Interactions of dopaminergic and histaminergic systems in health and disease

Inaugural-Dissertation

zur

Erlangung des Doktorgrades der

Mathematisch-Naturwissenschaftlichen Fakultät

der Heinrich-Heine Universität Düsseldorf

vorgelegt von

Roberto De Luca

aus Marino, Rom, Italien

Düsseldorf
2016

Aus dem Institut für Neuro- und Sinnesphysiologie

der Heinrich-Heine-Universität Düsseldorf

Gedruckt mit der Genehmigung der Mathematisch-Naturwissenschaftlichen

Fakultät der Heinrich-Heine-Universität Düsseldorf

First supervisor (Referent): Prof. Dr. O.A. Sergeeva (Institut für Neuro- und

Sinnesphysiologie und Institut für Klinische Neurowissenschaften und Medizinische

Psychologie, Heinrich-Heine-Universität Düsseldorf)

Second supervisor (Korreferent): Prof. Dr. H. Aberle (Institut für Funktionelle

Zellmorphologie, Heinrich-Heine-Universität Düsseldorf)

Tag der mündlichenPrüfung: 23.03.2016

Science knows no country, because knowledge belongs to humanity, and is the torch which illuminates the world.

Louis Pasteur

Table of content

Abbreviations (most frequently used)

3V: third ventricle

ACSF: artificial cerebrospinal fluid

AIN: acute isolated neurons

AP: action potential

cAMP: cyclic adenosine monophosphate

CB1: cannabinoid receptor 1

CNS: central nervous system

D2-type R: dopamine receptor type 2

DA: dopaminergic

DAT: dopamine transporter

DDC: L-dopa decarboxylase

DNA: deoxyribonucleic acid

eAPC: extracellular action potential current

eCB: endocannabinoids

FAAH: fatty acid amide hydrolase

FEPT: Fisher exact probability test

Fig: figure

GABA: gamma-aminobutyric acid

GPCR: G- protein coupled receptors

HA: histaminergic

H3R: histamine receptor 3

HCN channel: hyperpolarization and cyclic nucleotide activated channel

Hcrt/Orx: hypocretin/orexin

HDC: histidine decarboxylase

IHC: Immunohistochemistry

KO: knock-out

MEA: microelectrode array

mGluR: metabotropic glutamate receptor

mRNA: messenger ribonucleic acid

MWT: Mann-Whitney test

NADA: N-arachidonoyl-dopamine

NK1R: neurokinin 1 receptor

NTS: nucleus tractus solitarii

OLDA: N-oleoyl dopamine

PKA: protein kinase A

PKC: protein kinase C

PLC: phospholipase C

PCR: Polymerase chain reaction

PD: Parkinson´s disease

RAMH: R-alpha-methylhistamine

RT-PCR: reverse transcriptase-PCR

SNc: substantia nigra compacta

SP: substance P

TH: tyrosine hydroxylase

TMN: tuberomamillary nucleus

Tmt: Tomato

TRPV1: transient receptor potential vanilloid

VMAT2: vesicular monoamine transporter 2

WT: wild type

1. Introduction

1.1. The hypothalamic histaminergic (HA) system and arousal

The hypothalamus (Fig.1-1A) represents one of the oldest brain structures made up by a highly conserved circuitry involved in the integrative regulation of many vital functions such as feeding, metabolism, energy expenditure, reproduction, thermoregulation and sleep-wake cycles. The preoptic area contains mainly neurons responsible for thermoregulation and circadian rhythms; the tuberal hypothalamus, subdivided in anterior and lateral areas, in dorsomedial, ventromedial, paraventricular, supraoptic and arcuate nuclei, regulates feeding, nursing and several endocrine responses (Saper and Lowell, 2014;Saper, 2006). Finally, the posterior hypothalamus including the mamillary bodies overhung by the tuberomamillary nucleus (TMN) and supramamillary nucleus, provides a strong modulation of wakefulness (Haas and Panula, 2003), thus regulating the activity of different arousal centers that in concert inhibit sleep (Saper et al., 2005) (Fig.1-1B).
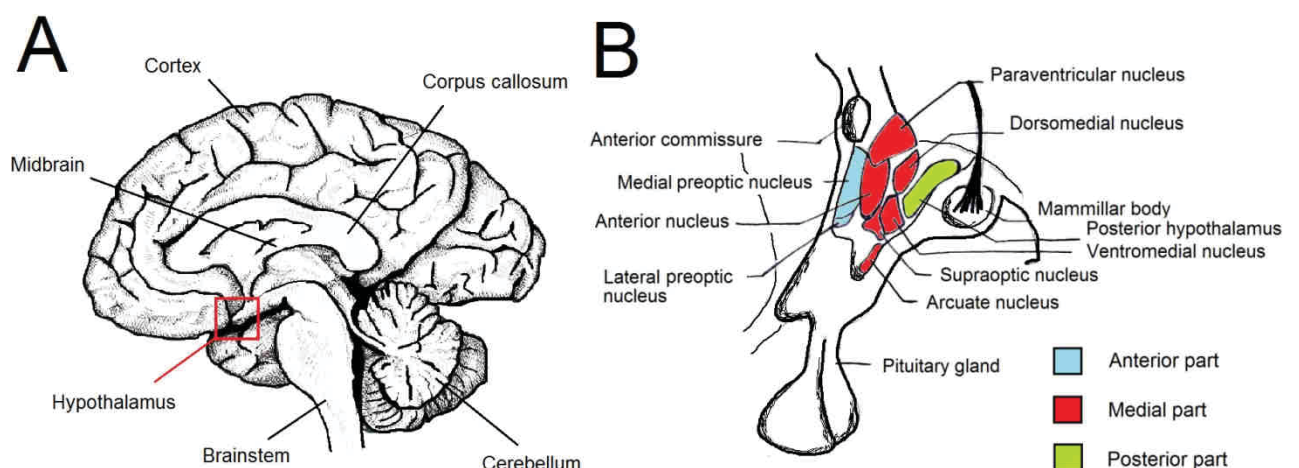
Fig.1-1. The human brain and its structures.
A. Sagittal brain section through the hypothalamus **B.** Anterior, medial and posterior hypo-
thalamus with bordering structures are represented. Modified from Kandel et al., (2000).

The physiological functions orchestrated by specific neuronal groups in the hypothalamus reflect the large diversity of the organization of its internal structure. Many studies have reported that specific hypothalamic lesions are responsible for distinct physiological impairments. Structural damages occurring in the preoptic area induce a loss up to 50% of daily sleep in rodents (Vetrivelan et al., 2012). Hetherington and Ranson provided experimental evidence that lesions of the dorso- and ventromedial hypothalamic and arcuate nuclei, increase body weight and cause accumulation of lipids in rats (Hetherington and Ranson, 1940). In addition, neurological and molecular impairments of the posterior

hypothalamus where the histaminergic (HA) system resides (Fig.1-2A and B) are responsible for somnolence, hypersomnia (Moruzzi, 1972), metabolic disorders and obesity (Jorgensen et al., 2006).

During the last decade it was recognized that the hypothalamic control of wakefulness and vigilance is a complex physiological process mediated by synergistic interactions between Hcrt/Orx (hypocretin/orexin) neurons of the perifornical area and the HA system (Haas et al., 2008). Von Economo in 1924, reported that profound lesions in the posterior hypothalamus (as we know now, involving HA and Hrct/Orx neurons), occurring in patients with encephalitis lethargica in the course of an influenza epidemic, are the basis of episodes of vigilance loss (Saper et al., 2005).
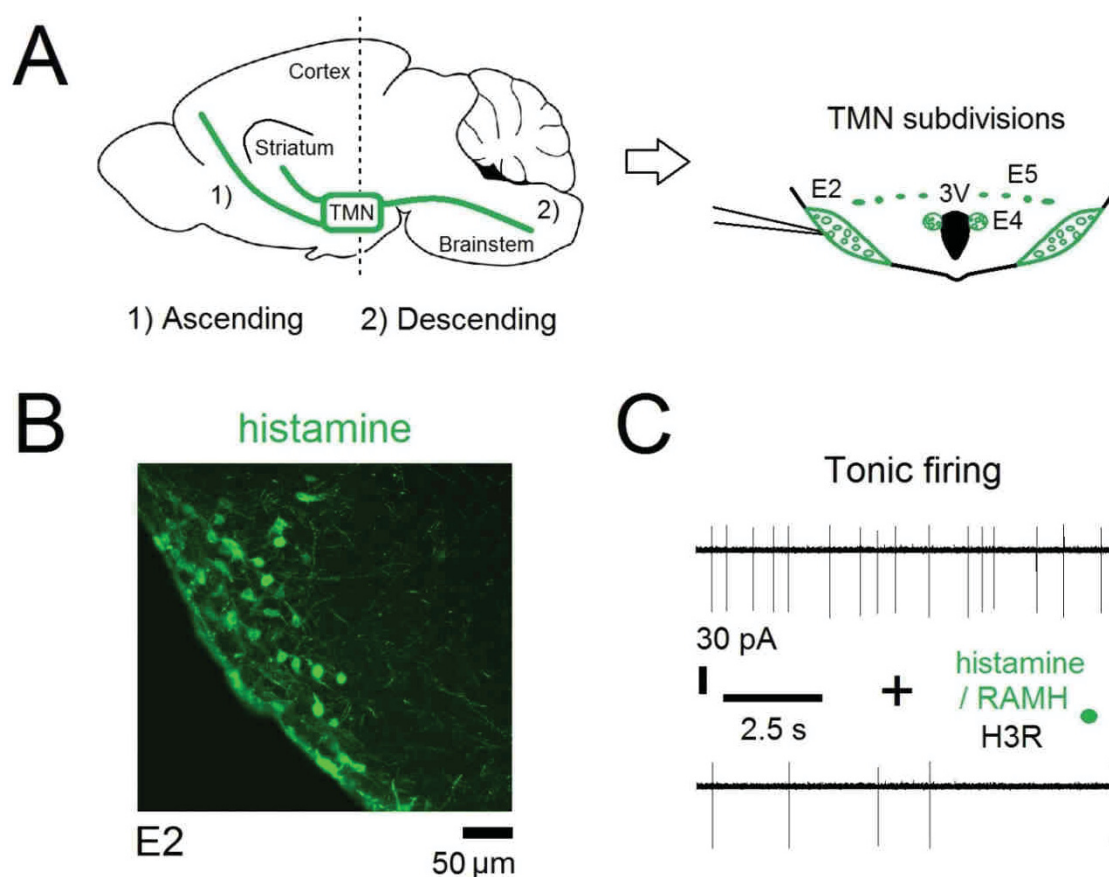
Fig.1-2. HA neuron populations in the TMN.
A. TMN is located in the posterior hypothalamus on the ventral surface of third ventricle (3V)-containing sections, from where it sends ascending (e.g. to striatum, cortex) and descending (e.g. to brainstem) projections. Coronal section made at the level indicated by dotted line is shown at the right side. TMN subdivisions and location of the typical recording site. **B.** Representation of mouse HA neurons (stained for histamine, in green) in the E2 subdivision. **C.** HA neurons display a regular firing pattern (extracellular recording) during waking *in vivo* and in brain slices *in vitro*. Histamine and R-alpha-methylhistamine (RAMH) trough histamine 3 receptor (H3R) inhibit firing of HA neurons.

The complex physiological changes induced by histamine in many districts of the body may explain why for a very long time, the specific action of this endogenous biogenic amine (like dopamine, adrenalin, noradrenalin and serotonin) in the brain was not fully accepted. Pioneering experiments from Henry Dale and JJ Abel (Riley, 1965; Abel and Kubota, 1919), the former working on muscle, the latter isolating the pituitary gland, gave the first important evidences that histamine could have a physiological action. It took nearly 20 years to have the complete acceptance that histamine truly behaves as a real neurotransmitter in the CNS. HA neurons were first identified exclusively in the TMN in 1984 by Panula and Watanabe (Panula et al., 1984;Watanabe et al., 1984) using antibodies against histamine (Fig.1-2B) or histidine decarboxylase (HDC, that produces histamine). In following studies the TMN was anatomically divided in several different subregions (in the rat): 1500 neurons are located in its ventral part (vTMN or E2) that includes also a less populated region called E3; nearly 500-600 in its medial part around the 3V (mTMN or E4) and 100 HA neurons are distributed between these two mentioned areas (diffTMN or E5) (Inagaki et al., 1988;Wada et al., 1991;Sarvari et al., 2012) (Fig.1-2A). TMN HA neurons innervate the whole CNS, with ascending (cortex and striatum) or descending projections (brainstem, i.e. nucleus tractus solitarii (NTS)) promoting wakefulness (Haas and Panula, 2003;Haas et al., 2008) (Fig.1-2A).

HA neurons have a membrane potential around -50 mV and display a regular and tonic firing pattern either in rat or in mouse brain slices (Fig.1-2C) (Haas and Reiner, 1988;Haas et al., 2008). The firing frequency correlates, when recordings are done *in vivo*, with the waking state: firing is fastest during active waking, slower during drowsiness and cessates during sleep (Takahashi et al., 2006). Retrograde tracing indicated that the TMN does not show a distinct or obvious topographical pattern (Kohler et al., 1985;Ericson et al., 1987). However, recent studies revealed that several subregions of HA neurons may react heterogeneously to different *stimuli,* such as stress (Miklos and Kovacs, 2003) and food restriction (Umehara et al., 2012) involving only E4-E5 and E3, respectively. The activation of specific TMN subregions is visualized by an increase of c-Fos (gene marker of metabolically active neurons) expression. Indeed, it seems that the heterogeneity of the HA population is not in the amount of TMN-projecting neurons to different brain areas but in their molecular identity that reflects the distinct pharmacological responses of HA neurons. Interestingly, microdialysis studies reported no increase of histamine content in striatum after the injection of H3R antagonists (like thioperamide) in TMN (Giannoni et al., 2010;Giannoni et al., 2009). Histamine is released from varicosities distributed periodically on the axons of HA

neurons, which rarely build up synaptic specializations (Diewald et al., 1997). The volume release controlling histamine levels represents an autocrine and paracrine regulatory effect that involves extra-synaptic receptors (Yu et al., 2015).

Rodent HA neurons may produce and release other neuroactive molecules like adenosine, galanin, metenkephalin, substance P (SP) (Airaksinen et al., 1992), GABA (Ericson et al., 1991) and dopamine (Yanovsky et al., 2011). HA neurons show immunoreactivity for GABA producing enzymes namely glutamate decarboxylase (GAD) 65 and GAD 67. Moreover, optogenetic stimulation of axonal fibers of mouse HA neurons innervating striatum and cortex, evoked robust GABA-mediated currents on target neurons (Yu et al., 2015). On the other hand, there is no direct evidence of GABA release inside TMN from light-stimulated HA collaterals (Williams et al., 2014).

The human TMN presents up to 40000 HA neurons in healthy subjects per side of posterior hypothalamus, detected by Nissl staining and histamine immunoreactivity (Shan et al., 2012). Similar to rodents in human HA neurons HDC co-localizes with GABA (Trottier et al., 2002). Histamine production is regulated by day and night fluctuations, reaching the highest peak during the dark period for rodents and during the light phase for healthy humans (around 6 *post meridiem*, p.m.). This supports the evidence for a role of the HA system in wakefulness. However the relationship between the ribonucleic acid messenger (mRNA) of HDC transcripts measured *post-mortem* and the histamine production is complex, since the fluctuations of histamine levels among the hours of the day are often different (Shan et al., 2012).

1.2. Histamine receptors

In mammalian brain histamine binds to four known G-protein coupled receptors (GPCR), called (H1-2-3-4Rs) (Panula et al., 2015). Histamine at physiological concentration has no major direct effect on mammalian ionotropic receptors such as: acetylcholine, GABA, glycine and glutamate (Haas et al., 2008;Smart and Paoletti, 2012;Panula et al., 2015). Interestinlgy, in invertebrates ionotropic histamine receptors are chloride channels structurally similar to glycine and GABAA receptors (Fleck et al., 2012).

1.2.1. H1 receptor (H1R)

H1R is considered to be the major responsible receptor for sedative effects in the CNS and of allergy symptoms outside the brain. The brain distribution of H1R was studied using selective radioligands such as [3H]mepyramine (Hill et al., 1977;Martinez-Mir et al., 1990) and later using *in situ* hybridization, showing particularly high expression levels in thalamus,

basal forebrain, hippocampus, brainstem and some nuclei in the hypothalamus. It is absent on HA neurons. The cellular function of H1R is excitatory inducing increase of firing frequency that is accompanied by a strong depolarization of the membrane potential. H1R is coupled with Gq/11 G-protein that activates the axis phospholipase C (PLC) – protein kinase C (PKC), that in turn increases intracellular calcium (Ca+2) levels (Leurs et al., 1994;Panula et al., 2015). The physiological function of H1R is in the promotion of arousal, wakefulness and food intake (Haas et al., 2008).

1.2.2. H2 receptor (H2R)

Studies on gastric acid secretion led to the discovery of a second class of histamine receptors, namely H2Rs (Panula et al., 2015). H2R is distributed in the whole brain like the H1R, in particular in the hypothalamus, basal ganglia and amygdala. It couples Gs G-protein leading to the accumulation of cyclic adenosine monophosphate (cAMP). The target of cAMP is the protein kinase A (PKA) that increases transcriptional activation (Panula et al., 2015). One of the most interesting actions mediated by H2R is a block of a calcium-dependent potassium (K+) channel responsible for the accommodation of firing (Haas and Konnerth, 1983). Finally, the H2R might be important for the maintenance of congnitive function in the CNS (Haas et al., 2008).

1.2.3. H3 receptor (H3R)

H3R was described on the basis of pharmacological evidence (Arrang et al., 1983;Drutel et al., 2001). It is highly expressed in many brain areas such as cortex, thalamus and basal ganglia, according to intensity of the signal given by radiolabeled RAMH (Panula et al., 2015). H3Rs act as autoreceptors (inhibiting synthesis and release of histamine) on HA neurons axons and somata or heteroreceptors (inhibit release of other transmitters) on non-HA neurons and are coupled to Gi/G0 proteins that once activated reduce intracellular cAMP levels. H3R activation reduces firing of HA neurons through inhibition of voltage-gated calcium channels (block of calcium current that is a feature of HA neuronal pacemaker activity) (Stevens et al., 2001). The physiological functions of H3R are many (i.e. H3R KO mice present reduced locomotion, Haas et al., 2008) from the regulation of metabolism to the control of wakefulness. The neurophysiological relevance of H3R increased the interest of clinical pharmacological research to develop novel H3R-specific compounds. Indeed, since H3R activation inhibits HA firing, H3R antagonists / inverse agonists (Pitolisant or Wakix ®) have a waking action and are available to combat exaggerated sleepiness in narcolepsy

and in other neurological disorders such as Parkinson's disease (Lin et al., 2008) (Dauvilliers et al., 2013).

1.2.4. H4 receptors (H4R)

H4Rs are the last class of newly discovered histamine receptors. Even though H4R mRNA was detected in the brain (Karlstedt et al., 2013), a possible role of H4R in the CNS requests further research. The major physiological function of this new receptor is in the modulation of immune responses (Panula et al., 2015).

1.3. Synergism between dopaminergic (DA) and HA systems in the control of arousal. DA excitation of HA neurons

Dopaminergic (DA) contribution to the maintenance of wakefulness is still under debate. Indeed, dopamine deficient mice do not move or sleep (Dzirasa et al., 2006). On the other hand, dopamine transporter knockout (DAT KO) mice have an increased level of dopamine in the brain and show locomotor hyperactivity (Jaber et al., 1999).

Innervation and release of dopamine in the hypothalamus by DA wake-on centers (e.g. from the periaqueductal gray and the zona incerta (A11)), provide a strong modulation of arousal, increasing the excitatory output to basal forebrain and cortex (Lin et al., 2011). HA neurons are excited by L-dopa (L-3,4-dihydroxyphenylalanine, precursor of dopamine) and agonists of D1-type and D2-type dopamine receptors and they express all five types of GPCR dopamine receptors (D1-2-3-4-5Rs) (Yanovsky et al., 2011). HA neurons do not produce tyrosine hydroxylase (TH, enzyme that converts L-tyrosine into L-dopa) but possess L-dopa decarboxylase (DDC) and the vesicular monoamine transporter 2 (VMAT2) for production (Yanovsky et al., 2011;De Luca et al., 2016) and release of dopamine (Yanovsky et al., 2011). Moreover, the wake-promoting action (monitored by electroencephalography (EEG)) of 1 mg/kg intraperitoneally injected quinpirole (a selective D2-type R agonist), is missing in histamine deficient mice (HDC KO) (Yanovsky et al., 2011). The role of DA (or dopaergic) projections to HA neurons is at present unclear. HA neurons located in the medial and dorsal TMN are closely connected to hypothalamic DA neuronal groups such as in the supramamillary nucleus, the ventral premamillary nucleus or the posterior periventricular nucleus (Yanovsky et al., 2011). TH-expressing fibers coming from the locus coeruleus and other brainstem areas can be visualized in the TMN (Yanovsky et al., 2011) (Fig.3-2).

1.4. Brain DA systems

Three DA systems are defined according to their projections (Fig.1-3A). (1) The *ultrashort system* that includes the amacrine-like neurons in the retina (A17) and the periglomerular DA neurons in the olfactory bulb (A16). (2) The *intermediate-length systems* composed of (i) the tuberoinfundibular dopamine neurons (TIDA) (in A12-14 groups) which deliver dopamine to the pituitary gland, (ii) incertohypothalamic neurons (A11) and (iii) the medullary periventricular nucleus that describe neurons connecting the dorsal and the posterior hypothalamus, and those located in the dorsal motor nucleus of the vagus nerve and the NTS in the brainstem. Finally, (3) the *long-length systems* include DA neurons of SN (substantia nigra) and VTA (ventral tegmental area) (A8-A9-A10) in the midbrain (Cooper et al., 1996). The heterogeneity of DA neurons regarding anatomical location and innervation pattern, reflects also the diversity at the molecular level and in terms of endocrinological and pharmacological responses. Diversity exists also within neuronal groups (e.g. midbrain DA neurons) previously thought to be homogeneous populations (Lammel et al., 2008). D2-type R-mediated autoinhibition in midbrain DA neurons is the most reliable marker for neuronal identification (Fig.1-3B), except for those neurons projecting to the prefrontal cortex, which express D2-type R at very low level (Lammel et al., 2008). DA neurons in the midbrain display a regular tonic firing frequency from 1 to 4 Hz *in vitro* (Tritsch and Sabatini, 2012) and 1 to 8 *in vivo* (Paladini and Roeper, 2014). Dopamine binding triggers different signalling cascades depending on the activated receptor (Tritsch and Sabatini, 2012). Focusing mainly on the inhibitory D2-type R, activation by dopamine (that shows the highest affinity for these receptors) downregulates cAMP levels through Gi/0 protein (Stoof and Kebabian, 1984; Tritsch and Sabatini, 2012) (Fig.1-3B). Quinpirole and other psychostimulants administered systemically in mouse suppress sleep, enhance arousal and stimulate locomotor activity in midbrain (in particular in SNc) (Fig.1-3C). Recently designed DAT-Cre mouse lines (Parlato et al., 2006) combined with optogenetic technology are about to reveal the particular role of diverse DA neuronal groups in this systemic action.

The production and the storage of dopamine are mandatory features for monoaminergic neurons to be defined as "truly" DA. Storage and release of dopamine are under control of DAT and VMAT2, respectively (Zoli et al., 1993). On the other hand, the biosynthetic machinery for dopamine production is represented by TH and DDC (Fig. 1-3D). In the midbrain most DA neurons are TH+/DDC+/DAT+, on the other hand in the hypothalamus the *scenario* is more complex since neurons fully expressing the complete enzymes for dopamine production and storage are rare, whereas many other populations that express

singularly TH, DDC and DAT, show differences in terms of DA nature (De Luca et al., 2016). Dopamine degradation involves several enzymes such as: catechol-O-methyl-transferase (COMT), monoamine oxydase (MAO) and dopamine beta hydroxylase (DBH) (Meiser et al., 2013).

Recently several lipid mediators produced in catecholaminergic neurons along with dopamine were described, such as N-oleoyl dopamine (OLDA) and N-arachidonoyl dopamine (NADA) (Huang et al., 2002;Chu et al., 2003) (Fig.1-3D). Their exact biosynthetic pathway is still unclear even though lipid acids produced by the fatty acid amide hydrolase (FAAH) activity, conjugate with L-tyrosine or dopamine to produce OLDA and/or NADA, respectively. OLDA shares with dopamine the COMT degradation pathway (Zajac et al., 2014).
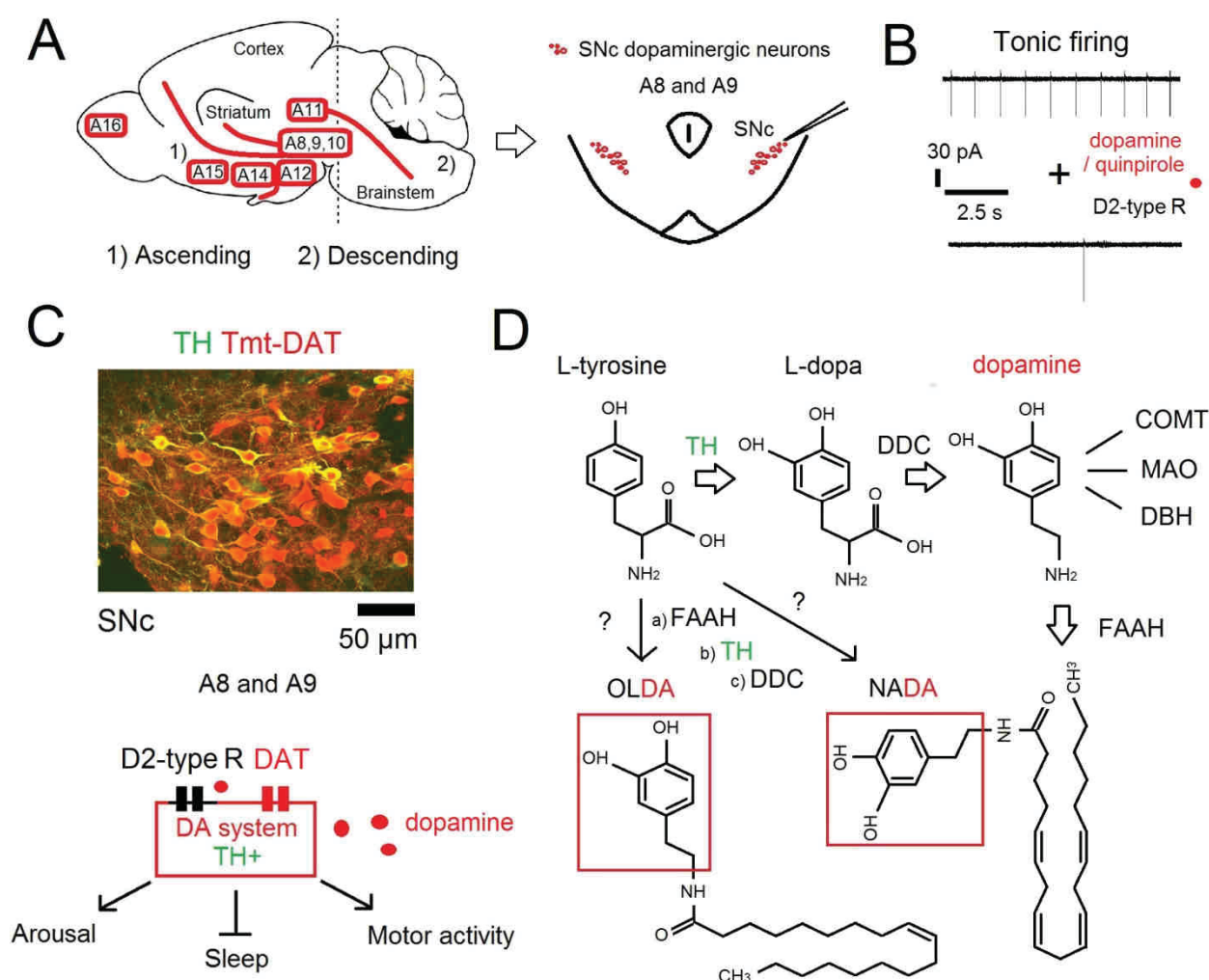
Fig.1-3. Brain DA systems.
A. DA clusters in CNS. The schematic representation shows different DA groups innervating distinct brain regions. Midbrain DA neurons in SN (A8-9) and VTA (A10) send ascending projections to striatum and cortex; DA neurons in the zona incerta (A11) present descending afferents to the brainstem; neurons in the arcuate nucleus (Arc, A12 and A14) innervate the

median eminence for the dopamine release in the pituitary gland. At the right: section made through the brain at the level indicated with dotted line. DA neurons of the SN pars compacta (SNc) with the location of the recording site. **B.** Firing of SNc neuron is regular and inhibited by dopamine or quinpirole (D2-type R agonist) through an auto-inhibitory mechanism activating the G protein-coupled inwardly-rectifying potassium (GIRK) channels **C.** Immunohistochemical co-localization of red "tomato" (Tmt)-DAT with tyrosine hydroxylase (TH, green) in neurons of SNc. Summary of SNc physiology below. **D.** Synthesis and degradation (MAO, COMT, DBH) pathways of dopamine. Note that conjugation of L-tyrosine with oleic acid produces the endocannabinoid N-oleoyl dopamine (OLDA), whereas conjugation of L-tyrosine or dopamine with arachidonic acid results in N-arachidonoyl dopamine (NADA). Oleic and arachidonic acid are produced by FAAH.

1.5. Parkinson´s disease (PD). Pharmacological progress in PD treatment: a focus on H3 and D2-type auto-inhibitory receptors

Deficits or impairments of dopamine transmission are implicated in the pathology of several neurological pathologies including PD, schizophrenia and attention deficit hyperactivity disorder (Grace et al., 2007;Schultz, 2007). PD is a severe and chronic neurological disorder that involves basal ganglia (structure formed by: SNc and SN pars reticulata (SNr), striatum, globus pallidus (GP) and subthalamic nucleus (STN)) and characterized by a progressive loss of pigmented DA neurons located in the SNc (Kish et al., 1988), leading to motor disabilities (bradykinesia and akinesia) (Agid, 1991), tremor, impairment of cognition and sleep disturbances (Boeve et al., 2007).

Two distinct pathways were identified in the basal ganglia thalamo-cortical connection: (a) the direct and (b) the indirect pathway. The first (a) facilitates voluntary movement and motor control suppressing the tonic active neurons in the internal part of globus pallidus (GPi), thus resulting in the only activation of thalamus and cortex. The second pathway (b) inhibits the involuntary movement increasing the inhibitory output to the thalamus, acting through the external part of pallidal (GPe) segment and also regulating the interplay between the globus pallidus and the STN (Braak et al., 2003). In other words, the direct pathway can be considered as a positive and the indirect pathway as a negative feedback in the connection between the basal ganglia and the thalamus. In PD the striatal dopamine defiency from SNc, leads to robust thalamic inhibition and diminished cortical activation that are responsible of bradykinesia and tremor.

Recent studies consider not only motor disabilities as the major core of PD symptoms but also the neurovegetative complications may play a considerable role in the pathogenesis of PD (Chaudhuri and Schapira, 2009). For instance sleep disturbances and excessive daytime sleepiness (EDS) are common symptoms in PD patients and their severity increases with the

progressive pathology (Simuni and Sethi, 2008). The hypersomnia may be explained by damaged arousal systems in PD, indeed noradrenergic neurons in the locus ceruleus, serotoninergic neurons in the dorsal raphe, cholinergic neurons in the basal forebrain (Jellinger, 1991) and Hcrt/orx neurons in the lateral hypothalamus (Thannickal et al., 2007), are affected in PD. Moreover, half of the patients surviving encephalitis lethargica displayed a Parkinsonian-like syndrome likely caused by chronic hypothalamic or mesencephalic inflammation (Berger and Vilensky, 2014). Lesions of the posterior hypothalamus and midbrain (Monti and Monti, 2007) impair the sleep-wake cycle.

Interestingly, HA neurons and DA neurons in the hypothalamus (Purba et al., 1994) preserve their number (Nakamura et al., 1996) and enzymatic activity (Garbarg et al., 1983) in PD brains (Prell et al., 1991). The intact HA function modulates, through the H3R, the release of other neurotransmitters such as: dopamine, serotonine, noradrenaline, acetylcholine and glutamate and H3R inverse agonists/antagonists are beneficial in combating sleepiness in PD patients (Arnulf and Leu-Semenescu, 2009). The first clinical signs of PD patients appear only after a loss of 50-70% of nigrostriatal neurons (threshold of pathological outcome), preventing an early intervention. Recent therapeutic strategies are directed to reduce the nigrostriatal loss, although the cellular and molecular mechanisms behind the vulnerability and the selective death of DA neurons are still unknown (Barzilai and Melamed, 2003). L-dopa represents from many years the "gold standard" treatment for PD, although unwanted side effects such as dyskinesia and motor complications appear especially after prolonged treatment (Weiss et al, 1971, Pechevis et al, 2005). Some explanations for L-dopa-dependent side effects are following: 1) newly synthesized excessive dopamine impairs function of DAT (Leenders et al., 1986); 2) Increased dopamine levels cause over-activation of D1R, which leads to dysregulation of motor functions (Calabresi et al., 2010); 3) high dopamine level downregulates or desensitizes D2-type R which elicits reduced L-dopa potency (Hurley and Jenner, 2006); 4) Finally, excessive dopamine might cause to oxidative stress due to auto-oxidation products of L-dopa metabolism, that exaggerate the degeneration of DA neurons in SN (Graham, 1978). Addictive behaviour (L-dopa overdosing) in some PD patients can be treated with partial D2-type R agonists e.g. aripiprazole (Mizushima et al., 2012). Therefore improvement of PD therapy is needed.

OLDA is an endogenous amide of DA and oleic acid (Chu et al., 2003) (Fig.1-3D) recently described as possible prodrug for PD treatment on the basis of its stability and penetration through the blood brain barrier (BBB) (Przegalinski et al., 2006). After intraperitoneal injection OLDA increased horizontal locomotor activity in the rat, which was abolished by

haloperidol (D2-type R antagonist) (Przegalinski et al., 2006). Cellular mechanims of OLDA action are unexplored. There are no studies proofing an interaction of this compound with dopamine receptors. Another endogeneous dopamine conjugate NADA (Huang et al., 2002) (Fig.1-3D) lacks significant action at dopamine receptors, but has high affinity for cannabinoid receptor 1 (CB1R) and FAAH (Bisogno et al., 2000). Modulation of SNc DA neuron activity by OLDA awaits to be explored.

1.6. Molecular targets of OLDA, a novel lipid mediator

In vitro studies showed that OLDA binds to the transient receptor potential vanilloid type 1 (TRPV1) with an equipotent action of capsaicin (Ki of 36 nM) and less efficiently to CB1R (Ki of 1.6 µM). A weak inhibitory action on FAAH was as well detected (Chu et al., 2003). Moreover, OLDA is described as a potent inhibitor of 5-lypoxigenase (5-LO) (half-inhibitory concentration (IC50) is 7.5 nM) (Tseng et al., 1992;Chu et al., 2003).

1.6.1. TRPV1 (VR1 or capsaicin receptor)

TRPV1 (also called vanilloid receptor 1 (VR1) or capsaicin receptor) belongs to a subfamily of TRP channels expressed on primary afferent nociceptors of the dorsal root ganglia, in some areas of the brain and in non-neuronal tissues (Cavanaugh et al., 2011;Kernder et al., 2014). TRPV1 is composed of 4 subunits consisting of 6 transmembrane domains (Garcia-Sanz et al., 2007). The pore-loop is formed by the fifth and the sixth domains (Clapham et al., 2005). Mutational analysis provided evidence of several sites on TRPV1, that are activated by different *stimuli*. The vanilloid (capsaicin) site is located intracellularly between the second and third transmembrane domains, whereas the proton site is on the external part of the receptor in close neighbourhood to the pore-loop structure (Julius, 2013). This non-selective cation channel (calcium > sodium (Na+)), is also activated by heat (thermal activation threshold is around 43°C) (Caterina et al., 1997), thus participating not only in nociception but also in thermosensing (Tominaga et al., 1998). Mice without this functional receptor (TRPV1 KO) display partial impairments in pain sensitivity and thermal nociception even though their responses to noxious mechanical *stimuli* are indifferent from WT mice (Caterina et al., 2000).

1.6.2. Endocannabinoids (eCB) and their receptors

Endocannabinoids (eCB) derive from polyunsaturated fatty acids and show different chemical structures than THC (Δ9-tetrahyrocannabidinol, a phyto-active compound isolated from *Cannabis Sativa*). Development of THC analogues led to the discovery of cannabinoid-

sensitive targets, namely cannabinoid receptors (CBRs) in the brain (Devane et al., 1988). Once eCB are released in the synaptic cleft, activation of CBRs may cause either increase or decrease of the classical transmitter release (Piomelli, 2003). The first eCB discovered was the amide of arachidonic acid called anandamide (N-arachidonoylethanolamide, AEA) (Devane et al., 1988). AEA synthesis and release are calcium-dependent processes (Di Marzo et al., 1994). On the other hand, a role of GPCR in AEA release has been proposed. Indeed application of a D2-type R agonist causes a huge release of AEA outflow in striatum, blocked by the D2-type R antagonist raclopride (Giuffrida et al., 1999). Another THC-like compound, which was detected later is 2-arachidonoylglycerol (2-AG). Like for AEA, 2-AG production is initiated by an increase of intracellular calcium. However, AEA and 2-AG synthesis are independent processes since D2-type R activation in striatum does not influence 2-AG concentrations (Giuffrida et al., 1999). AEA and 2-AG can diffuse passively across the membrane. Usage of eCB transport inhibitors, enhances biological effects of AEA and 2-AG (Piomelli et al., 1999). FAAH is an intracellularly bound-serine hydrolase that cleaves AEA into arachidonic acid and ethanolamine, which is widely expressed on axon terminals. In contrast to WT mice, administration of AEA induces a robust loss of motility together with analgesic and cataleptic effects in FAAH KO mice that is abolished in the presence of a CB1R antagonist (Lichtman et a., 2002). The FAAH inhibitor URB 597 augments eCB levels in the tissue causing strong-anxiolytic or analgesic effects, which are mainly mediated through the CB1R (Piomelli et al., 2006).

Metabolism of 2-AG occurs mainly through enzymatic hydrolysis by monoacylglycerol lipase (MGL) action (Dinh et al., 2002). Lately identified eCB are: noladin ether, oarachidonoyl-ethanolamine and N-arachidonoyl-dopamine (NADA). AEA and NADA do not only bind to CB1 or CB2 receptors but also show affinity for TRPV1 acting on thermoregulation and pain sensation in the peripheral nervous system (Kim et al., 2007).

Both CB1 and CB2 receptors belong to the large family of the GPCR. They are of the Gi/0-coupled type, opening potassium channels and inhibiting cAMP activity. In addition, other mechanisms have also been observed, for instance interaction with certain ion channels (such as: A-type or inwardly rectifying potassium channels) (Pertwee, 1997).

CB1R is among the most abundant and widely distributed GPCRs in the brain. High levels of CB1R expression are found in basal ganglia (for motor activity regulation), hippocampus, cerebral cortex and brainstem (Farquhar-Smith et al., 2000). The CB2R is mainly expressed on immune cells and regulates the release of cytokines. Recent studies also report a moderate

expression of CB2R in the midbrain (Zhang et al., 2014), hippocampus and brainstem (Gong et al., 2006).

Additional cannabinoid receptor subtypes functionally related to CB1 and CB2R are most likely existing (Begg et al., 2005). For instance the anorexic effect of N-oleoylethanolamine (OEA) was suggested to be mediated by GPR119 (G protein-coupled receptor 119, mainly found in pancreas) in the hypothalamic regulation of metabolism (Wang and Ueda, 2008). Anorectic action of OEA is missing in histamine-deficient mice (Provensi et al., 2014).

1.7. Objectives

Previous studies reported that HA and DA systems share physiological features and anatomical locations (Yanovsky et al., 2011). Clarifying histamine - dopamine interactions might help to better understand the developments of neurological disorders (like PD) and their possible treatment (Panula and Nuutinen, 2013). Finally the usage of hybrid molecules (such as OLDA) interacting with common molecular targets of the histamine-dopamine axis may open a new frontier for the pharmacological treatment of PD.

(1) Identification criteria for diverse subgroups of aminergic neurons in TMN and DA neurons in midbrain should be worked out using different transgenic mouse lines. Focus on H3R-mediated inhibition of HA neurons in TMN and its possible impairment in patho-physiological conditions.

(2) OLDA targets should be characterized in midbrain DA neurons (especially in SNc) and in HA neurons of TMN: role of TRPV1, D2-type R and cannabinoid receptors.

2. Materials and Methods

2.1. Solutions and materials for mouse brain slicing and electrophysiological recordings

2.1.1. Cutting and recording solutions

Anoxia and neurotoxicity are pathophysiological conditions caused by invasive operations, injury and brain damage. In order to keep the experimental conditions as optimal during slices preparation, a neuroprotective ice-cold sucrose-containing solution modified from recording solution (also called artificial cerebrospinal fluid (ACSF)) was prepared. This solution was kept on ice (to maintain temperature around 0°C) and continuously saturated with carbogen (5% CO_2/95% O2) to maintain pH 7.4 during slice preparation and is composed of (in mM): Sucrose 202 (VWR International GmbH, Darmstadt, Germany), D-Glucose 12, NaHCO3 26, KCl 3.75, NaH2PO4 * H2O 1.25, MgSO4 * 7H2O 1.3, $CaCl_2$ * 2H2O 2 mM (Merck, KgaA, Darmstadt, Germany). After cutting in this solution brain slices were immediately placed into an incubation glass with ACSF of similar composition except for the sucrose, which was replaced by 125 mM NaCl. Preparation of slices in sucrose-containing solution reduces neuronal depolarization, swelling and osmotic damage (induced by water entry) during cutting. The low temperature minimizes the cellular metabolism of the brain slices, allowing a better recovery throughout the incubation period, 1 hour, or longer, at room temperature (22-25°C).

In some recordings ACSF with nominally zero calcium level was used: it contained 0.5 mM ethylene glycol tetraacetic acid (EGTA) (Endo et al., 2014;De Luca et al., 2016). Either for cutting or recording solutions $CaCl_2$ was firstly dissolved before adding other compounds to the stock solution (10X) in order to prevent the calcium carbonate precipitation. In some experiments another variant of recording solution with high potassium (KCl 4 mM) was made. This last solution depolarizes neurons enhancing their excitability. Recordings were done either at room temperature (22-25°C) or at 33°C. In the latter case the ACSF was warmed up in the heated perfusion tube (ALA scientific instruments, NY, USA) by a temperature controller (NPI, electronic GmbH, Tamm, Germany), before reaching the slice inside the warmed recording chamber.

Acute isolated neurons (AIN) were dissociated from TMN slices incubated for at least one hour. The dissected TMN region was placed in a small volume of HEPES-based AIN recording solution (50-70 µl) and triturated with the help of 100 µl Eppendorf pipette (Eppendorf-Sigma,Steinheim, Germany) until the tissue was fully homogenised. HEPES-based solution was composed of (in mM): NaCl 150, KCl 3.7, $CaCl_2$ 2.0, $MgCl_2$ 2.0, HEPES

(4-(2-hydroxyethyl)-1-piperazine-ethanesulfonic acid (Sigma, Steinheim, Germany) 10, glucose 10 (pH 7.4). Recordings were done at room temperature (22-25°C).

2.1.2. Patch pipette (intracellular) solutions

For the whole-cell current clamp and voltage clamp recordings electrodes contained (in mM): KCl 130, NaCl 10, MgCl$_2$ 2, CaCl$_2$ 0.25, glucose 5 ,HEPES 5, EGTA 10, MgATP 5, MgGTP0.3 (Sigma, Steinheim, Germany), pH 7.2 adjusted with KOH 1 M. In some experiments EGTA 0.1 mM instead of 10 mM was as well as biocytin (0.05-0.1%) (for neuronal labelling). For a better use the aliquotes of these solutions were kept at -20°C into 1ml Eppendorf tubes. All solutions (fresh or frozen) were filtered (using a filter paper, Whatman, Sigma, Steinheim, Germany; or a syringe, Thermo Fisher scientific, Dreieich, Germany) for daily use.

2.1.3. Plastic wares and glasses

Tubes and all plastic wares (tips, petri dishes and wells) were purchased from Starlab GmbH Hamburg; Eppendorf Eppendorf-Sigma,Steinheim, Germany; Falcon NY, USA; Sarstedt, Nuembrech, Germany and Wilcowell, Amsterdam, Nederland. Bottles and glasses were bought by VWR International GmbH, Darmstadt, Germany.

2.2. Animals and surgery

Animal transportation, handling and experiments were conducted according to German law (TierschutzgesetzBGBl. I,S. 1206, revision 2006), EEC directives 86/609/EEC and the local guidelines (LANUV FB Tierschutz, BezirksregierungDuesseldorf). Permission for the animal studies was provided by the regional government of Germany (Landesamt für Natur, Umwelt und Verbraucherschutz Nordrhein-Westfalen, AZ 84-02.04.2013.A213) and the experiments were performed according to the guidelines for the use of experimental animals, as given by the German „Tierschutzgesetz" and the „Guide for the Care and Use of Laboratory Animals" of the U.S. National Institutes of Health. Juvenile and adult C57Bl6J, TRPV1-/- (KO), TRPV1+/- (heterozygous, HT) mice and their wild-type (WT) littermates (Caterina et al., 2000) as well as mouse lines either expressing the fluorescent Tmt protein under control of the HDC promoter (Tmt-HDC) (JacksonLaboratory, #007908) (Cg Gt(ROSA)26Sortm14(CAG−tdTomato)(Yanovsky et al., 2012;De Luca et al., 2016) or Tmt-DAT (DAT-Cre mouse line provided by Prof.G.Schütz, University of Heidelberg (Parlato et al., 2006;De Luca et al., 2016)) were used. Previous studies have shown that in mice carrying both transgenes (HDC-*Cre* and Rosa26-lox STOPlox- tdTomato) the majority of HA

neurons of vTMN express Tmt protein and virtually all Tmt-HDC positive neurons are HA (Yanovsky et al., 2012). All mice were kept in Zentrale Einrichtung für Tierforschung und Tierschutzaufgaben (ZETT), in Duesseldorf University. Animals were held at 12/12 hours dark/light cycle and the free access to water and food. The food provided contained 6% fat (SSNIFF Spezialdiaeten GmbH, Germany). Animal ordering was arranged every day with the help of a specific web program Ticket@lab (provided by ZETT). All surgery was performed under isofluoran (Abbott, Wiesbaden, Germany) anesthesia, and all efforts were made to minimize the number of animals and their suffering. Mice were held by the tail and quickly kept in the hand for a fast decapitation using big scissors. The head is harvested and skin together with muscles surrounding the skull were removed with the help of small scissors, starting from the basis of the head until the nasal part. Once the skull is visible two cuts were usually made to complete the brain removal: 1) the first cut (longitudinal) is done at the level of the occipital bone, crossing the interparietal, parietal and frontal lines; 2) the second one (transverse) between nasal and frontal bones, allows the complete opening of the hemispheres using small forceps (Fig.2-1A). Some additional cuts were made to remove the resting bones surrounding the brain. At this stage dura mater (the most external layer of meninges) was removed. With the help of a spatula the brain was detached from the basis of the skull and put into a glass containing ice-cold fully oxygenated sucrose-ACSF for 2-3 minutes. Cerebellum and olfactory bulbs were removed with the scalpel in order to keep a coronal brain section containing brainstem (and NTS), midbrain (SN), hypothalamus (TMN) and striatum. Finally, this section was fixed with a tissue adhesive (Histoacryl, B. Braun Melsungen AG, Germany) on a round platform inside an ice-cold chamber to be cut with blades (Credo, Solingen, Germany) mounted on a tissue vibro-slicer (HR2, Sigmann Elektronik, Germany) (Fig.2-1B).
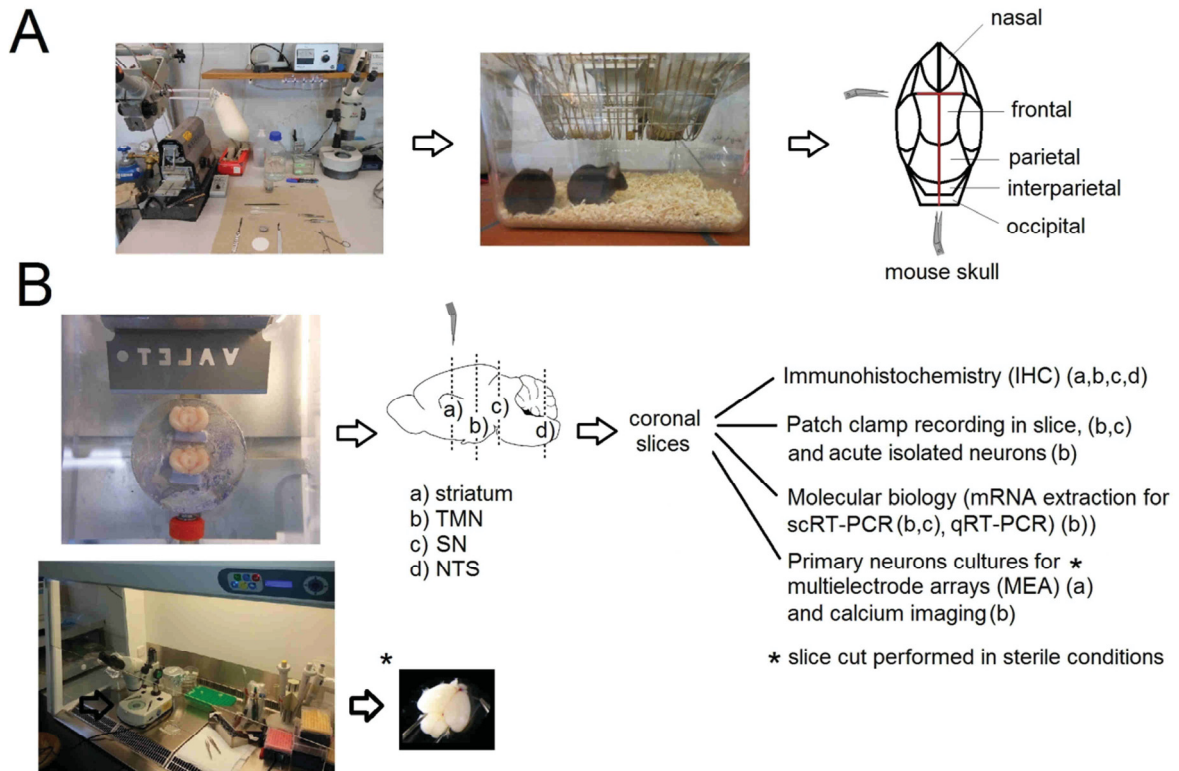
Fig.2-1. Surgery and mouse brain cutting.
A. Photographs showing table of surgery and mice used for experiments. On the skull representation (right), cutting lines (in red) between bones for opening are depicted. **B.** Brain coronal slices were prepared either using a tissue micro-slicer or a scalpel for acute experiments (i.e. patch clamp, immunohistochemistry (IHC) and molecular biology) and for primary neurons cultures preparations (in sterile conditions), respectively. The considered brain areas for experimental investigations are anatomically indicated using letters: a) striatum; b) TMN; c) SN; d) NTS.

2.3. Description of patch clamp technique and its components

After the first evidences from Luigi Galvani about electrical activity inducing muscular contraction in animals (Verkhratsky et al., 2006), the desire to measure a low-noise ion channel current on single cells, became reality with the development of the patch clamp technique (Fig.2-2) by Neher and Sakmann (1976), awarded with the nobel prize in Physiology and Medicine in 1991. Four configurations are known for patch clamp: 1) cell-attached; 2) whole-cell; 3) outside-out and 4) inside-out. The configurations: 3 (obtained pulling the pipette out from whole-cell) and 4 (pulling the pipette away from cell-attached), will not be discussed here in detail. The most physiological approach to measure firing properties of neurons (spontaneous firing) is the cell-attached configuration, since the pipette

adheres on the cell membrane keeping only a gentle suction (gigaseal). Recording this configuration in voltage clamp (VC) mode allows to measure the ionic currents crossing the cell at given voltage and to visualize the extracellular action potential currents (eAPCs, reduced in a depolarized neuron). Indeed the transmembrane voltage recorded, passing through the amplifiers is converted into a current by a current-voltage converter. A negative feedback is inside the circuit to keep always the patched cell at the fixed voltage (0 mV) (Fig.2-2A and D upper part). This approach is particularly important to measure the activity of voltage-gated channels that are opened only at certain values of potential.

In the whole-cell configuration after a small suction of the cell membrane, next step is its rupture with a strong pulse of negative air pressure. The membrane opening creates a low-resistance unity between the pipette and the cellular volume. Recording this configuration in current (CC) clamp mode allows to visualize action potentials (APs) and measure the membrane potential of the neurons by the application of a fixed value of current on the cell (zeroing of voltage amplifier, C_0). The CC amplifier changes minimally the small voltage signals coming from the cell. This mode is very useful to study cellular responses to surrounding neurotransmitters acting on ion channels (Fig.2-2B and D lower part) (Liem et al., 1995).

Nevertheless VC and CC can be either applied on whole-cell or cell-attached, respectively. The whole-cell VC is largely used to measure the activity of different channel populations (i.e. ligand gated ion channels) in terms of current (i.e. spontaneous GABAergic inhibitory postsynaptic currents, sIPSCs or hyperpolarization-activated cyclic nucleotide-gated, HCN channel currents) (Jackson, 2001).The cell-attached CC is better suitable respect to VC to record the cell resting membrane potential (Perkins, 2006).
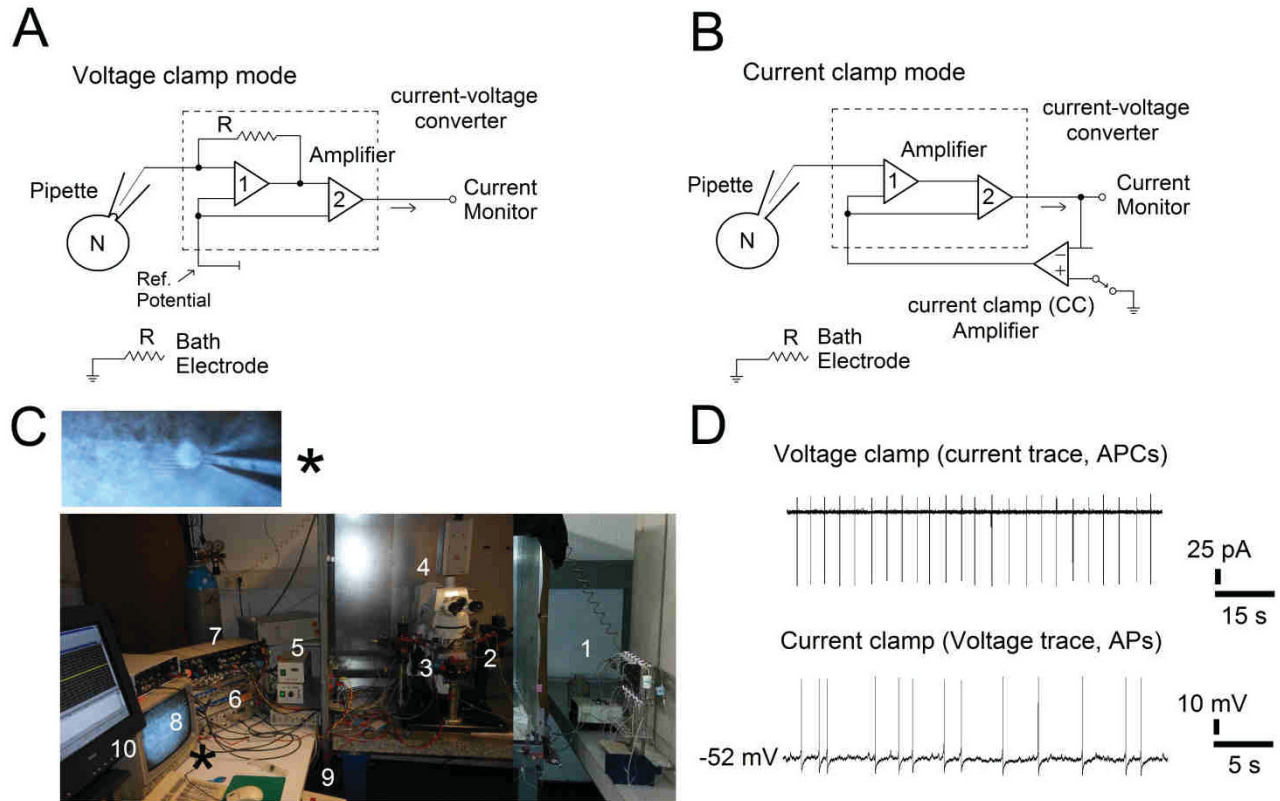
Fig.2-2. Patch clamp modes and equipment.
A. B. Simplified circuits of voltage clamp and current clamp modes. In ideal conditions (without compensation) the electrode resistance is negligible, so recorded potential equals the membrane potential of the cell. N, neuron; R, resistance; Ref., referring; CC, current clamp. **C.** Patch clamp setup and electronic devices: 1) peristaltic pump and drug application apparatus; 2) electro-mechanic arm connected to the manipulator, on which are mounted: pipette, holder and preamplifier; 3) slice chamber and perfusion tubes; 4) infrared-differential interference contrast camera, fluorescent lamp and optical/fluorescent microscope; 5) camera, light and lamp power supplies; 6) amplifier; 7) temperature controller; 8) monitor; 9) manipulator; 10) computer. Voltage or currents recorded are converted to digital signals to be elaborated by PC programs. **D.** Examples of true traces of voltage clamp and current clamp, showing eAPCs and intracellular APs, respectively.

2.4. Electrophysiology on slices and AIN

All animals of both genders were divided in two groups: juvenile (below postnatal day 14) and adult (more than 21 days old). Juvenile neurons are usually more clearly visible in the slices because of incomplete myelination. Moreover, the quality of the juvenile tissue after the incubation is much better compared to adult preparations.

Slices of 200 μm (2 midbrain slices per mouse) or/and 250 μm thickness (2 TMN slices per mouse) were incubated for at least 1 hour at room temperature and than transferred to the recording chamber that was continuously perfused with ACSF in order to start

electrophysiological *ex-vivo* recordings. The speed of perfusion (volumetric) was around 1.7 ml/minute given by a peristaltic pump (Ismatec, Wertheim, Germany) (Fig.2-2C). Every tested drug was applied for 7 minutes at least and compared with the frequency recorded during 7 minutes of control. Antagonists were applied for 14 minutes or for the whole duration of the experiment if it is not mentioned otherwise.

For recordings from AIN drug application was performed by gravity force in vertical tubes. Midbrain neurons of SNc and HA neurons in TMN, were identified at first sight looking at their anatomical locations (for SNc: group of dark neurons above VTA directed to the surface of the midbrain slice; for TMN: posterior hypothalamic neurons in close contact to the brain surface) under an upright fluorescent microscope (Zeiss, Goettingen, Germany) using infrared-differential interference contrast (IR-DIC) (Hamamatsu photonics K.K., Japan); Tmt-HDC and Tmt-DAT neurons were identified by both, IR-DIC and fluorescence (HBO 100, Zeiss, Goettingen, Germany). Pictures of living neurons and slices with visible recording site reported by the electrode pipette, where taken after every recording using an AxioCamMRc camera (Zeiss, Goettingen, Germany) and ZEN 2012 lite software (Zeiss, Oberkochem, Germany) either with natural or fluorescence light if any. Pictures of living AIN were taken with the Q-capture program (Q-imaging, Canada), positioning the pipette with the patched neuron under the objective of a Rolera XR camera (Q-imaging, Canada). Healthy neurons look bright, well defined and with visible borders (Fig.2-3). Only big neurons in the cellular suspension (20 µl, acutely isolated) with processes coming from TMN dissociation were patched for recording. After electrophysiological recording AIN were harvested for single-cell reverse transcriptase-polymerase chain reaction (scRT-PCR) (Fig. 2-3). In some experiments cytoplasm of neurons recorded in slices was harvested to confirm cellular identification.

For cell-attached (extracellular) recordings the patch pipettes were made from 1.5 mm (OD) borosilicate glass (Science Products GmbH, Hofheim, Germany) using micropipette puller (P-87, Sutter Instrument C., Novato, CA, USA). Pipettes were filled with ACSF and carefully inserted into the holder (HekaElectronik, Lambrecht/Pfalz, Germany) in tight contact with the Ag/AgCl wire. The patch pipette resistance (5 MΩ) was measured with the TIDA program (HekaElectronik, Lambrecht/Pfalz, Germany).

In the whole-cell configuration (intracellular recordings) pipettes were filled (to 1/3 of their volume) with intracellular solutions. The resistance for these pipettes was around 4 MΩ (allowing a better recording stability in the whole-cell configuration).
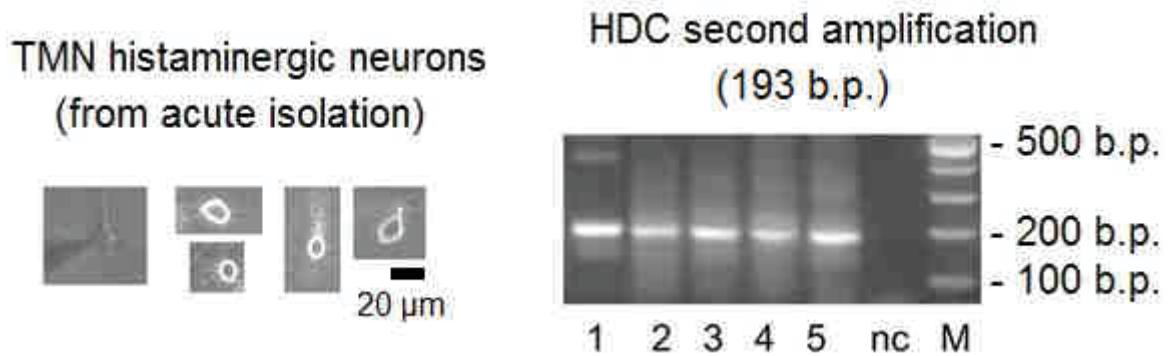
Fig.2-3. scRT-PCR for HA neurons identification.
Pictures of AIN from mouse TMN (left) and PCR products obtained after amplification of complementary deoxyribonucleic acid (cDNA) derived from these cells with primers specific for HDC (right). M: DNA size marker, 100 b.p. (base pairs) ladder, nc: negative control (picture from Olga Sergeeva).

The system (wire + pipette + holder) is connected to the preamplifier (building up the headstage), thus driving the signal to the amplifier (HekaElectronik, Lambrecht/Pfalz, Germany) (Fig.2-2C). At the beginning of the experiment, in order to have a stable wiring connection, chlorations of Ag/AgCl (using FeCl3 solution, Sigma, Steinheim, Germany) wire and ground electrode were properly made.

Using a manipulator (LN, Ratingen, Germany) the headstage was moved (first fastly and then slowly) leading the pipette into the bath upon the slice fixed at the bottom of the chamber with a micro-wired mesh (Fig.2-2C).

In the whole-cell configuration, application of positive pressure (given by a syringe connected with tubes to the holder) is followed (after a perfect seal that increases the electrode resistance) by a strong and fast negative pulse, leading to the membrane rupture. In CC whole-cell recordings after the gigaohm seal was obtained the amplified voltage was zeroed. On the other hand, in VC whole-cell the membrane potential was clamped either to -70 mV (at the Cl- equilibrium potential, for sIPSCs measurements) or -50 mV (typical resting potential of monoaminergic and HA neurons in particular. Indeed neurons with values more depolarized than -42 mV were discarded), before breaking the membrane. After membrane rupture the capacitance was gradually compensated at this stage. Cells were discarded if their capacitance transients changed during recordings by more than 10 %. Values of membrane potential were not corrected for the liquid junction between pipette and the bath solution (2.4 mV, calculated using the built-in software in pClamp9).

An EPC7 patch-clamp amplifier (HekaElectronik, Lambrecht/Pfalz, Germany) and a Digidata 1200 interface board (Axon Instruments, USA) were used for whole-cell VC, CC or

cell-attached VC recordings. For cell-attached VC electrical signals were filtered between 1 and 10 kHz, using low pass and high pass filters, respectively. For whole-cell VC the signals were filtered at 0.1 Hz only by a low pass filter. For whole-cell CC signals were filtered at 2 Hz only by a low pass filter. Every recording was sampled at 20 KHz and analysed with pClamp9 software (Axon Instruments, USA). The frequency of intracellular and eAPC (in bins of 15 s duration) and their shape were analysed with the program Mini analysis 6.0.1. (Synaptosoftinc, Fort Lee, NJ, USA).

2.5. Criteria for midbrain and HA neurons identification

In extracellular firing rate recordings <u>HA neurons</u> were visually identified before recording based on their anatomical location, soma size (18 - 25 μm, or smaller if they were located in the compact TMN cluster; De Luca et al., 2016) and shape (pyramidal-like) or using Tmt-HDC mice (Fig.2-4 left). After establishment of gigaohmic seal with the cellular membrane, spontaneous activity was observed for at least 5 minutes. In cases when a neuron was silent or its firing unstable, recording was interrupted and next neuron was approached. Only neurons with regular and stable firing rate (mainly from 0.3 to 4 Hz) were subjected to the pharmacological treatment. At the end of pharmacological testing the H3R agonist RAMH (2 μM), was applied. Only neurons with significant inhibition of firing (paired t-test with 7 minutes baseline before drug application) were considered for further analysis. Measurements of eAPC duration were done. Reliability of this identification *criterium* was investigated in the present study (see 3. Results).

In whole-cell current clamp recordings <u>HA neurons</u> were approached, recorded and analysis performed if neurons had regular spontaneous firing (at membrane potentials around -50 mV) that was significantly increased by thioperamide (1 μM). *Post-hoc* identification was performed after histamine immunostaining (for biocytin-loaded neurons either in WT, TRPV1 KO or Tmt-HDC mouse (Fig. 2-4A right).

In whole-cell voltage clamp recordings <u>HA neurons</u> were identified through scRT-PCR for HDC expression (Fig.2-3) or through biocytin labelling combined with histamine immunostaining. In majority of slice experiments Tmt-HDC mice were used (Fig.2-4A right). Measurements of HCN-mediated currents were done in some recordings. HCN channels were activated by 9 consecutive 2.5 s pulses increasing incrementally by 10 mV. The HCN-mediated current (or Ih) amplitude was calculated by subtracting the instantaneous current at the beginning of voltage step from the current present at the end of the pulse. If hyperpolarization at the last step (to -140 mV) did not induce a current significantly different

from the instantaneous current at the beginning of the pulse, the neuron was considered Ih–negative. Recorded HCN-mediated current amplitude was 0.3 nA, on average.

In extracellular firing rate recordings <u>DA neurons</u> of SNc were identified by anatomical location, soma size (15-20 μm) and regular firing (typically 1-4 Hz). At the end of pharmacological testing quinpirole (0.05-1 μM) was applied. Only neurons showing significant inhibition of firing by quinpirole were further analysed. Tmt-DAT mice were used in some experiments (Fig.1-3C). In all of Tmt-DAT neurons in SNc quinpirole-mediated inhibition of firing was significant compared to baseline activity.

For the extracellular and intracellular recordings **from** <u>DA neurons</u> of TMN usage of Tmt-DAT mice was necessary (Fig.2-4B).
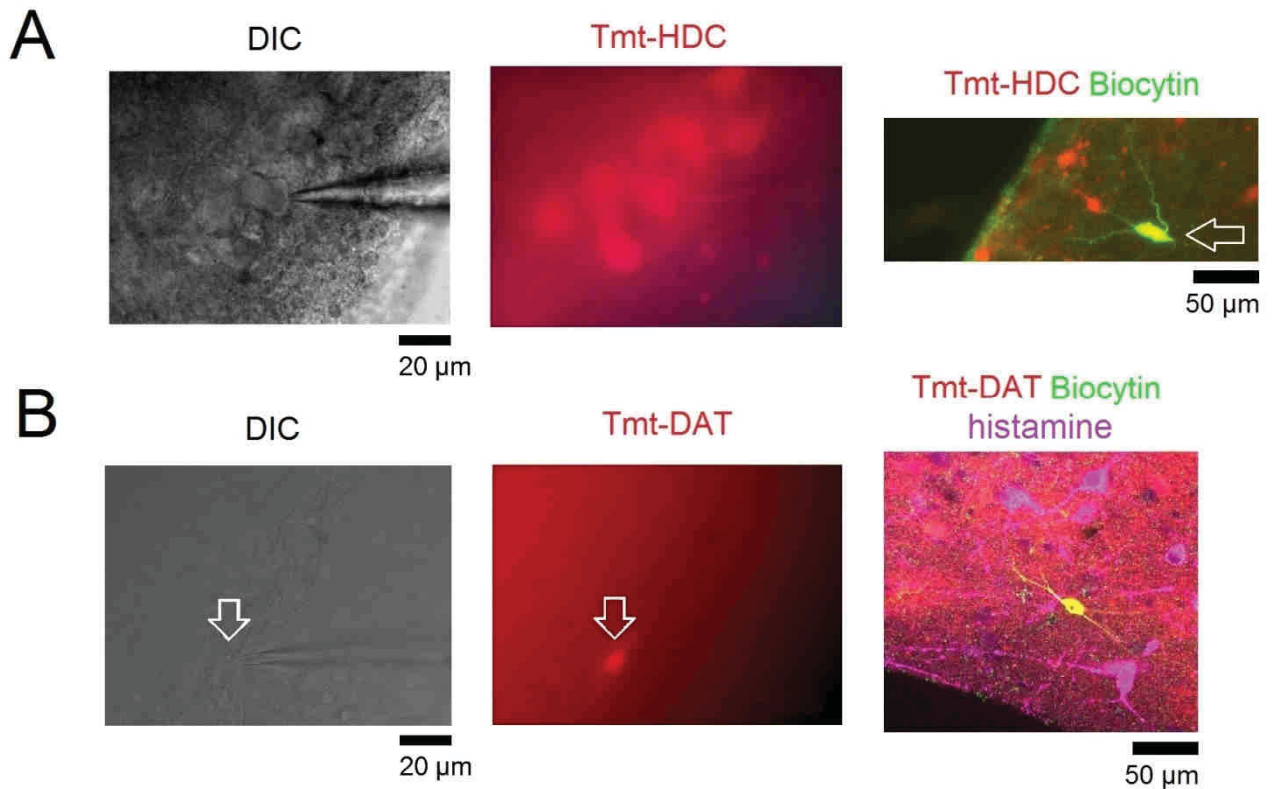
Fig.2-4. Examples of patched monoaminergic neurons in TMN either in cell-attached or in whole-cell configuration in different reporter mouse models.
A. DIC picture of a patched (cell-attached configuration) HA neuron in E2-containing slice (left). The very same neuron was photographed with a fluorescence microscope and found to be Tmt-HDC-positive (in red, middle). Picture of a Tmt-HDC-expressing neuron loaded with biocytin (in green, whole cell-configuration) (right). **B.** DIC picture of a patched (cell-attached configuration, right) monoaminergic neuron (Tmt-DAT-positive, in red) in E2-containing slice (middle). Image of a Tmt-DAT-expressing neuron loaded with biocytin (in green, whole cell-configuration) surrounded by histamine-positive neurons (in pink, left, modified from De Luca et al., 2016).

2.6. Molecular biology

2.6.1. scRT-PCR

The cellular cytoplasm is harvested before or after electrophysiological recording either from slices or AIN (after the seal, a strong negative pressure was applied on the neuron under visual control to be sure that only the cytoplasm was sucked in the pipette containing 7 µl of intracellular recording solution). Electrode content was expelled in a tube containing 3.5 µl of mixture of 3 components of first strand cDNA synthesis kit (GE Healthcare, GB): Bulk mix with reverse transcriptase, DTT (dithyotreitol) and random hexamer primer pdN6 in a ratio of 5:1:1. After all components were added sample was mixed in the vortex (Neolab, Heidelberg, Germany) for 10 s and centrifuged at 14000 rmp (revolutions per minute) for 1 minute using an Eppendorf *minispin* centrifuge and kept for at least 2 hours in the thermoblock (HLC HTM 130, DITABIS Pforzheim, Germany) at 37°C to allow the starting of cDNA production from cellular mRNA. Finally, labelled samples (with a code for every different cell) were stored at -20°C. The PCR reaction amplifies a selected DNA region within the cellular genome or a cDNA library. One pair of primers (short oligonucleotide sequences complementary to the 5′ and 3′ ends of DNA strands) called sense and antisense is designed to amplify the region of interest. PCR steps (cycle) can be divided in 1) denaturation, 2) annealing and 3) elongation. During the denaturation the double-stranded DNA (dsDNA) is separated in single strands (ssDNA) and occurs at 94°C for 48 - 50 s. In the annealing, sense and antisense primers hybridize the complementary DNA regions on the strands, a process done in the present study at 49-60°C for different protocols with step lasting from 48 s to 1 minute. Finally, during elongation primers initiate DNA synthesis starting from the annealing point at 72°C (optimal condition for DNA polymerase) for 90 s. Several cycles (40) are requested to amplify the searched DNA product. In all experimental conditions a two-round strategy was performed (first and second amplification, respectively) for every scRT-PCR protocol (Yanovsky et al., 2012;Kernder et al., 2014;De Luca et al., 2016). Preparation of the PCR reaction was performed under laminar flow (sterile conditions, avoiding any possible DNA contamination), adding at the end neuronal cDNA volume (1 µl) outside of the bench. Thinwalled PCR tubes were prepared containing a mixture of 10X PCR buffer (that provides the optimal chemical environment for activity and stability of the DNA polymerase), 10 pM each of sense and antisense primer (designed with BLAST program, NCBI), 200 µM of each deoxynucleoside triphosphates (dNTP) and 2.5 units Taq polymerase (stable at high temperatures, isolated from *Thermus Aquaticus* bacteria). The final reaction volume was adjusted to 10 µl with nuclease-free water

(Promega, Mannheim, Germany). The magnesium (Mg2+, bivalent cation useful for the optimization of the polymearase) was taken from 1.5 to 3 mM. For the second amplification protocol, 1 µl of the obtained product from first amplification was used as a template. Annealing temperature, primers and magnesium concentration were variable in different reactions. As a rule the annealing temperature was at least 5°C lower than the melting temperature of primers used. The Taq enzyme, PCR buffer, Mg2+ solution, and four dNTPs were all purchased from Qiagen (Erkrath, Germany). All oligonucleotides were synthesized by MWG-Biotech (Ebersberg, Germany). PCR amplifications were performed using a thermal cycler (Mastercycler, Eppendorf, Germany).

The used criteria for primer design were the following: 1) oligo nucleotides sequence lenght (max 25 b.p.); 2) less than 60% of AT/GC content; 3) melting temperature (Tm) above 54°C; 4) melting points among primers used in the first and second amplifications (very similar;) 5) complementarity of regions between primers (close to zero). Primer were designed to span introns on genomic DNA which allows to discriminate between genomic-DNA and cDNA amplicons with respect to their size. In the case of intronless sequences (e.g. CB1R and CB2R) samples were halfed to be processed in parallel: only one half of mRNA-sample was subjected to the reverse transcription (RT+), the other half being "RT-". RT+ samples were positive, RT- were negative in case of CB1R PCR amplification indicating presence of mRNA species encoding for the CB1R in these samples.

Electrophoretic run of PCR products was performed with TAE buffer (for 50X: Tris base 2M (Sigma 7-9), Ethylenediaminetetraacetic acid (EDTA) 0.5 M (Sigma, Steinheim, Germany); glacial acetic acid 1 M (100%, Merck, KgaA, Darmstadt, Germany) and pH 8.0, to dissolve EDTA) at 100 V and 100 mA using a power supply (EPS 301, GE Healthcare, GB). Gels were made of 2% agarose (Sigma, Steinheim, Germany) heated until boiling in TAE buffer afterwards with 0.005% „GelRed Nucleic Acid Gel Stain" (Biotium, Hyward, CA, USA) added. DNA bands were visualised with the help of a bright UV transilluminator (TFX-20M, Thermo Fisher Scientific, USA). Analyzed pictures were aquired with Photodoc-it (UVP, Cambridge, GB). Representative PCR products were sequenced (by BMFZ facility, University of Düsseldorf) on an automatic sequencer (model 377; Applied Biosystems International, Weiterstadt, Germany) to proof the correctness of PCR reactions. Obtained sequences were compared to the known gene sequences listed in the GenBank NCBI. In none of our scRT-PCR experiments genomic-DNA-derived amplicons larger than the cDNA-derived ones were obtained. Amplifications of TRPV1 and neurokinin 1 receptor (NK1R) were conducted also with the help of Anna Kernder.

2.6.2. Real Time RT-PCR (qRT-PCR)

Experiments were conducted by Olga Sergeeva. See (Chepkova et al., 2015) for Materials and Methods. All reactions were normalized on ribosomal protein L13a (RpL13a) expression (that does not change during tissue maturation). Primers are listed in the next paragraph.

2.6.3. List of primers and cDNA products (in alphabetic order)

cDNA name	Forward sequence(s)	Reverse sequence(s)	Product size (b.p.)
CB1R up	5'-GTG GGC AGC CTG TTC CTC A-3'	5'-CAT GCG GGC TTG GTC AGG-3'	401
CBR Deg up	5'-GCC AGC AG(AC) T(GC)G CC(AG) T(GC)G C(GT)G T-3'		
CB2R lo2		5'-TCC ACC CCA TGA GCG GCA GGT A-3' 5'-TCC ACC CCA TGA GCG GCA GGT A-3'	227
HDC	5'- GAT GAT GGA GCC C(A/T)G TGA ATA-3	5'- TCA GAG GTG TAG GCA ACG A-3	193
HDC		5'-GAT GCT GTC CCA GCT GTC G-3'	
NK1	5'- GAT ATG GAT CAT TTT GGC CCA C-3'	5'- GGT AGA ACT CAT GGC CAG CC-3'	124
NK1	5'- GCA AGG TGG TCA AAA TGA TGA T-3'	5'- TGC TGG ATG AAC TTC TTA AGG TAG-3'	
pre-SP	5'- TGA GCA TCT TCT G(T)CA GAG AAT CGC-3'	5'- CAA TGT TTA TTG GCA CAA TAT G-3'	215
pre-SP	5'-GGC TTA TGA AAG AAG CGC A(G)AT G -3'		
TRPV1 (exon 13)	5'-TCA TGG GCG AGA CTG TCA ACA AG-3'	5'-CTG GCT AAA GGG ATC CCG TAT AGT-3'	107 - 111
TRPV1 (exon 13)		5'-TCC TCA TGC ACT TCA GGA A-3'	
TRPV1 (exon 7)	5'-TTG TGG AGG TGG CAG ATA A-3'	5'-AGG GCT CCA CGA GAA GCA T-3'	381 -201

For following primer sequences (published):

- GluN1, GluN2A, GluN2B, GluN2C, L13A (see Kernder et al., 2014)
- DAT, DDC, TH, VMAT2 (see De Luca et al., 2016)

2.7. Primary cultures

Newborn Tmt-HDC and WT mice were anesthetized by ether or isofluoran (Abbott, Wiesbaden, Germany) and killed by a heart cut. Brains were removed and collected as mentioned before (see paragraph: 2.2. Animals and surgery) under sterile conditions (Sergeeva et al., 2005). Forceps and scalpels were autoclaved for the purpose.

Primary dissociated Tmt-HDC-expressing neurons cultures were prepared cutting coronal posterior hypothalamic-containing slices (of variable thickness) in which TMN was carefully isolated. Efforts were made to dissect preferentially the vTMN. Sectioned vTMN was later on incubated in PBS (phosphate-buffered saline), triturated after trypsinization (10 minutes) and washed in nutrient medium (MV10) consisting of: fetal calf serum (10%), minimal essential medium (MEM Eagle, 89 %, Life technologies, Eugene, Oregon, USA), glucose

(0.8 %), glutamine (2 mM, Sigma, Steinheim, Germany), insulin (0.1 U/ml, Life technologies, Eugene, Oregon, USA) and HEPES (10 mM). After mild centrifugation (1000 rpm, 1 minute), the cells were re-suspended in the required volume of the nutrient medium. The same protocol was followed for the preparation of striatal culture, as no clear border between striatum and globus pallidus can be visualized in thick slices (Sergeeva et al., 2007), neurons from both structures were likely cultivated, although efforts were made to dissect preferentially the dorsal part of the striatum. Dissociated vTMN cells were plated with a density of 1 to 2 x 10^5 /cm^2 onto polyethylenimine-coated optical dishes (diameter of 12 mm; three per 35 mm-diameter Petri dish) in a volume of 50-60 μl and cultured in an incubator with 5 % CO_2, 95 % air and 98 % relative humidity, at 37 ± 0.5 °C. On the second day fresh MV10 was added to the final volume of 1 ml. Cultures were grown for at least 6 days before recordings were started. Dissociated striatal cells were plated at the same density as vTMN cells onto polyethylenimine-coated microelectrode arrays (MEAs, Multi Channel Systems, Reutlingen, Germany); in a volume of 60 μl and cultured in an incubator. On the second day serum-free neurobasal medium (NBM) composed of: supplement B-27 (2%, Life technologies, Eugene, Oregon, USA), glutamine (0.5 mM) and Penicilline/Streptomicine (50 U/ml, Life technologies, Eugene, Oregon, USA) was added to the final volume of 1 ml for striatal cultures.

2.8. Microelectrode array (MEA) recordings

Striatal cultures were grown attached to the wired system of MEA biosensors for at least 6 days before MEA recordings were started (Fig.2-5A).

After 4 control recordings, each 2 minutes long, 0.5 μl retrobeads were added to the 1ml of growth medium. Then spontaneous firing of cultured neurons was monitored with interruptions as indicated in the results section for 2 more days (Fig.2-5B). Extracellular potentials were recorded on MEAs with a square grid of 60 planar Ti/TiN-microelectrodes (30 μm diameter, 200 μm spacing, Fig.2-5A, left) at 37°C with the help of a temperature controller. Signals from all 60 electrodes aligned in a 8x8 grid (Fig.2-5A right), were simultaneously sampled at 25 kHz, visualized and stored using the standard software MCRack provided by Multi Channel Systems. Spike detection and analysis was performed offline with the software SpAnNer (RESULT MedizinischeAnalyseverfahren, Tönisvorst, Germany) as previously described (Sergeeva et al., 2007). After recordings MEAs were carefully cleaned and sterilized to be used for new plated cultures. MEA recordings were performed with the help of Prof. Olga Sergeeva.
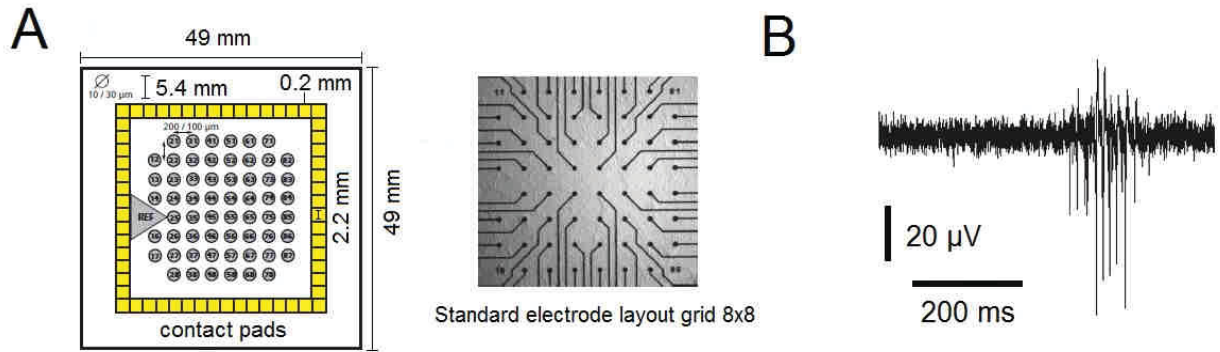
Fig.2-5. Picture of MEAs biosensors (pictures adapted from: MEA Manual Multi Channel Systems).
A. Picture of 60-square MEAs having 60 electrodes of 50 x 50 µm size and inter-electrode distances of 200 µm (left) in an 8x8 layout grid (right). **B.** Example picture of striatal culture firing recorded during control.

2.9. Calcium imaging on TMN primary cultures

Primary dissociated Tmt-HDC culture preparations were incubated with Fluo4 (1:100, diluted in the culture medium, Life technologies, Eugene, Oregon, USA) for 1 hour in the incubator. Cultures were washed three times with HEPES-based solution before starting the imaging recording. Selection of the region of interest (ROI) was taken looking at the co-localization between the calcium dye (488 nm) and Tmt-HDC (530 nm) using a TILLvisION programmed monochromator (T.I.L.L. photonics GmbH, Germany). During imaging recordings perfusion of HEPES-based solution at physiological temperature was performed (a setup composed of drug application system, temperature and peristaltic pump, was used for the purpose. At the end of each experiment KCl 30 mM in modified-HEPES solution (in mM): NaCl 120, KCl 30, $CaCl_2$ 2.0, $MgCl_2$ 2.0, HEPES 10, glucose 20 (pH 7.4) was always applied as positive control for responsiveness and calibration. Drug application was done for 5 minutes taking 300 s as the fixed recording frame. Only neurons responding to KCl 30 mM with an increase of intracellular calcium levels, were taken in account for further analysis.

2.10. Stereotaxic injection of retrobeads in striatum and brainstem

Stereotaxic injections of retrobeads were organized and performed by T. Suvorava and G. Kojda. One or two injections (one on each side) of undiluted Lumafluor IX retrobeads were done in the region containing NTS at coordinates: from -6.72 to –7.32 mm anteroposterior (bregma), 0.25-1.25 mm mediolateral and 4.25-4.6 mm dorsoventral (skull surface). For the Method about injections in striatum see (De Luca et al., 2016).

2.11. Immunohistochemistry (IHC)

Fresh coronal brain slices containing SNc or TMN were fixed in 4% EDC (1-ethyl-3(3-dimethylaminopropyl)-carbodiimide, Sigma) in 0.1M phosphate buffer (PB, pH 7.4) for 6-8 hours and post-fixed for 30 minutes in 4% paraformaldehyde in 0.1 M PB. Finally, the samples were put in 20% sucrose-PBS solution at 4°C (until slices will drop down at the bottom of the glass). Slices were cryosectioned on a Leica cryotom (Wetzlar, Germany) at 25 μm thickness and sections mounted on gelatin-coated slides, dried and stained according to the immunofluorescence staining protocol. For some preparations floating slice were stained without being cryosectioned.Tmt-HDC primary brain cultures were grown on glass coverslips and fixed after 14–21 days *in vitro*.

Slices and cultures were first washed in PBS with 0.8% Triton X-100 (PBS-T) for 5 minutes (3 times) in dishes or multiwell platforms and then incubated overnight at +4°C with the primary antibodies. Neurons recorded in TMNv-containing slices with biocytin (Sigma, 0.1%) were visualized by streptavidin Alexa Fluor 488 conjugate (1:500). After 3 times rinsing with PBS-T, immunoreactivities were visualized following 2 hours of incubation with secondary antibodies conjugated with different flurophores. All secondary antibodies were obtained from Life technologies, Eugene, Oregon, USA. After 3 rinsings with PBS, sections and primary cultures were coverslipped with Aqua Poly Mount (Polysciences, Warrington, England) and kept at +4°C (for few days) or at -20°C (for longer periods). TMN neurons were visualized, photographed and measured (major axis) with the Zeiss laser scanning microscope 510 META (confocal) or/and Axioskop 2 Plus supplied with the AxioCamMRc camera (Zeiss, Goettingen, Germany) and ZEN 2012 lite software (Zeiss, Oberkochem, Germany). The usage of a confocal microscope was helpful either to have an high quality three-dimensional view or to visualize triple fluorescent preparations (3 lasers with excitation wave length (in nm): for red (HENE 1, 543 nm), green (Argon/2, 488 nm) and infrared (HENE2, 633 nm)). The lists of primary and secondary antibodies used are provided in the next paragraphs.

2.11.1. List of primary antibodies (in alphabetic order)

Name	Concentration(s)	Specie	Storage	Firm
Biocytin	0.05%-0.1%	-	-20°C	Sigma, Germany
Anti-D2-type R	1:100	rabbit	-20°C	eBioscience, USA
Anti-histamine	1:1000 (1:1 PBS and glycerol)	rabbit	-20°C	Merck-Millipore, Germany
Anti-MAP-2	1:200 – 1:500	mouse	-20°C	BioTrend, Germany
Anti-NK1R	1:200	goat	+4°C	Santa Cruz, USA
Anti-SP	1:50	goat	+4°C	Santa Cruz, USA
Anti-TH	1:100 – 1:200	chicken	+4°C	Abcam, UK
Anti-TRPV1	1:200 – 1:1000	rabbit	-20°C	Merck-Millipore, Germany

2.11.2. List of secondary antibodies (after primary antibody order; Alexa Fluor AF)

Name	Concentration	Anti-, in Specie	Storage	Firm
Bio StreptavidinAF 488	1:500	biocytin	+4°C	Thermo Fisher Sci.
AF 647 (Cy5)	1:500	rabbit, in goat	+4°C	Thermo Fisher Sci.
AF 488	1:500	rabbit, in donkey	+4°C	Thermo Fisher Sci.
AF 546	1:500	mouse, in goat	+4°C	Thermo Fisher Sci.
AF 488	1:500	mouse, in donkey	+4°C	Thermo Fisher Sci.
AF 594	1:500	mouse, in goat	+4°C	Thermo Fisher Sci.
AF 647 (Cy5)	1:500	goat, in donkey	+4°C	Thermo Fisher Sci.
AF 488	1:500	goat, in donkey	+4°C	Thermo Fisher Sci.

AF 488	1:500	chicken, in goat	+4°C	Thermo Fisher Sci.
AF 594	1:500	chicken, in goat	+4°C	Thermo Fisher Sci.
AF 647 (Cy5)	1:500	chicken, in goat	+4°C	Thermo Fisher Sci.

2.12. List of drugs

Name	Concentration(s)	Solvent	Storage	Firm(s)
AM 251	1 μM	DMSO	+4°C/-20°C	Sigma
AM 630	1 μM	DMSO	+4°C/-20°C	Sigma
capsaicin	100 nM – 1 μM – 10 μM	Ethanol (<0.1%)	-20°C	Sigma
(+)- CP-99994	100 nM & 1 μM	water	+4°C	Sigma
(+)-CP-96345	1 μM	DMSO	room temperature	Sigma
CNQX	20 μM	DMSO	+4°C/-20°C	Abcam, UK
D-AP5	50 μM	water	+4°C/-20°C	Abcam, UK
D-609 (T8543)	30 μM	water	-20°C	Sigma
gabazine	10 μM	water	+4°C/-20°C	Abcam, UK
GR-73632	10 nM & 30 nM	water	+4°C/-20°C	Sigma
histamine	5 nM – 30 μM	water	+4°C/-20°C	Sigma
LY 294002	10 μM	DMSO	+4°C	Sigma
MPEP	10 μM	DMSO	+4°C/-20°C	Sigma
OLDA	200 nM & 2 μM	DMSO	-20°C	Sigma
(-) quinpirole	100 nM - 1μM	water	+4°C/-20°C	Tocris, UK
R-alpha-metyl-histamine	2 μM	water	+4°C/-20°C	Sigma
sDHPG	0.5 μM - 5 μM - 20 μM	water	+4°C/-20°C	Tocris
(+)- Sulpiride	10 μM	DMSO	+4°C/-20°C	Sigma
thapsigargin	1 μM	DMSO	+4°C/-20°C	Sigma
thioperamide	1 μM	water	+4°C/-20°C	Sigma
TTX	1 μM	water	-20°C	Sigma
U 0126	10 μM	DMSO	+4°C/-20°C	Sigma
U 73122	10 μM	DMSO	+4°C	Sigma
URB 597	1 μM	DMSO	+4°C/-20°C	Tocris, UK
WIN 55-212,2	10 nM –1 μM	DMSO	+4°C/-20°C	Tocris, UK

2.13. Statistical analysis

Control period recording and bath application of drugs were performed as previously described (see paragraph: 2.4. Electrophysiology on slices and AIN). Slices were normally hemi-sectioned and only one neuron (with several drug applications) per section was recorded. Only neurons with a stable baseline period were recorded.

All values are reported as means ± s.e.m. Statistical analysis and comparison between 2 groups was done with the non-parametrical Mann-Whitney U test (MWT), unpaired t-test or Wilcoxon test (Statistics Version W 1.54, Oxford, UK). In particular, MWT test was applied to compare for instance mean values of firing frequencies and eAPC durations (first 5 minutes of control recording period, average of 30 to 2292 events) between different neuronal groups (different age, different location).

Comparison between control (baseline) activity and activity after treatment was done with the paired t-test. Occurrence of the effect was compared between groups using the two tailed Fisher´s exact probability test (FEPT). Data analysis and presentation was performed with GraphPad Prism version 5.03 for Windows (GraphPad Software, San Diego, California, USA). A value of $p < 0.05$ was considered statistically significant.

3. Results

3.1. Development of new aminergic neuron identification strategies. Validation of transgenic animal models.

3.1.1. Co-localization of histamine immunoreactivity with Tmt-HDC in TMN

In juvenile mice 98 ± 2% of Tmt-HDC-expressing neurons from vTMN or E2 showed histamine immunoreactivity (4 mice; 472 neurons Tmt-HDC-positive of which 464 were histamine-positive) (Fig.3-1). This strict HA nature of Tmt-HDC neurons was maintained in adult mice (98.4 ± 0.6% of Tmt-HDC neurons contained histamine; 4 mice; 182 Tmt-HDC-positive neurons of which 179 were producing histamine). These findings were similar to previously published observations about E2 in the adult mouse (Yanovsky et al., 2012). Note that the large population of vTMN histamine-immunopositive neurons (25 ± 3 %, data between adult and juvenile were pooled, n=8, p=0.11, MWT) was not Tmt-HDC-positive (neurons in green on Fig.3-1). In mTMN or E4 from the same mice which were used for the E2 immunostainings only 37 ± 4% of juvenile Tmt-HDC-positive neurons were immune-positive for histamine (4 mice; 207 Tmt-HDC-positive neurons, 81 of them histamine-positive), whereas in adults 96 ± 2% of all neurons bearing one or several processes, soma sizes larger than 10 μm and expressing Tmt protein, contained histamine (4 mice, 156 Tmt-HDC-positive neurons from which 150 contained histamine) (Fig.3-1). Therefore, electrophysiological investigations were performed only on adult E4 neurons. Note that the large population of mTMN histamine-immunopositive neurons (27.5 ± 5%, n=4 in juvenile and 51.5 ± 7%, n=4, in adult, p=0.11, MWT) lacked Tmt-HDC expression (neurons in green on Fig.3-1). These experiments revealed that big fraction of HA cells can not be visualized and recorded in living brain slices.
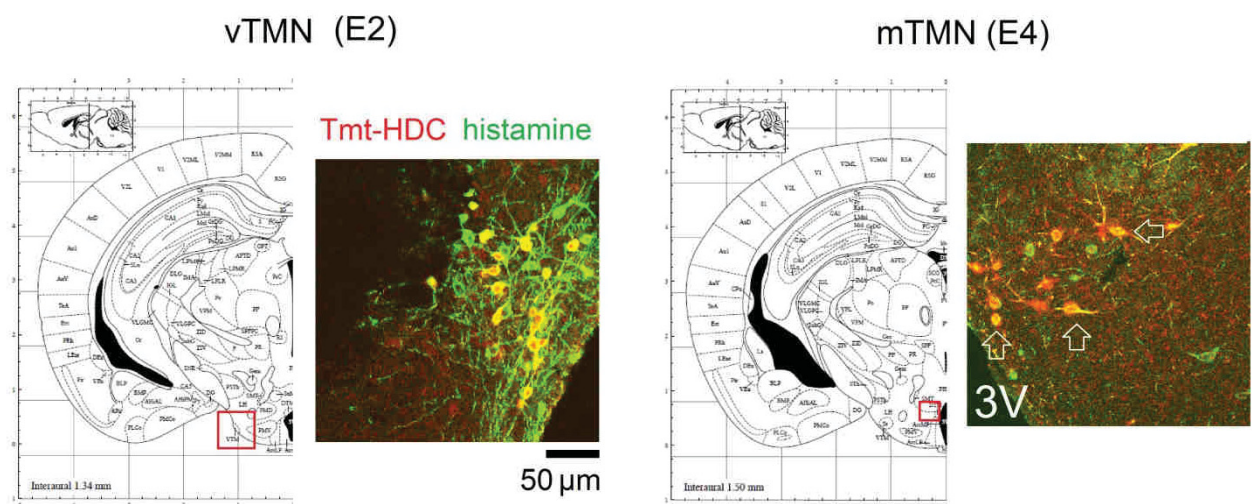
Fig.3-1. Anatomical locations and Tmt-HDC/histamine expression of juvenile/adult vTMN (E2) and adult mTMN (E4).
TMN-containing hemi-sections taken from mouse brain atlas (Franklin and Paxinos, 2008). Co-localization of red fluorescent Tmt-HDC with green-labelled histamine immunoreactivity in juvenile E2 (left) and adult E4 (right). The whole HA population is visible only after histamine staining. Histamine-containing Tmt-HDC neurons of E4 indicated by the arrows near the 3V.

3.1.2. Identification of DAT-positive "conditionally DA" neurons in TMN

The Tmt-DAT mouse line was generated to enable investigations of DA inputs to TMN. A small number of Tmt-DAT positive cells was detected in vTMN (Fig.3-2A). The soma size of these neurons was 11 μm on average. Electrophysiological and pharmacological properties of Tmt-DAT cells of vTMN were analyzed in detail (De Luca et al., 2016). Briefly, spontaneous firing of these neurons was more irregular than firing of HA neurons. AP duration was shorter in these cells than in HA neurons. In contrast to HA neurons which were inhibited by histamine (30 μM) through the H3R, Tmt-DAT neurons were excited (effect abolished in the presence of the H1R antagonist mepyramine). The vast majority of Tmt-DAT neurons was immune-negative for TH, but expressed DDC or/and VMAT2 (scRT-PCR analysis, Fig.3-2B), thus belonging to the "conditionally DA" neurons of the posterior hypothalamus.

Fig.3-2. Morphological and molecular characterisation of aminergic neurons of the vTMN.
A. Coexistence of neurons expressing red fluorescent Tmt-DAT with HA neurons in green. Note non-overlapping fluorescences. TH immunoreactivity is visualized with cy5 (in pink). Open arrows point to two TH-and Tmt-DAT-positive neurons located in premamillary nucleus ventralis (PMV). Thin orange arrows point to TH-positive axons located in vTMN. **B**. scRT-PCR analysis of TH, VMAT2 and DDC expression done in 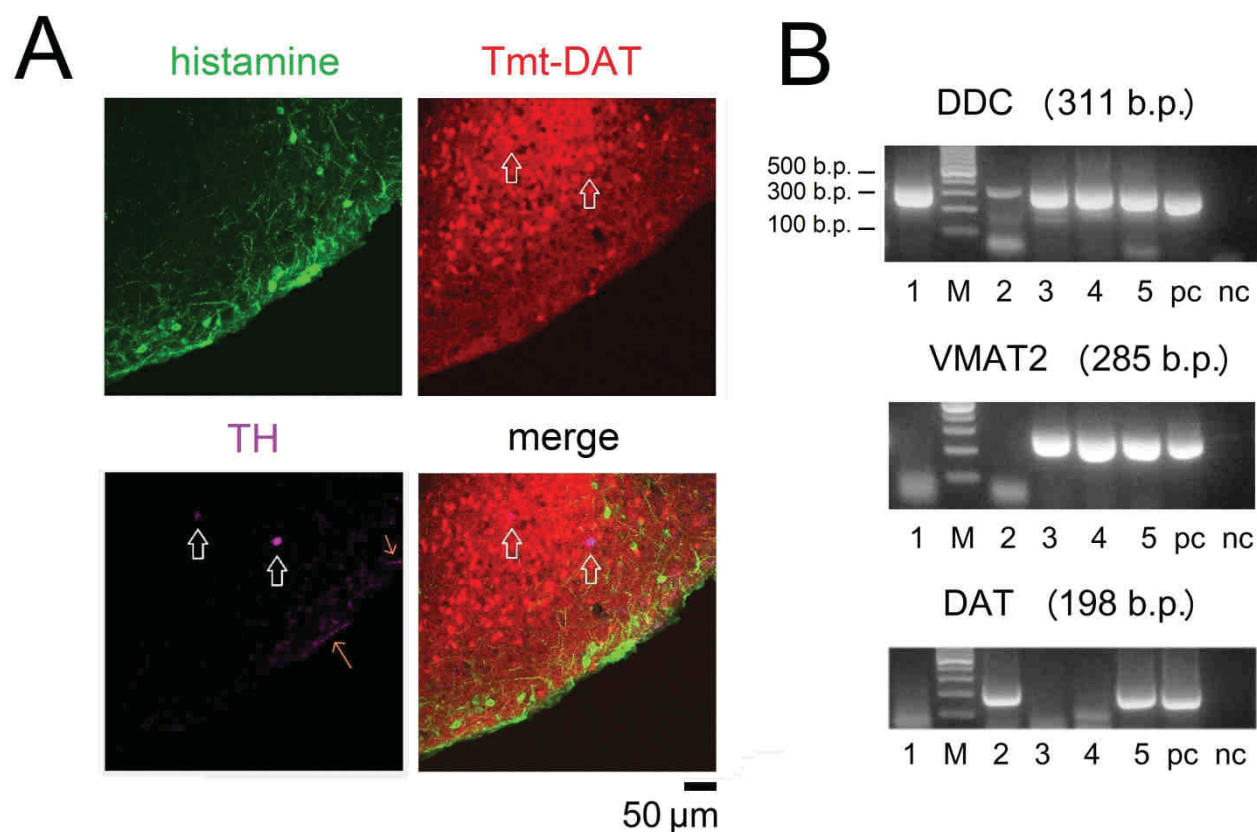5 Tmt-DAT neurons harvested from vTMN (data from Olga Sergeeva and Roberto De Luca). Modified from (De Luca et al., 2016). Pc: positive control (whole TMN).

3.1.3. Co-localization of TH immunoreactivity with Tmt-DAT in SNc

Tmt-DAT+/TH+ neurons in adult and juvenile SNc (data were pooled as no significant difference was found between ages) represented $83 \pm 4\%$ of the total number of Tmt-DAT positive cells (7 mice, 272 neurons, 1 section per mouse was analyzed) (Fig.3-3).
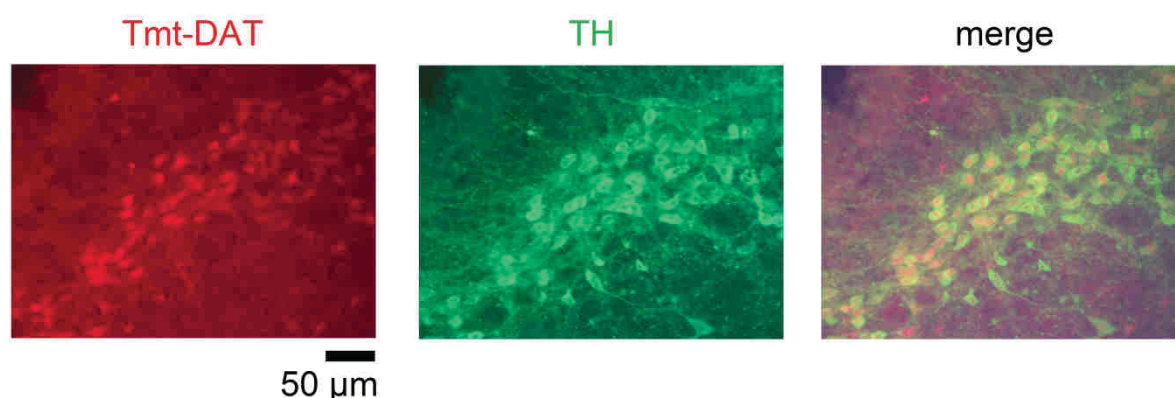
Fig.3-3. Co-localization of TH immunoreactivity with Tmt-DAT in SNc.

3.1.4. Electrophysiological properties of HA neurons of TMN.

3.1.4.1. AP duration

As previous studies reported that aminergic neurons have action potential durations longer than 1.5 ms compared to the other cell types in SNc and TMN (Ungless et al., 2004; Takahashi et al., 2006; Grace and Bunney, 1983) (Fig.3-4A), comparative measurements of eAPC and intracellular AP duration were done. In order to select the right paradigm for estimation of the eAPC duration sequential recordings from E2 neurons first extracellular (cell-attached mode, holding potential 0 mV) followed by the whole-cell configuration (CC mode) on the same neurons were performed. Juvenile E2 neurons were used for this purpose. Superimposed AP and eAPC from one such experiment is shown in Fig.3-4B. Previous studies performed *in vivo* suggested different paradigms for the estimation of AP duration (Ungless et al., 2004; Grace and Bunney, 1983). Time from start to peak of the AP

corresponded to the time from start to the first zero crossing of the eAPC (2.7 ± 0.24 ms vs 3.1 ± 0.9 ms, respectively, p=0.42, MWT; 6 neurons) and the time from the start to the negative trough of eAPC (6.6 ± 0.9 ms) corresponded well to the AP duration measured at its half amplitude (5.7 ± 0.7 ms, MWT p=0.29). This latter measure was previously found to be the most reliable *criterium* for *in vivo* identification of extracellularly recorded DA neurons (Ungless et al., 2004) and is provided further for different neuronal groups. Moreover *in vivo* recordings from mouse TMN neurons (Takahashi et al., 2006) showed a clear-cut difference only for this parameter between HA (average 1.52 ms) and non-HA neurons (average 0.94 ms) of TMN. Using Tmt-HDC mice we determined lower threshould for eAPC duration as 1.52 ms for the identification of HA neurons in slices at room temperature. Note that at 33°C AP duration is shorter (Fig.3-4C), which explains the difference with values provided in Takahashi et al., (2006) study.

Fig.3-4. AP duration: intracellular and extracellular recording.
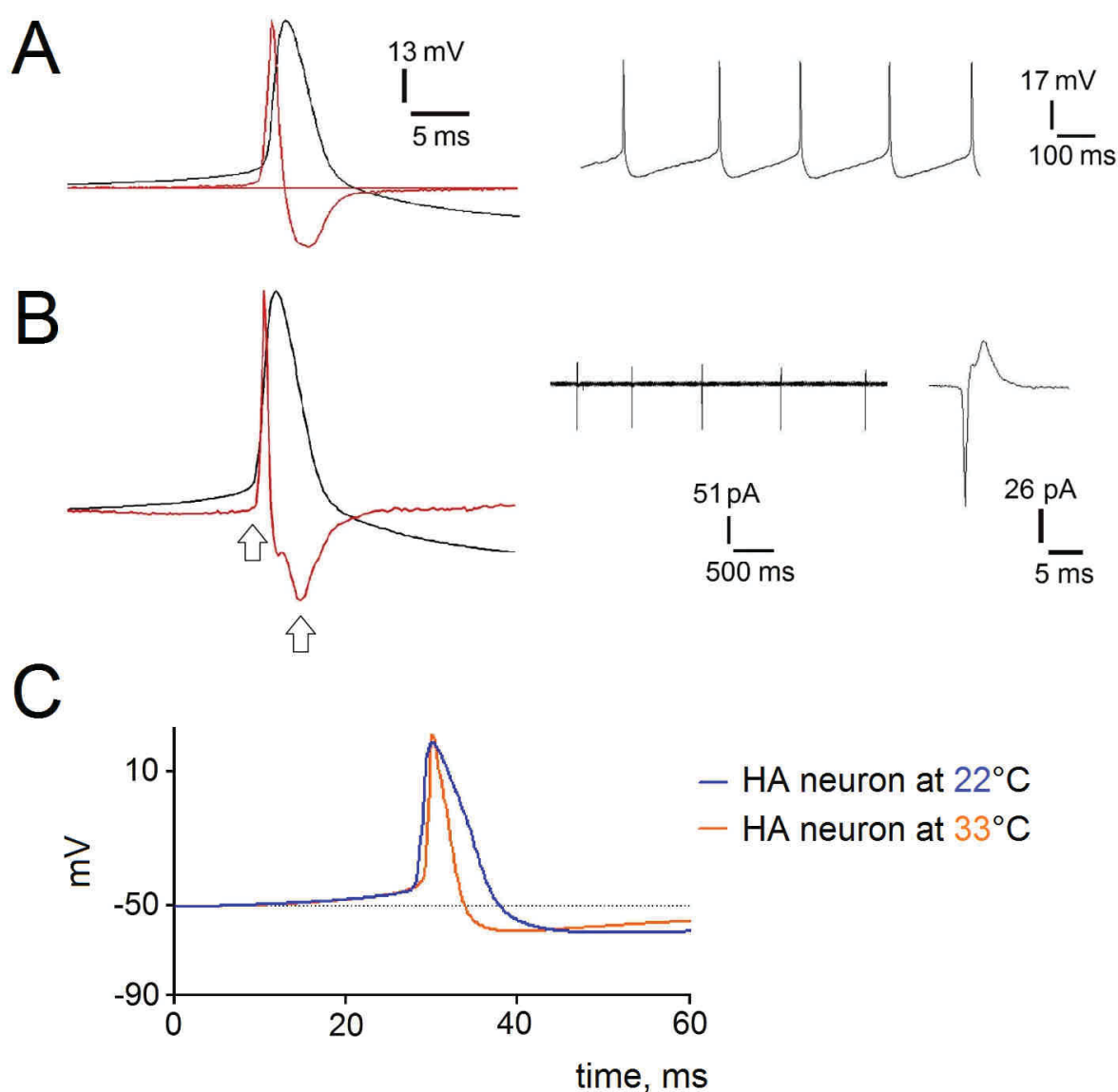**A.** Averaged AP (in black) recorded from vTMN neuron in whole-cell CC mode and its first differential (in red). At the right individual APs recorded from the same neuron. **B.** eAPC normalized to the first peak and inverted in polarity (average of 25 individual traces) laid over and scaled to the intracellularly recorded AP (in black) peak. The eAPC shows close similarity to the first differential of the intracellularly recorded APs. Two arrows mark action potential width: from the start of action potential to the negative trough. Recording trace at the right shows firing in cell attached (loose patch) voltage clamp (Vh=0 mV) mode obtained from the same neuron as in A; averaged eAPC is shown next to it. **C.** Representative averaged action potentials recorded at indicated temperature. Panel C modified from De Luca et al., (2016).

3.1.4.2. Comparison between E2 and E4 subdivisions of mouse TMN

Electrophysiological properties such as the Ih (HCN-mediated) current, firing frequency, input resistance and extracellularly measured eAPC duration of adult E4 neurons located around the 3V were compared with the respective values in adult/or juvenile E2 neurons (Fig.3-5A and B). In 70% (7 out of 10) of E4 Tmt-positive neurons HCN currents showed amplitudes of 0.26 ± 0.5 nA. There was no difference in occurrence (p=1, FEPT) but HCN current amplitude was significantly different (p=0.003, MWT) compared to the adult E2 HA neurons: 17 out of 23 (74%) showed HCN currents of 0.15 ± 0.08 nA amplitude (Fig.3-5C). No difference was detected in terms of input resistance (Rm) (p=0.74, MWT): 171.8 ± 27.5 MΩ (n=23) and 182.3 ± 61.4 MΩ (n=10), for E2 and E4 HA neurons, respectively. Firing frequency of adult E4 neurons did not differ significantly from E2 neurons and represented 1.16 ± 0.42 Hz (n=10) vs 1.13 ± 0.3 Hz (n=22), respectively. Adult E4 neurons were characterized by an eAPC duration of 4.6 ± 0.4 ms (n=10), which was not different from the identified adult E2 neurons (4.5 ± 0.3 ms, n=22). The longer duration of eAPC in comparison to the study by Takahashi et al., (2006) is due to the room temperature (25°C) in our *ex-vivo* recordings. Taken together these data show that adult E4 do not differ from adult or juvenile E2 HA neurons except for HCN current amplitude, even though this characteristic does not reflect a visible difference between E2 and E4 in terms of firing properties.
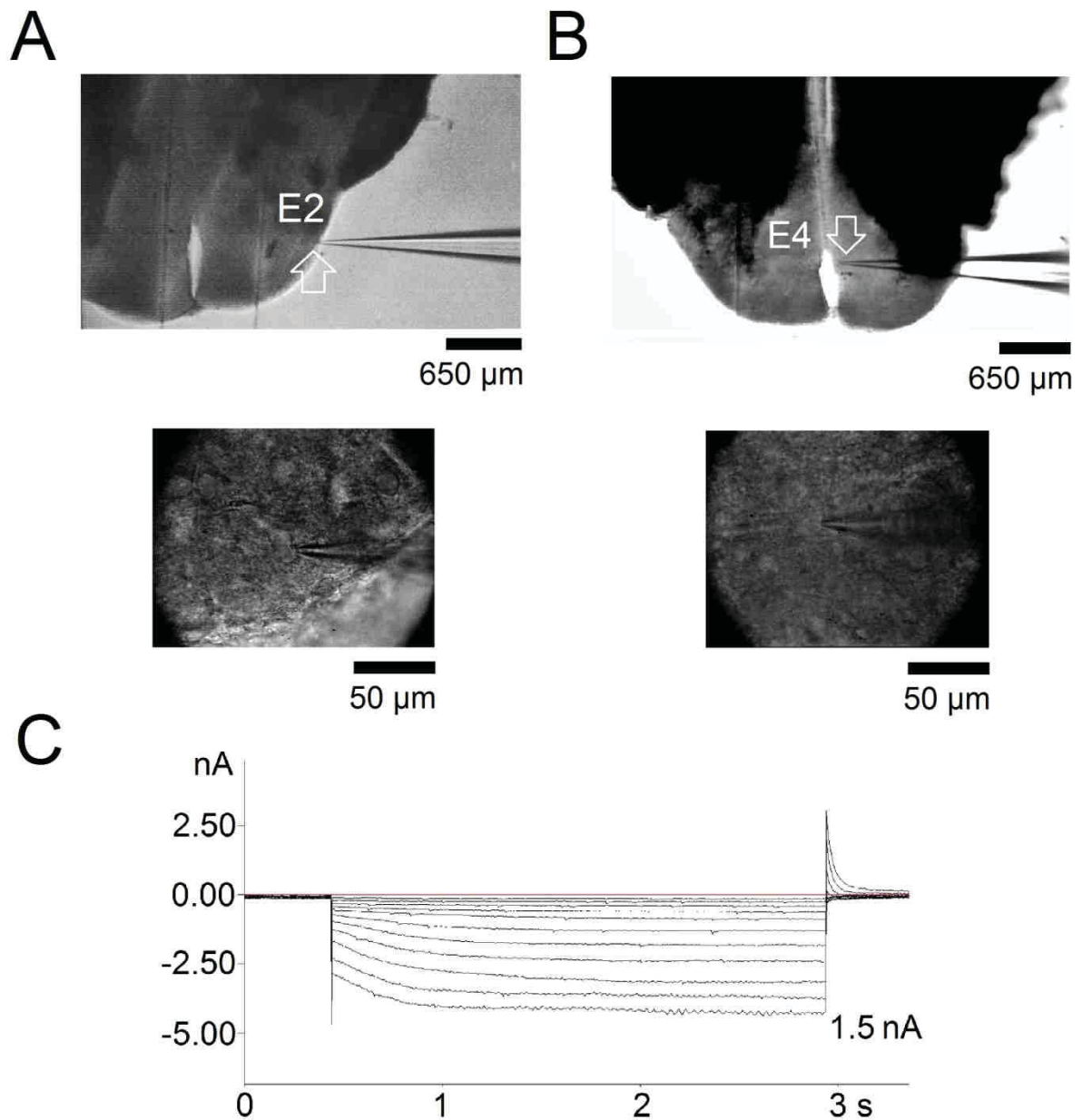
Fig.3-5. E2 and E4 HA neurons recording sites and HCN-mediated current.
A. B. DIC microscopy picture shows location of E2 and E4 recording site with respective patched neurons below. **C.** Representative HCN-mediated current activated by 9 consecutive 2.5 s pulses increasing incrementally by 10 mV on HA neurons.

3.1.4.3. Electrophysiological properties of TRPV1 KO and WT HA neurons

Firing frequency of TRPV1 KO neurons (1.03 ± 0.14 Hz, n=26) was not significantly different from "WT" neurons (1.6 ± 0.25 Hz, n=51). The same eAPC duration (5.4 ± 0.6 ms vs 6.0 ± 0.25 ms) was measured from "WT" and TRPV1 KO neurons, respectively. TRPV1 KO neurons recorded in CC experiments showed similar membrane potentials (between -45 and -52 mV) and similar action potential duration measured at half-amplitude: 5.12 ± 1.2 ms (n=5) (difference from WT neurons is not significant: p=0.65, MWT).

3.1.5. Pharmacological identification of HA neurons through auto-inhibitory H3R activation.

3.1.5.1. Recordings from HA neurons projecting to the striatum

Microdialysis studies have shown no histamine release in the striatum after the injection of H3R antagonist in TMN (Giannoni et al., 2009;Giannoni et al., 2010), suggesting low or no expression of H3R in these neurons. Indeed, application of RAMH (after 7 minutes of control period) reduces firing either in randomly recorded E2 HA neurons or in those retrogradely traced from striatum, without significant differences in the amount of inhibition (De Luca et al., 2016) (Fig.3-6).
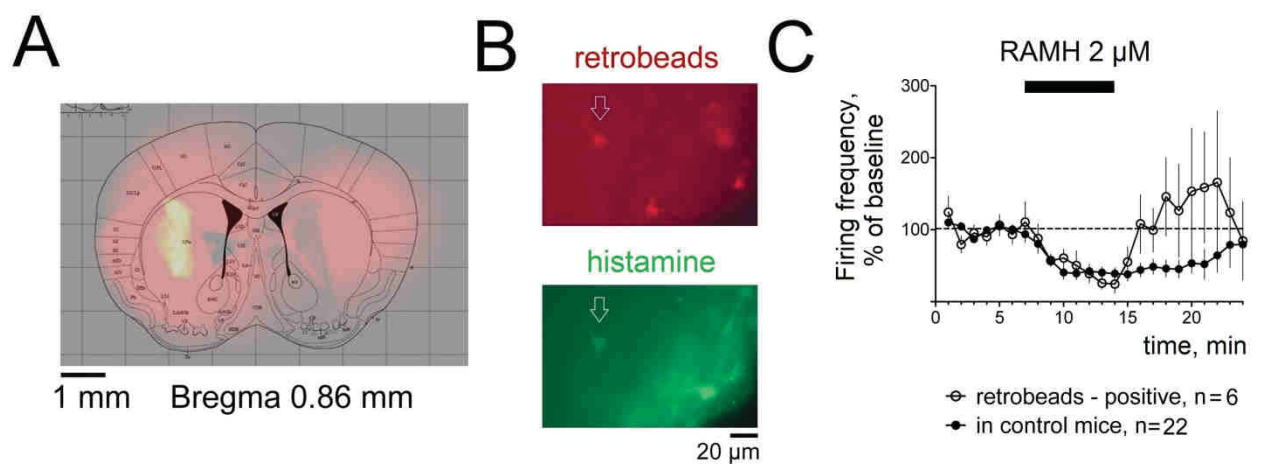
Fig.3-6. Functional expression of H3R in hypothalamo-striatal projections of vTMN.
A. Coronal brain slice from a mouse injected with red fluorescent retrobeads overlaid with the map from a mouse brain atlas (Franklin and Paxinos, 2008) corresponding to the injection site (picture made with the help of Tatsiana Suvorava). **B.** Coronal brain slice containing TMNv. Location of recorded HA neuron is indicated with arrow. Neuron is identified *post-hoc* by green histamine-immunoreactivity. **C.** Averaged time course diagrams plotted for the neurons projecting to the striatum (open circles) or for the neurons with unknown projections recorded in control mice (closed circles). No difference between individual data points was detected with the unpaired t-test. Modified from (De Luca et al., 2016).

3.1.5.2. Calcium and depolarization affect H3R-mediated auto-inhibition

It was already reported that in the presence of zero or low extracellular calcium, release of endogenous histamine and potency of H3R-ligands (in other systems) were strongly reduced (Arrang et al., 1985). Therefore, the effect of extracellular calcium on H3R-mediated inhibition of HA neuron firing was investigated. Several sub-maximal concentrations of histamine were applied either in normal ACSF or in calcium-free solution on WT HA

neurons and Tmt-HDC-expressing neurons with maximal inhibition of firing (>50%, recorded in loose patch) in order to determine the IC50 of histamine (see next paragraph).

The reduction of histamine potency in calcium-free solution could be explained by a strong patho-physiological change (likely a damage) of exposed HA neurons.

For these reasons, effect of calcium-free solution was also tested in CC to investigate the response (shifting) of membrane potential of HA neurons under this condition.

In CC recordings bath perfusion of calcium-free solution for 7 minutes induced a transient increase of firing frequency in HA neurons (from 1.8 ± 0.2 Hz during control to 2.6 ± 0.4 Hz), followed by a dramatic drop (to 0.7 ± 0.2 Hz; n=7). Increase of firing was accompanied by a significant depolarization (in 9 out of 10 neurons, $p<0.05$, paired t-test) with a shift from the resting membrane potential (-55.1 ± 0.2 mV) to more depolarized values of -48.3 ± 0.5 mV (data not shown). For the comparison with baseline (paired t-test) the last 3 minutes of the calcium-free perfusion period were considered (De Luca et al., 2016).

In normal ACSF solution, CC experiments showed that histamine (25-250 nM) induced a significant reduction of firing frequency in 6 out of 9 neurons (from 0.3 ± 0.01 Hz in control to 0.15 ± 0.02 Hz, during 7 minutes presence of HA). The membrane potential of responding neurons was maintained at around -51.6 ± 1.9 mV (n=6). After the washout period the neurons were depolarized by 5-7 mV with positive current injection and HA was reapplied (Fig.3-7B). During baseline recording the membrane potential was -45.9 ± 3.9 mV and -48.7 ± 6 mV in the presence of HA (the difference between these two periods was not significant, paired t-test). The amount of auto-inhibition was dramatically reduced: firing frequency in control was 1.3 ± 0.1 Hz and in the presence of HA 1.5 ± 0.1 Hz.

Thus nominal zero extracellular calcium level caused depolarization of HA neurons by ca 7 mV and was accompanied by the reduction in potency of histamine to produce auto-inhibition of spontaneous firing.

Other possible mechanisms affecting H3R functionality were additionally investigated such as: extracellular GABAergic contribution and intracellular calcium levels.

Histamine release induced by optogenetic stimulation suppressed GABAergic input to TMN via presynaptic H3 heteroreceptors on not-HA neurons, suggesting a minor role of H3 autoreceptors for HA neurons inhibition (Williams et al., 2014).

On the other hand application of gabazine (GABA$_A$R antagonist) did not affect the exogenous HA-mediated inhibition through H3R (De Luca et al., 2016) in calcium-free condition, in which the content of endogenous HA release is reduced in regard to normal ACSF (Arrang et al., 1985).

As H3Rs may stimulate release of calcium from intracellular stores (Bongers et al., 2007), thapsigargin (a non-competitive inhibitor of sarco/endoplasmatic reticulum calcium ATPase, also called SERCA pump) was used to block accumulation of calcium in intracellular compartments (thus resulting in the increase of cytosolic calcium, a process enhanced in calcium-free condition) prior to the application of histamine. In the presence of thapsigargin autoinhibition by histamine 250 nM was significantly reduced (data not shown) (De Luca et al., 2016).

Taken together these data show that H3R-mediated inhibition is affected (reduced) by prolonged depolarization accompanied by an increase of intracellular calcium, a process that was also induced through strong TRPV1-activation by capsaicin (further described).

3.1.5.3. HA neurons from WT and TRPV1 KO mice show no difference in H3R-mediated auto-inhibition

Dose-response curve for the inhbition of firing by histamine was done in WT neurons of vTMN in ACSF and in calcium-free ACSF (De Luca et al., 2016) (Fig.3-7A left). Histamine potencies (IC50) yielded 0.1 ± 0.03 μM vs 3.4 ± 0.6 μM respectively. Action of histamine was abolished in the presence of thioperamide, thus indicating a specific involvement of H3R either in calcium-free or in normal ACSF (De Luca et al., 2016).

Similar protocols were applied to TRPV1 KO neurons recorded in calcium-free ACSF, as no endogeneous histamine release occurs under this condition. Histamine IC50 (3.4 ± 1.3 μM) was not different from WT measurements (Fig.3-7A right).
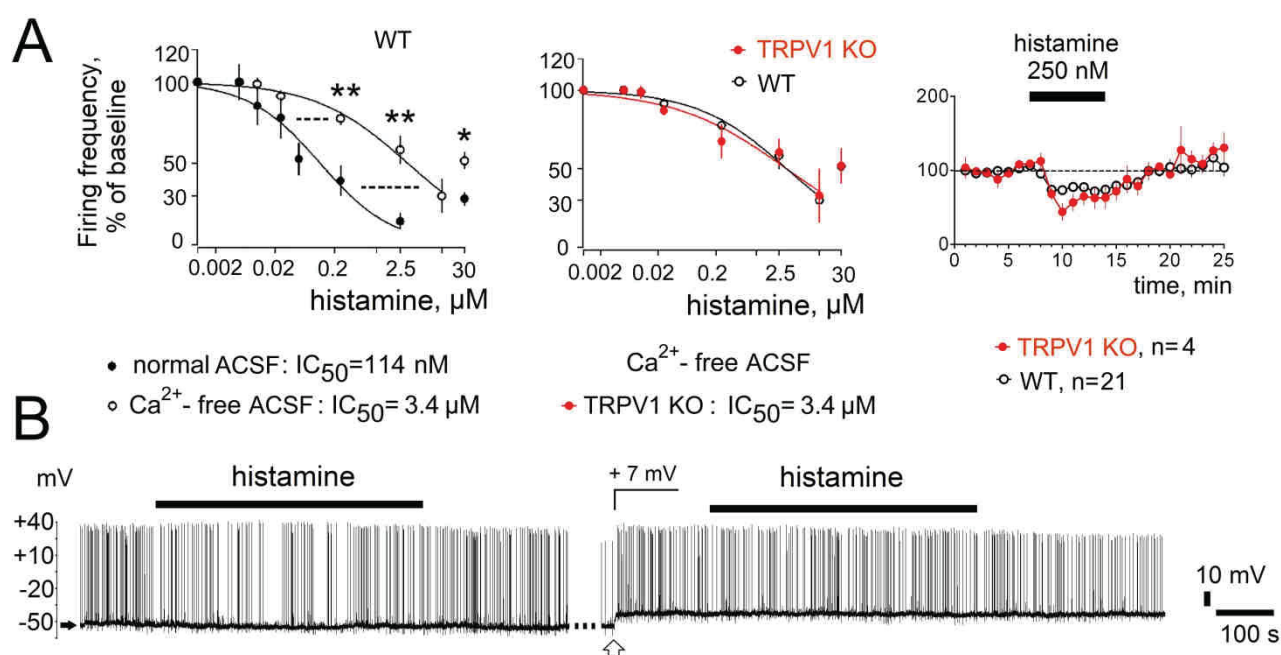
Fig.3-7. HA neurons auto-inhibition is reduced by zero extracellular calcium levels and prolonged depolarization.
A. Left: dose-response relation for the inhibition of firing in control and calcium-free condition obtained from WT neurons (% of baseline, average of 7 minutes of histamine application, 4 to 21 neurons;* p<0.05; ** p<0.01, MWT). Middle: Histamine dose-response curves for the TRPV1 KO and WT neurons. Right: Averaged time course diagrams of histamine 250 nM responses as used for the construction of dose-response plots. Modified from De Luca et al. (2016). **B.** Example of CC recording showing inhibition of firing by histamine (at different concentrations) at resting membrane potential and under enforced depolarization (+7 mV on average).

3.1.6. Identification of DA neurons in SNc of TRPV1 KO and WT mice

Firing frequencies of DA neurons of SNc, identified by the response to quinpirole, were comparable between genotypes and represented 1.7 ± 0.3 Hz (n=8, WT) and 2.4 ± 0.3 (TRPV1 KO, n=13, MWT p=0.11), eAPC durations were similar: 3.9 ± 0.4 ms and 3.4 ± 0.4 ms, respectively. Magnitude of quinpirole (0.1 - 1 µM) inhibition of firing was similar between these two groups (to $57 \pm 12\%$ of baseline in WT and to $58 \pm 9\%$ in KO, average of first 7 minutes of washout). Experiments where sulpiride co-application with OLDA was performed following testing with quinpirole demonstrated irreversible block of D2-type R. In these experiments cytoplasm of recorded DA neurons was sucked into the electrode and scRT-PCR for TH was performed (Fig.3-8). If no significant inhibition of firing by quinpirole was seen but TH expression was detected the cell was considered DA and was used for the analysis.
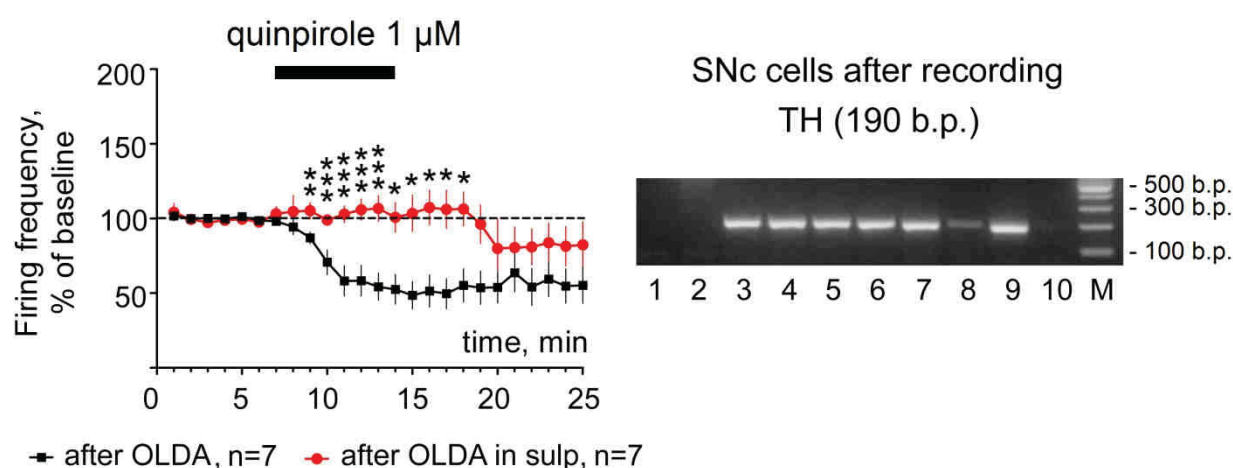
Fig.3-8. Identification of DA neurons of SNc in Tmt-DAT, TRPV1 KO and WT mice.

A. Comparison of quinpiriole responses in naïve and sulpiride-pretreated DA neurons (left) (* p<0.05; ** p<0.01; *** p<0.005, MWT). scRT-PCR shows TH expression in 5 DA neurons exposed to sulpiride (sulp) (D2/3R antagonist) (right).

3.2. Identification of OLDA targets in selected subgroups of aminergic neurons controlling wakefulness

Since TRPV1 is a temperature-sensitive channel above 25°C, capsaicin and OLDA-mediated responses were studied at room temperature if not mentioned otherwise.

The second aim of the present study was to compare effects of OLDA on spontaneous firing of aminergic neurons in wild type and TRPV1 KO mice. For this purpose neurons in the most compact ventrolateral part (E2) of TMN were visually selected with the help of DIC microscopy.

3.2.1. Effect of OLDA and capsaicin on firing frequency of DA neurons in the SNc

OLDA (0.2 or 2 µM) enhanced firing frequency of 4 SNc neurons to $113 \pm 7\%$ of control (average of 6 last minutes of the recording period shown in Fig.3-9). Quinpirole applied at the end of OLDA recordings inhibited (in a reversible manner) spontaneous firing of investigated cells to $30 \pm 11\%$, supporting anatomical identification of visually selected cells (Fig.3-9 A).

Previous studies reported an impact of TRPV1 activation on presynaptic glutamate release in SNc (Marinelli et al., 2003, 2005, 2007). However, whether and how capsaicin affects the firing frequency of DA neurons was not investigated. Capsaicin significantly increased firing in 3 neurons and did not affect it in one neuron tested. Capsaicin slightly increased firing frequency in 3 out of 4 tested neurons ($110 \pm 7\%$ of baseline, 7 minutes during washout period). The effect of OLDA was similar in time course and magnitude to the effect of capsaicin (Fig.3-9B).
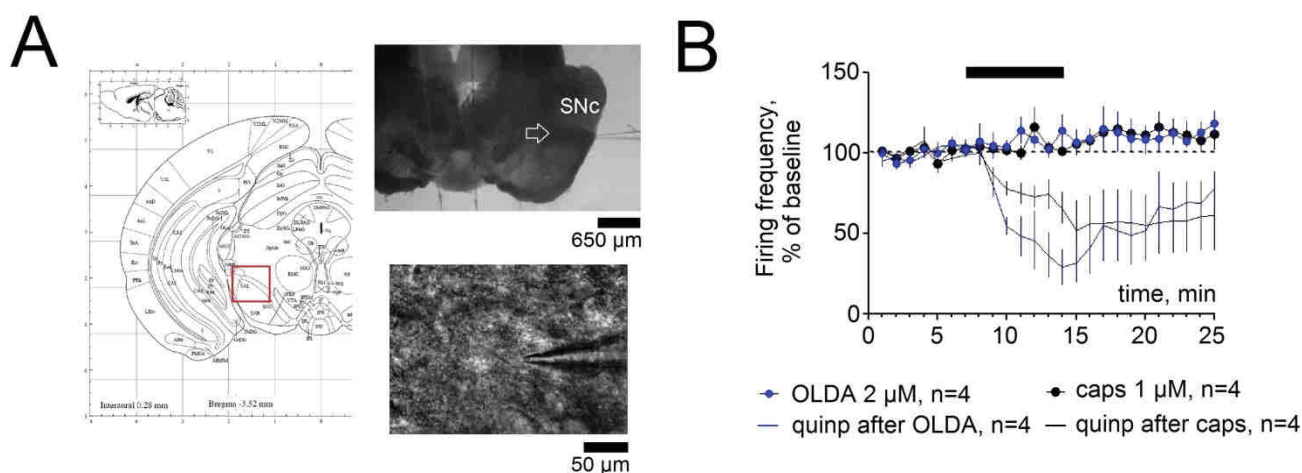
Fig.3-9. Anatomical location of SNc DA neurons.
A. Red frame in picture from mouse brain atlas (Franklin and Paxinos, 2008) indicates area visually inspected with DIC microscopy. Slice and recorded neuron were photographed, an example is shown next to the diagram. **B.** Normalized firing frequencies of DA neurons exposed either to OLDA or capsaicin (caps). All neurons responded to quinpirole (quinp) applied at the end of experiment.

As TRPV1 is considered to be the major target of OLDA we applied OLDA to SNc neurons from TRPV1 KO mice. OLDA slightly but significantly inhibited firing frequencies (to $90 \pm 4\%$ of control in the last 6 minutes of recording period) in all 8 investigated neurons (Fig.3-10). Difference from WT neurons, where only excitation by OLDA was seen, is highly significant (p=0.008, MWT).

An excitatory action of CBRs (especially CB1R) on DA neurons in SNc was reported recently (Marinelli et al., 2007). Application of WIN 55-212,2 (10 nM or 1 µM), non-selective agonist of CB1 and CB2 receptors, increased firing frequency of SNc DA neurons to $120 \pm 9\%$ of baseline (n=7, 7 minutes of washout period). Due to the big variations no difference was seen between responses to 10 nM and 1 µM of WIN 55-212,2.

In the presence of the D2-type R antagonist sulpiride 10 µM inhibition by OLDA was reversed to excitation. Next we applied OLDA to TRPV1 KO SNc DA neurons in the presence of sulpiride and CB1R antagonist AM251 (1 µM). A small residual excitation by OLDA was still seen in these experiments. Finally, combined application of CB1R and CB2R antagonists AM251 and AM630 together with sulpiride, abolished OLDA-mediated excitation (Fig.3-10).
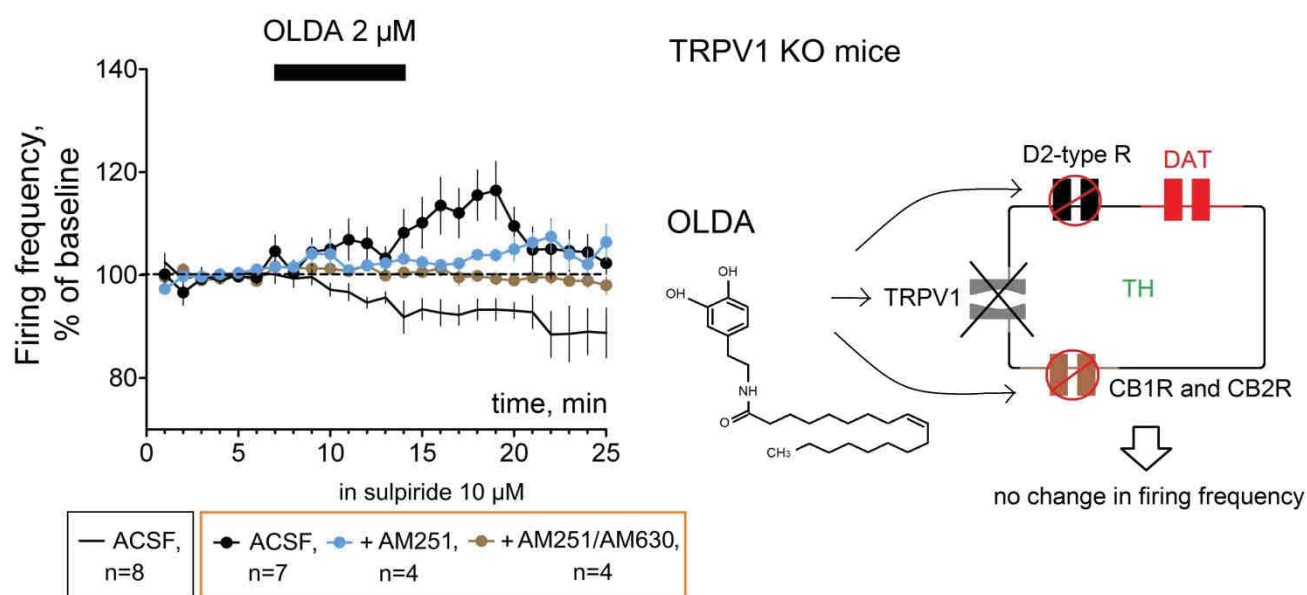
Fig.3-10. OLDA inhibition of DA neuron firing is reversed to excitation in the presence of sulpiride 10 µM, a D2-type R antagonist.
This excitation is explained through the recruitment of CB1R (antagonized by AM251, 1 µM) and CB2R (antagonized by AM630, 1 µM).

Previous studies described and clarified mechanisms of activation of cannabinoid and TRPV1 receptors and functional consequences of their activation for the physiology of midbrain DA neurons (Marinelli et al., 2003, 2005, 2007). Therefore expression of these receptors and their functional mechanisms are not addressed in the present study.

As OLDA effect through the D2-type receptors determined response in TRPV1 KO but not WT mice, D2-type receptors expression was investigated with IHC between these two genotypes. Majority of TH-positive neurons of SNc were D2-type receptor positive in TRPV1 KO (88 ± 4%, 5 mice, 229 neurons on total) and in WT (86 ± 4%, 5 mice, 213 neurons on total). No difference was detected for D2-type receptor expression between these two genotypes (p=0.67, FEPT) (Fig.3-11).
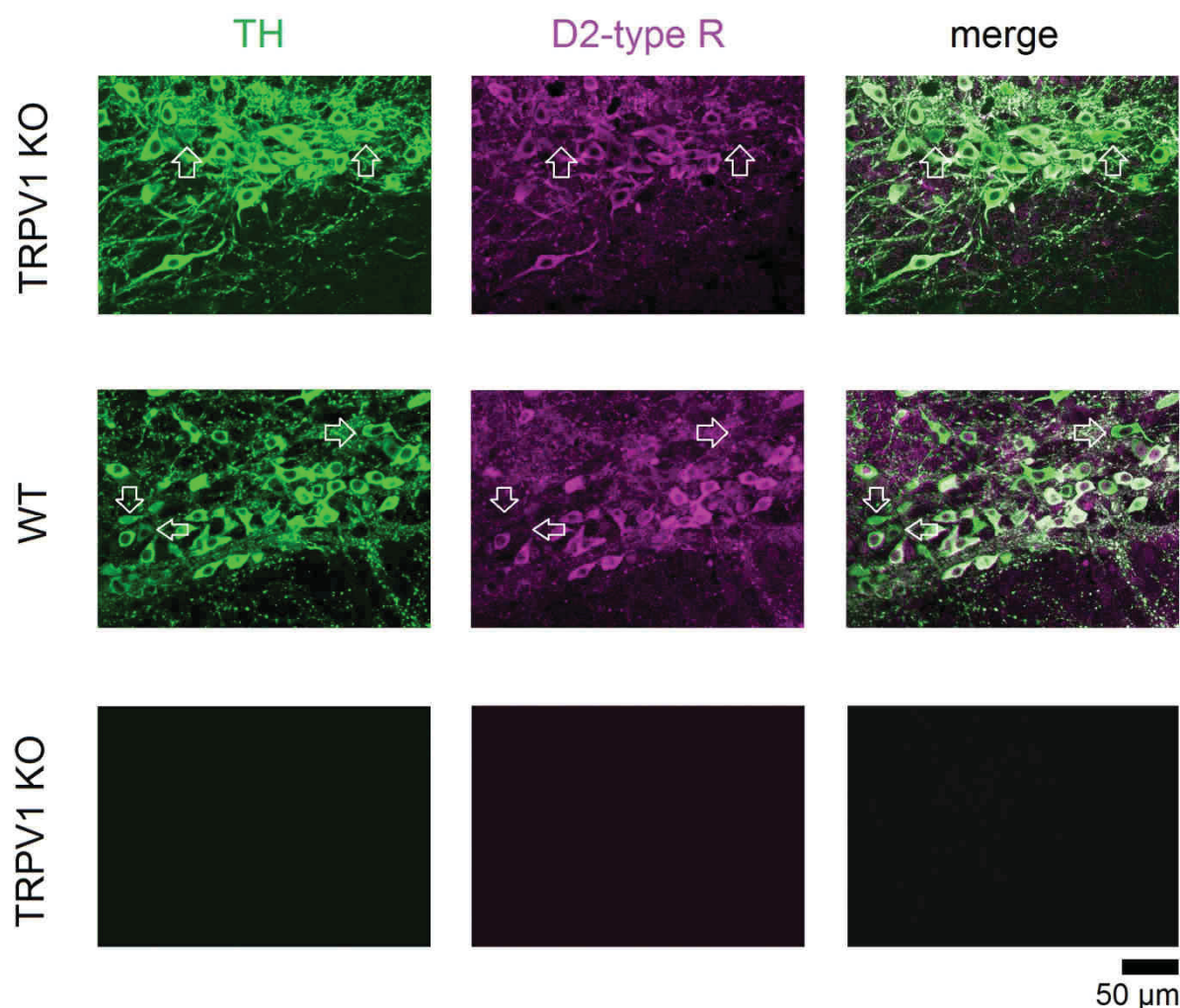
Fig.3-11. D2-type R staining in TH-positive neurons in SNc of WT and TRPV1 KO mice.
Opened arrows indicate TH-expressing neurons (in green) that clearly co-localize with D2-type R immuno-reactivity (in pink). Negative control (without TH and D2-type R primary antibodies incubation) was performed on the same day of previous stainings (above) to test possible unspecific fluorescence from secondary antibody incubation.

Expression and function of TRPV1 was not yet investigated with an electrophysiological approach in the mouse TMN region. We recorded responses to the classical ligand of TRPV1 capsaicin in neurons from the densest subdivisions of TMN in the mouse: vTMN and medial mTMN, followed by their morphological and molecular biological analysis. Developmental change in TRPV1 expression was also studied.

3.2.2. TRPV1 activation depolarizes HA neurons of the TMN and increases their firing frequency

Application of capsaicin 0.1 and 1 μM in CC experiments (using EGTA 10 mM-containing intracellular solution) caused transient increase ($266 \pm 14\%$, n=7) of firing frequency that returned to the baseline level by the end of the drug application period. At the same time a significant depolarization (4.8 ± 1.1 mV) was observed in 6 out of 7 neurons ($p<0.05$, paired t-test) during capsaicin perfusion, which continued throughout the washout period (Fig.3-12A).

In order to test TRPV1-mediated direct or indirect actions, capsaicin was also applied on HA juvenile AIN in E2. The majority of neurons (12 out of 17, 71%) responded to capsaicin with inward currents larger than 5 pA. On average capsaicin 1 μM evoked currents of -19 ± 6 pA (n=7) and capsaicin 10 μM of -33 ± 12 pA (n=5) amplitude (Fig.3-12B below). Taken together these data show a clear postsynaptic TRPV1 response to capsaicin application on HA neurons.

In VC cell-attached (also called loose patch) a large fraction of HA neurons from juvenile E2 compared to the adult E2 neurons, responded to capsaicin 0.1 μM (8 out of 10 neurons, data not shown) and 1 μM (17 out of 22 neurons) with an increase in firing frequency. Difference in occurrence of capsaicin 1 μM-induced excitation between juvenile (77%) and adult E2 HA neurons (41%) was significant ($p=0.0305$, FEPT) (Fig.3-12C, left). As in none of the adult E2 neurons capsaicin 0.1 μM enhanced firing frequency (n=3), this concentration was not further applied to adult HA neurons.

3.2.2.1. TRPV1 expression in TMN and individual HA neurons scRT-PCR

TRPV1 transcripts (107 b.p.) were detected by scRT-PCR only in 33% of juvenile (5 out of 15) HA (HDC-expressing) E2 neurons (Fig.3-12B, above), which indicates a low expression of this channel (below detection level) in about half of the neurons, as the majority of juvenile neurons were responding to capsaicin in electrophysiological experiments (see below) (Fig.3-12C, left). Analysing adult E2 neurons for TRPV1-expression 6 out of 12 were found PCR-positive. No difference in occurrence of transcripts of this channel was detected between juvenile and adult HA neurons (p=0.21, FEPT). Considering juveniles and adults as one group the final percentage of TRPV1 expression was 40%.

qRT-PCR in which TRPV1 mRNA levels of E2 juvenile mice relative to the mature adults (100%) represented $381 \pm 139\%$ (n=5; p=0.022, MWT), when primers spanning cDNA fragment including exon7 were used. When qRT-PCR was conducted with primers spanning exon 13 of TRPV1-gene, mRNA levels in juvenile TMN comprised $330 \pm 48\%$ of adult TMN (n=5; p=0.012, MWT). Note that 2 different primer pairs (spanning exon 7 or exon 13) show higher expression of TRPV1 in immature E2 (Fig.3-12C, right). These results demonstrated that the amount of TRPV1 expressed and capsaicin occurrence are higher in E2 of juvenile mice compared to the adult ones, even though this difference remained undetected at the single cell level.

3.2.2.2. Dose-dependent action of capsaicin. Impairment of capsaicin-excitation of TMN neurons in TRPV1 KO mice

Excitation of juvenile E2 HA neurons by capsaicin 0.1 μM to $235 \pm 39\%$ during drug perfusion and $175 \pm 40\%$ of control during the minutes 6-10 after drug withdrawal from the bath, n=8 (data not shown). This second, outlasting, phase of excitation is further called "long lasting enhancement by capsaicin (LLEcap). This prolonged TRPV1-induced excitation (up to 20 minutes after drug withdrawal) can be detected in some experiments during the application of capsaicin 1 μM. The initial excitation by 1 μM capsaicin ($165 \pm 16\%$ and $280 \pm 31\%$, n=17) was indifferent from the excitation by 100 nM (p=0.086, MWT) but caused a stronger LLEcap (p=0.036, MWT). In addition, amplitude (or amount) of capasicin 1 μM response between adult and juvenile E2 HA neurons, showed no difference among 25 minutes data points (unpaired t-test).

The first phase of direct excitation of E2 HA neurons by capsaicin 0.1-1 μM was significantly impaired in juvenile TRPV1 KO mice (p=0.046, MWT) (Fig.3-12D). As no difference in response to capsaicin was seen between heterozygous and wild type mice, data were pooled (this group is called "WT" mice). LLEcap was abolished in TRPV1 KO HA

neurons (p=0.02, MWT) when compared to the whole population of "WT" neurons (responding and non-responding to capsaicin) (n=22). The statistical difference between individual data points is illustrated on Fig.3-12D.
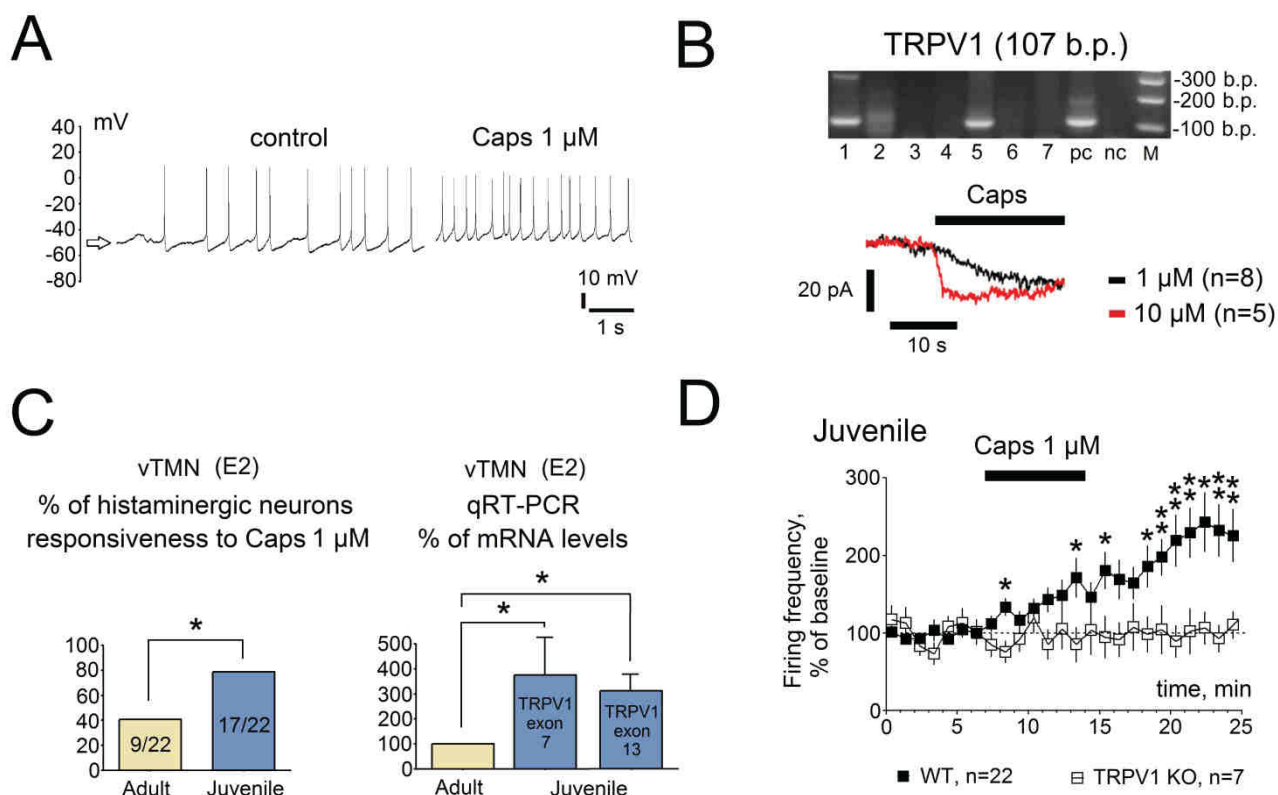
Fig.3-12. TRPV1 expression and excitation by capsaicin of HA neurons.
A. Representative CC recording trace showing increase of firing and depolarization (~5 mV) during capsaicin application, with respect to control. **B.** Picture of scRT-PCR analysis of TRPV1 expression in 7 juvenile HA neurons (data from Olga Sergeeva and Anna Kernder). Averaged current responses to different capsaicin concentrations (caps 1 and 10 μM) obtained from 8 and 5 HA E2 AIN, respectively (below). **C.** Percentage of capsaicin (1 μM) responsiveness (occurrence) (left, * p<0.05, FEPT) and TRPV1 mRNA expression between adult and juvenile HA neurons (right * p<0.05, MWT) (data from Olga Sergeeva). **D.** Firing frequency versus time course diagram of E2 HA neurons averaged responses during control and capsaicin 1 μM application. HA neurons recorded in wild type „WT" mice respond to capsaicin with an excitation that is strongly impaired in TRPV1 KO mice (* p<0.05; ** p<0.01, unpaired t-test).

TRPV1 staining was also performed to clarify the postsynaptic location of this channel on HA neurons but in WT and TRPV1 KO posterior hypothalamic cultures (n=4 and n=4, respectively) no difference was detected for TRPV1 immunoreactivity (Fig.3-13).
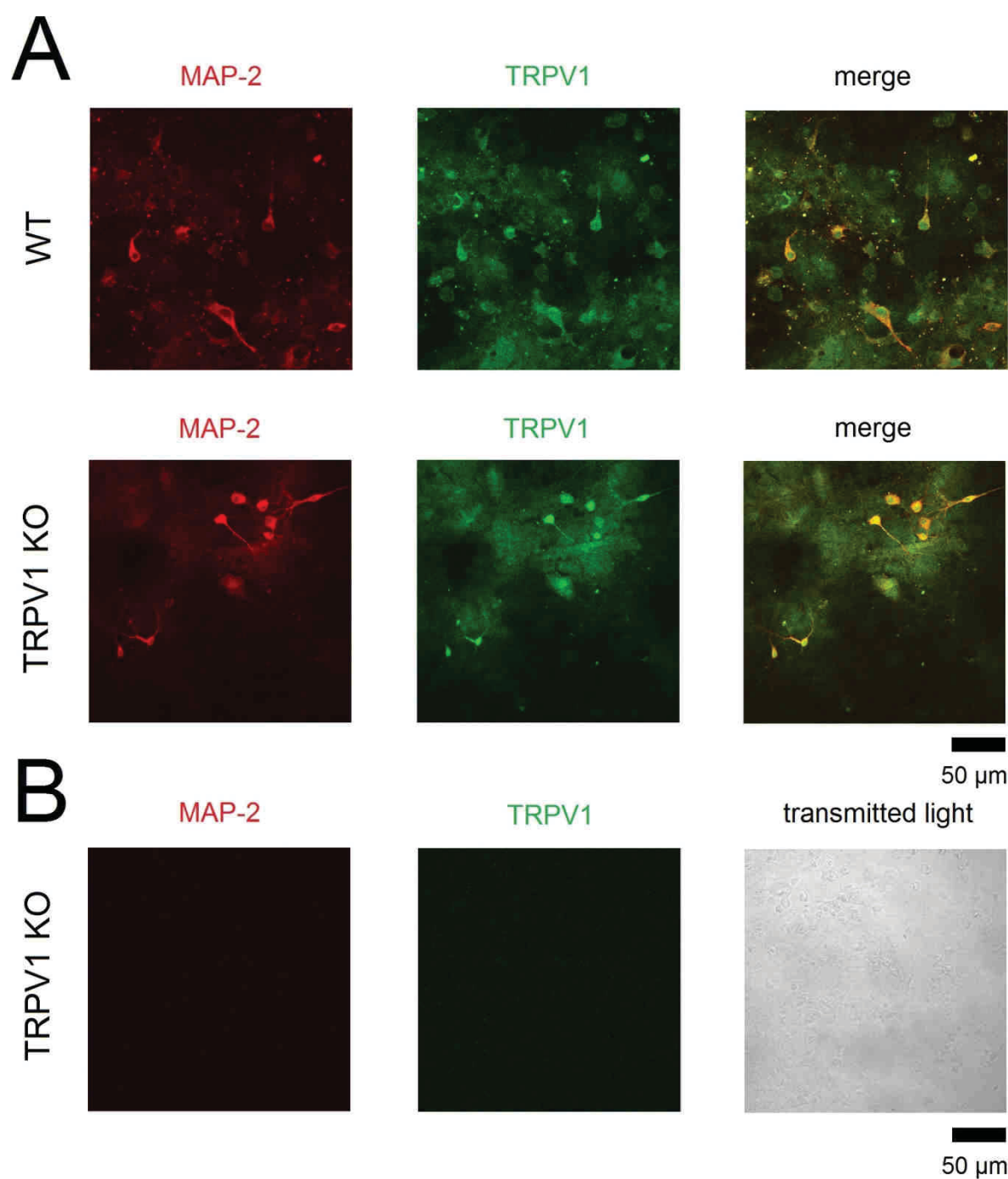
Fig.3-13. TRPV1 staining in WT and TRPV1 KO mouse posterior hypothalamic neuronal cultures.
A. TRPV1 immuno-reactivity (in green) on red MAP-2-expressing neurons in WT and TRPV1 KO mouse posterior hypothalamic cultures. Note that WT and TRPV1 KO preparations present no differences for TRPV1 immuno-reactivity. **B.** Negative control (without MAP-2 and TRPV1 primary antibodies incubation) on TRPV1 KO cultures was performed on the same day as previous stainings (in B).

3.2.2.3. TRPV1 expression in E4 subdivision of TMN is higher than in E2 and goes along with higher responsiveness to capsaicin in adult E4 neurons

The majority of investigated adult E4 neurons were excited by capsaicin 1 μM (9 out of 10); during the last 5 minutes in the presence of a TRPV1 agonist the firing frequency represented 169 ± 21 % of control (n=9), during the minutes 6-10 after drug withdrawal from the bath (LLEcap) the firing represented 354 ± 113% of control.

In contrast to the E4 neurons a larger fraction of adult E2 neurons were not responding to capsaicin (13 out of 22). The difference in occurrence of capsaicin potentiation between adult E2 and E4 neurons was significant (p=0.0189, FEPT). In 9 E2 neurons excitation by capsaicin 1 μM amounted to 136 ± 19% of control during drug perfusion and 199 ± 37% of control during LLEcap (difference in the amount of potentiation between E2 and E4 responsive to capsaicin neurons was not significant, (p=0.33 and p=0.29, for the first and second phase, respectively; MWT).

Semi-quantitative real time PCR was performed to compare the amount of mRNA encoding for TRPV1 in E4 relative to E2 in adult mice: it represented 335 ± 40% of E2 taken as 100% (5 mice; p=0.037, MWT, data from Olga Sergeeva). Thus E4 shows higher TRPV1 expression and capsaicin sensitivity relating to the E2 region in adulthood.

In a study by Cavanaugh et al., (2011) unidentified neuronal populations around the 3V in the caudal hypothalamus were shown to express TRPV1 (using a TRPV1-reporter mouse for the purpose), whereas other hypothalamic regions showed hardly any expression. In our experiments excitation by capsaicin (0.1-1 μM) of HA neurons (both, the first phase and LLEcap) were missing in TRPV1 KO mice, supporting expression of this channel in this neuronal population.

3.2.2.4. Retrograde tracing of HA system reveals higher probability of TRPV1–mediated excitation of descending than ascending pathways. Are retrobeads toxic for the neurons?

The next aim was to investigate the role of capsaicin responding neurons in adulthood and whether they display a different physiological role with respect to the other fraction of non-sensitive HA neurons in E2. For these reasons tracing studies were designed in striatum and brainstem as well known projection areas of TMN in rodents. Retrograde tracing experiments on adult mice allowed the comparison of capsaicin effects in HA neurons with descending (to brainstem) versus ascending projections (to striatum).

First of all, immunostainings for histamine and TH (the latter as marker of catecolaminergic neurons) were performed in the brainstem at the level of NTS. The striatum was stained only

for histamine (Fig.3-14A). Many HA axons and fibres were found in such preparations entering NTS (left) from the dorsal surface of the brainstem and striatum (right), making contacts with neurons located in those regions.

In 7 mice injections of retrobeads were done bilaterally or unilaterally at the level of NTS and unilaterally in striatum. Retrobeads-containing neurons were found 5-14 days after operation in E2 or E4-containing slices.

Occurrence of retrobeads in HA neurons of E2 and E4 was investigated *post-hoc* from fixed slices after recording. Only immuno-reactive cells for histamine were considered. In E2, $9 \pm 2\%$ of histamine positive neurons (n=351, 6 mice) contained retrobeads, whereas $13 \pm 3\%$ of HA neurons of E4 were retrogradely labelled (from 185 investigated histamine-positive neurons in 4 mice). The difference between two TMN subdivisions in occurrence of labelled neurons is not significant (p=0.18, FEPT) (Fig.3-14B).

Striatal injections were done only unilaterally and in the dorsal part, thus resulting in the presence of retrobeads-labelled HA neurons only in E2 (not calculated for IHC, but only recorded). This protocol was performed with the purpose to have an experimental control, measuring the rate of success of NTS injections.

HA identification of retrobeads-containing neurons was performed considering their location, spontaneous firing (with typical frequency), eAPC duration and sensitivity to RAMH. In the E2 subdivision all retrobeads-containing neurons (n=5) after NTS injections, significantly increased their firing frequency in response to capsaicin 1 µM to $198 \pm 52\%$ and $178 \pm 32\%$ of baseline during the first and second (LLEcap) phase of response, respectively (Fig.3-14C). All 7 E4 neurons labelled from NTS, were excited by capsaicin with no difference in amplitude of response from E2 neurons either in the first ($215 \pm 81\%$ of control, p=0.62, MWT) or the second phase ($427 \pm 92\%$, p=0.072, MWT). The occurrence of a capsaicin response in E4 was not different from the control adult neurons (see above, p=1, FEPT). The occurrence was significantly higher in E2 neurons traced from NTS (p=0.0407, FEPT), than in the whole E2 population, indicating a higher expression level of TRPV1 in descending projections of the HA system.

The majority of E2 neurons retrogradely traced from the striatum (6 out of 7, Fig.3-14C) displayed no response to capsaicin 1 µM (difference with E2 and E4 neurons traced from NTS is significant: p=0.0003, FEPT; difference with total population of adult E2 neurons is not significant, p=0.08, FEPT).

Firing frequency of *ex-vivo* recorded E4 neurons carrying retrobeads was not different from control adult E4 neurons (1.85 ± 0.8 Hz (n=7) vs 1.2 ± 0.42 Hz (n=10)) as well as their

eAPC durations (3.1 ± 0.3 ms vs 4.6 ± 0.4 ms). The same was true for the E2 neurons: retrobeads-containing neurons fired at 1.55 ± 0.4 Hz (n=12) whereas adult control E2 neurons at 1.2 ± 0.3Hz (n=22), their eAPC durations represented 3.6 ± 0.4 ms vs 4.45 ± 0.3 ms, respectively.

These results demonstrated that TRPV1 may serve as target for the pharmacological identification of the descending pathway of the HA system in adulthood, since all neurons labelled from NTS responded to capsaicin.
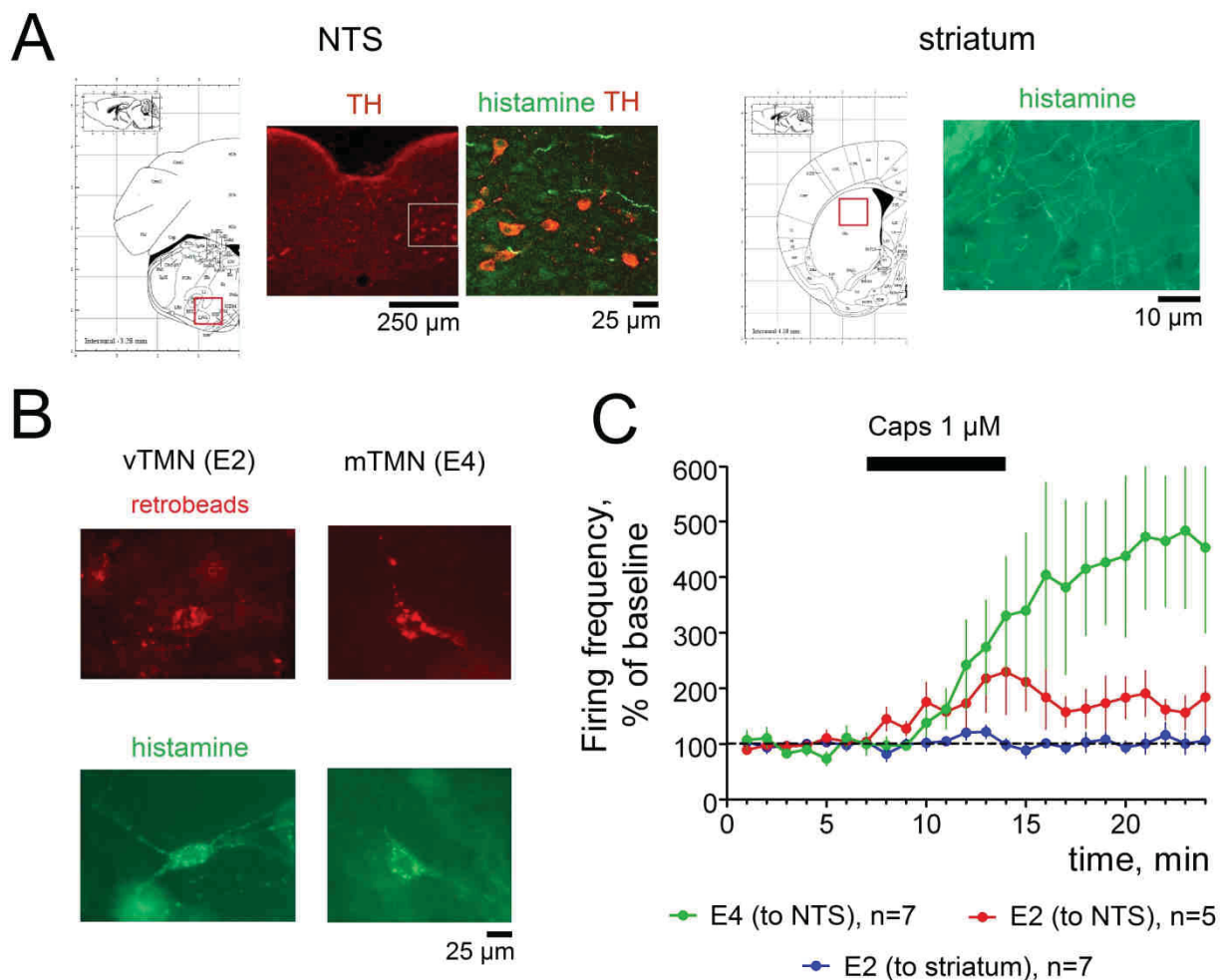
Fig.3-14. HA neurons in E2 and E4 labelled from NTS and striatum, differ in capsaicin sensitivity.
A. Anatomical locations and staining of brainstem-containing NTS and striatum slices. NTS region was stained with TH (red), identifying TH-expressing catecolaminergic neurons (left). HA axons were visualized in green either in NTS or in striatum (right). NTS enlarged image showed a TH-positive neuronal group surrounded by a robust HA innervation. **B.** Pictures of retrobeads-containing (red) HA neurons (green) in E2 and E4 after NTS or striatal injections. **C.** Firing change induced by capsaicin application in retrobeads-containing neurons of different subdivisions of TMN projecting to different brain regions.

Tracing studies give important insights into the neuronal connectivity and are becoming an important experimental tool in combination with electrophysiology and optogenetics to elucidate functional connectivity. Interestingly until now, actions of retrobeads on the cellular metabolism or physiology (once they are taken up by neurons) were never considered during anatomical and electrophysiological studies. A screening analysis of possible retrobeads-induced toxicity that may also affect responses to capsaicin, was performed on striatal cultures: changes in their electrophysiological properties was monitored using the multichannel electrode system for 3 consecutive days (Fig.3-15 right). Striatal primary neuronal cultures were prepared as previously described in material and methods (Sergeeva et al., 2007).
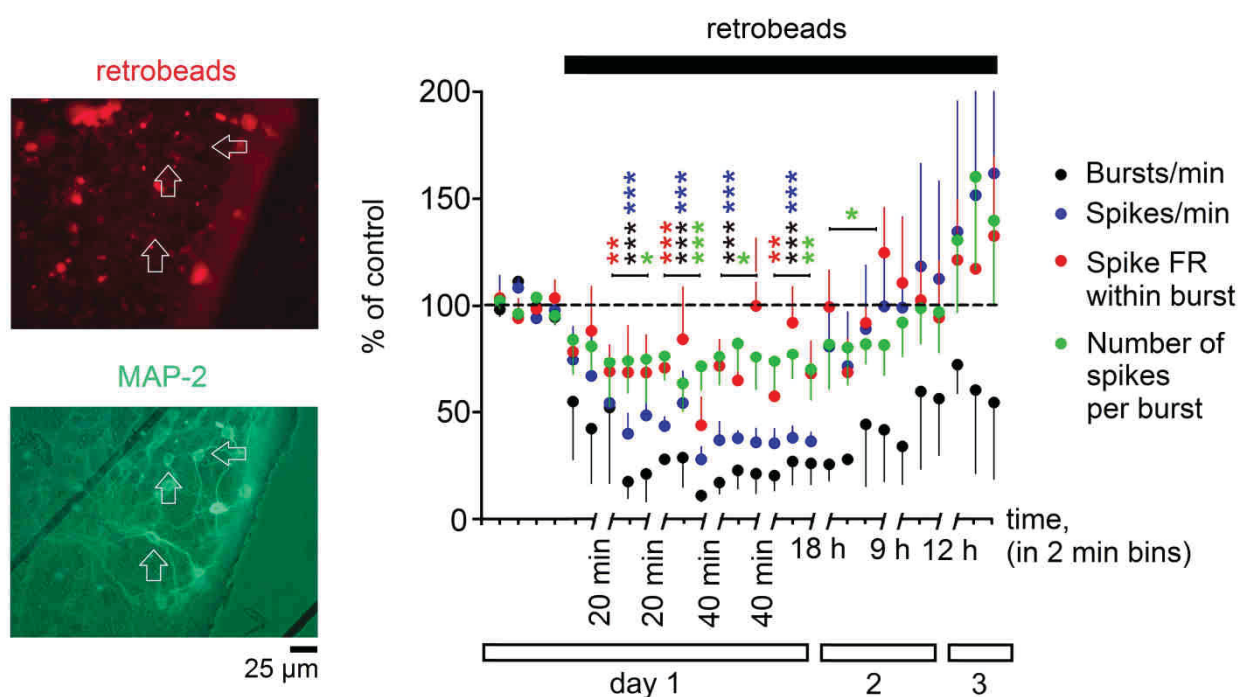
Fig.3-15. Exploring striatal toxicity of retrobeads.
Fluorescence images of MEAs with striatal culture grown on it after incubation with retrobeads (red), fixed and stained after recording for the neuronal marker MAP-2 (green) (left). Red retrobeads–fluorescence partially overlaps with MAP-2, indicating retrobeads uptake occurred either in neurons or glia. Time course diagrams normalized to the control period (8 minutes) showed the 4 parameters characterizing electrical activity of striatal network measured using MEAs (right) (* $p<0.05$; ** $p<0.01$; *** $p<0.005$, MWT) data from Olga Sergeeva and Roberto De Luca.

Suppression of striatal neuronal activity in terms of frequency (spikes per minute) and spike bursts (burst per minute) was observed in all cultures tested (n=5, plated in different experimental days) during the first day of retrobeads application. Recovery of spontaneous activity in striatal cultures was observed the following day. Interestingly, firing frequency

within bursts was less affected than other parameters. These findings justify the experimental *ex-vivo* protocol for retrobeads-containing neuron recording in slices performed later than 6 days after retrobeads injection. Longer waiting periods (in some studies up to 2 weeks) are necessary for the retrograde labelling of neuronal somata from far remote projection areas allowing travelling of retrobeads along the axons (Lammel et al., 2008).

After recordings we fixed striatal cultures and investigated neuronal content with the microtubule-associated protein-2 (MAP-2) immuno-reactivity. Uptake of retrobeads by striatal neurons was detected by co-localization of retrobeads fluorescence (red) and MAP-2 labelling (green) (Fig.3-15 left). Neuronal loss after retrobeads application was not observed. The recovery of physiological functions observed either in animal or in culture system demonstrates that application of retrobeads is a non-toxic approach *in vivo* or *in vitro*, respectively. The method of *in vitro* retrobeads testing using MEAs is thus a safe tool for screening of chemical compounds for toxicity.

3.2.2.5. Retrograde tracing of HA system. Problem with identification of HA neurons after capsaicin application

RAMH inhibited all E2 neurons of TMN projecting to the striatum (after capsaicin application) to $55 \pm 8\%$ of control (n=7 last 5 minutes of application period). To be sure that inhibition of firing was due to the interaction of ligand with the H3R and not to the run down of activity due to cell death or lost contact with the cell membrane we considered only neurons showing recovery of firing frequency to a level higher than that during drug application. In 3 neurons traced from NTS RAMH had no effect, so they could not be considered HA, even though these neurons shared the electrophysiological properties with truly HA neurons, such as regular firing frequency and eAPC width longer than 1.5 ms. In 5 other cells (2 E2 and 3 E4) firing frequency was reduced in the presence of RAMH to $15 \pm 10\%$ of control, however recovery was not observed in 3 of them. A striking coincidence was noticed between large responses to capsaicin and lack of response to RAMH.

Every recorded neuron belonging to "WT" and TRPV1 KO groups where capsaicin either caused LLEcap>160% or failed to do this with regard to their responsiveness to the H3R agonist RAMH, was deeply analysed. A significant difference in relative firing frequencies (p=0.02, MWT) during the RAMH application period (last 5 minutes) between capsaicin-responding ($70 \pm 12\%$ of baseline, n=12) and non (weak)-responding cells ($42 \pm 8\%$, n=14), was found.

Next we took advantage of the transgenic mouse model expressing red fluorescent Tmt-HDC were HA neurons could be visualized and recorded in the living brain slice and their responses to RAMH could be compared in control and after capsaicin application.

In 8 Tmt-HDC neurons, which were excited by capsaicin (183 ± 40 % of control) the response to RAMH 2 μM was reduced (n=1) or abolished (n=7). The difference in occurrence of RAMH-inhibition between non-responding and capsaicin-responding groups was significant (p=0.0005, FEPT) (De Luca et al., 2016).

The impairment of H3R-mediated inhibition caused by capsaicin on HA neurons may be explained as follows: 1) Capsaicin- induced excitation may cause swelling and cellular damage (Pecze et al., 2013) leading to H3R internalization (Osorio-Espinoza et al., 2014); 2) Calcium and depolarization through TRPV1 receptor activation could affect the potency of H3 receptor action (Arrang et al., 1985) explaining the reduced auto-inhibition.

We found that depolarization and/or intracellular calcium rise (both achieved following TRPV1 activation) can reduce H3R-mediated auto-inhibition on HA neurons (De Luca et al., 2016). Possible protocols allowing the preservation of autoinhibition in neurons exposed to capsaicin were explored.

Capsaicin-induced excitation on Tmt-HDC-expressing neurons in calcium-free condition was 121 ± 15% during the first phase (8-14 minutes) and 152 ± 12% in the late phase (20-25 minutes) in respect of control (all responsive, paired t-test, n=6) (Fig.3-16A left). No difference was detected regarding the first phase between the 17 juvenile HA neurons (capsaicin-sensitive) recorded in normal ACSF (nSol) and Tmt-HDC-positive neurons in calcium-free (CF) (p=0.42, MWT). Statistical difference was indeed detected only for late phase (p=0.007, MWT) (Fig.3-16A right).

RAMH was applied after capsaicin perfusion in calcium-free solution, inhibiting all Tmt-HDC-positive neurons (67 ± 9% of baseline, p<0.05 paired t-test, n=6) previously excited by TRPV1 activation (Fig.3-16B). The experiments demonstrated that a reduced excitation through TRPV1 (by sodium entry, Fig.3-16C) was still possible in the absence of calcium.

Interestingly, the occurrence of capsaicin responses between normal and calcium-free solution remained unchanged (p=0.6, FEPT) among juvenile HA neurons, but RAMH responsiveness increased significantly (p=0.0047, FEPT).

For safe identification retrobeads-containing neurons traced from NTS and located in E2 and E4 areas, will be recorded applying RAMH in calcium-free condition.
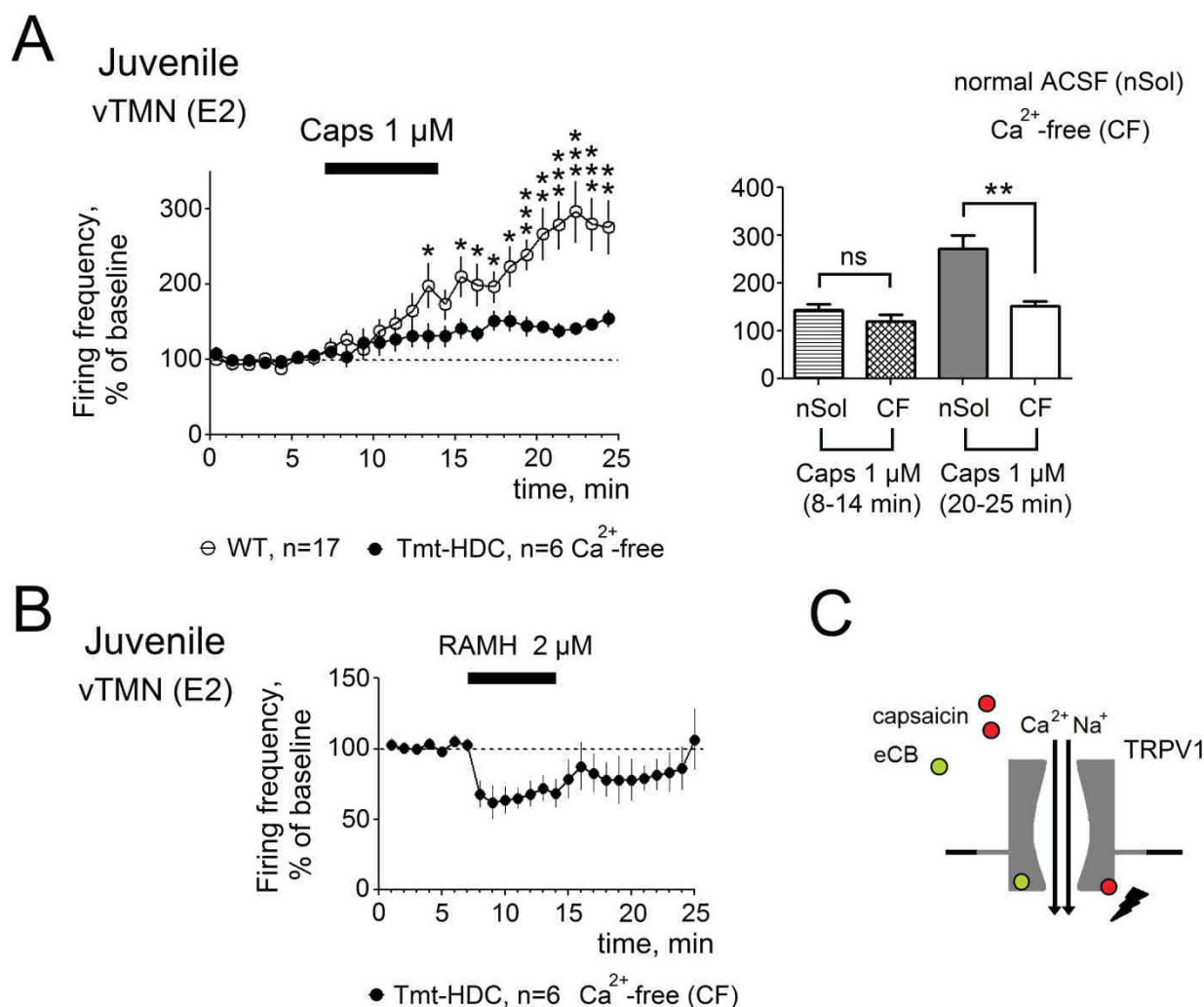
Fig.3-16. TRPV1 activation in calcium-free condition and autoinhibition through H3R on E2 juvenile HA neurons.
A. Capsaicin responsiveness was unchanged in calcium-free solution but the amount of excitation was reduced compared to normal ACSF in juvenile E2 HA neurons (left) located in E2 (* $p<0.05$; ** $p<0.01$, *** $p<0.005$, unpaired t-test). No difference was detected during the first phase (8-14 minutes) of capsaicin-induced excitation (right) (* $p<0.05$, MWT). **B.** H3R functionality is not affected by capsaicin application in calcium-free solution. All capsaicin-sensitive Tmt-HDC-positive neurons were significantly inhibited by RAMH. **C.** Schematic model of TRPV1 channel. Capsaicin (red dots) or endocannabinoids (green dots) activate the receptor leading to sodium (Na+) and calcium (Ca+2) entrance.

3.2.2.6. TRPV1–mediated excitation of HA system is independent of glutamate

Capsaicin-induced LLEcap could be explained through the release of other transmitters following TRPV1 activation. We also searched an explanation for the developmental down-regulation of capsaicin responsiveness as we found no difference in the occurrence of TRPV1 expression in juvenile and adult HA neurons (scRT-PCR). Glutamate release was reported in the hypothalamus after TRPV1 activation (Bourque et al., 2007).
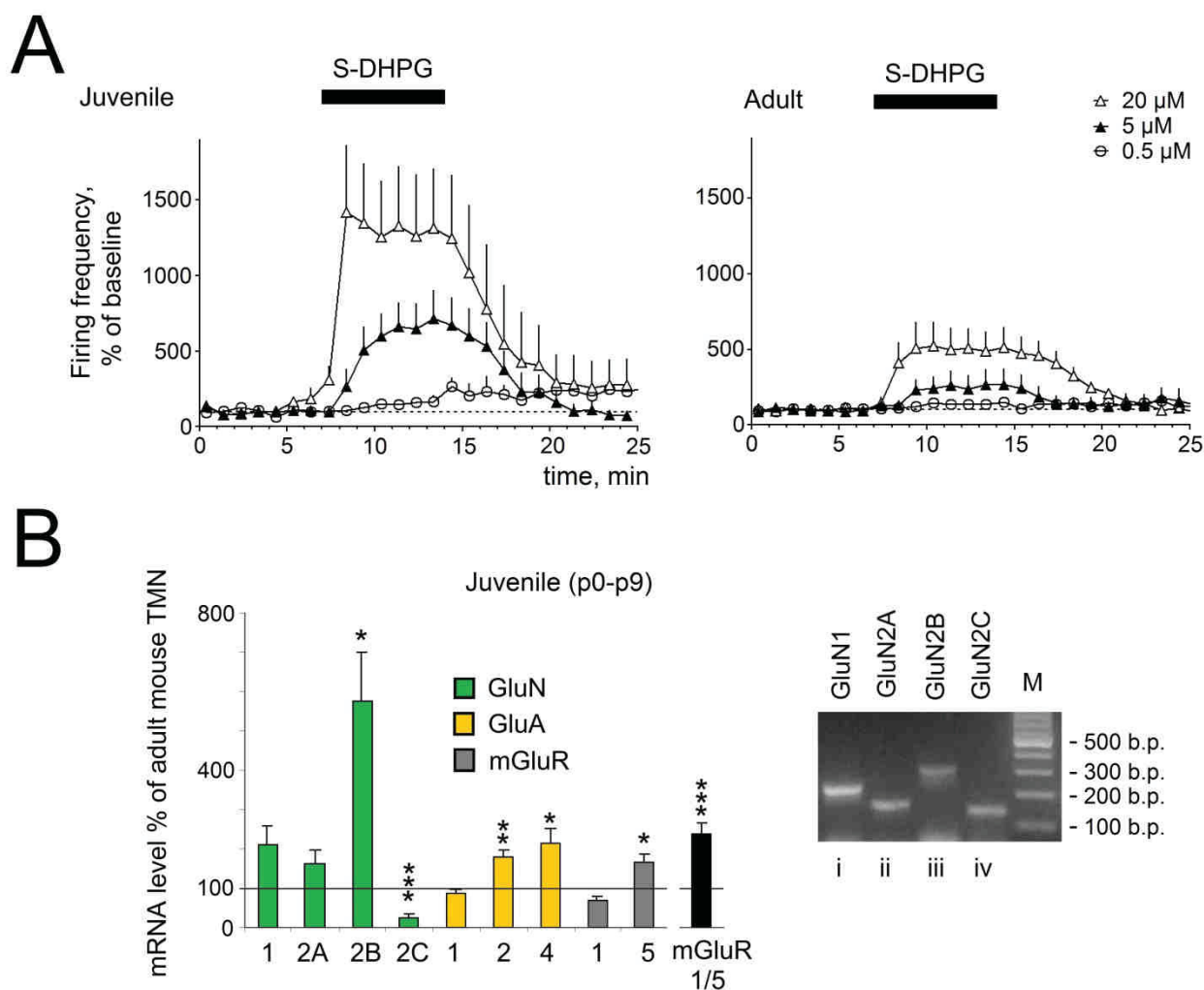
Fig.3-17. Glutamate receptors expression and sensitivity during maturation in mouse TMN.

A. Larger responses to different concentrations of mGluR1/5 agonist sDHPG were recorded in juvenile compared to adult HA neurons. **B.** qRT-PCR analysis of transcription of indicated genes. All reactions were normalized on RpL13a (for primers see Kernder et al., 2014 and paragraph: 2.6.3. List of primers and cDNA products) except for the black bar (mGluR5 was normalized on mGluR1). Averaged value for the adult group (4-7 mice) was taken as 100% (left). Example of gel shows amplicons of such amplification for the GluN from p9 TMN (* p<0.05; ** p<0.01; ***p<0.005, MWT) (modified from Kernder et al., 2014).

HA neurons present very high sensitivity to the group I-mGluRs agonist (*R,S*)-3,5-dihydroxyphenylglycine (sDHPG) (Kernder et al., 2014). This group includes mGluR1 and 5 which are coupled to PLC for the internal release of calcium (Wang et al., 2007). Excitation by sDHPG 0.5 μM application on HA neurons (mainly recorded in E2) was smaller in adult (p25-p51) than in juvenile (p9-p13) mouse brain: 128 ± 6 % (n=10) versus 156 ± 11 % (n=4) (p=0.02, Wilcoxon test). At higher concentrations (5 μM) sDHPG was able to increase firing of juvenile HA neurons to $500 \pm 88\%$ (n=4) against $214.2 \pm 22.8\%$ in the adults (n=4)

(p=0.04, Wilcoxon test), with respect to their control. Finally sDHPG 20 µM excited juvenile HA neurons to $1177 \pm 146\%$ (n=4) versus $440 \pm 51\%$ (n=5) in adulthood (p=0.02, Wilcoxon test), respect to their control (Fig.3-17A). These findings were similar to what was found in the rat (Yanovsky et al., 2012).

On the molecular level expression of mGluR1 transcripts were not age-dependent in mouse TMN, whereas mGluR5 transcript numbers declined with age (Fig.3-17B), most likely reflecting a developmental down-regulation of mGluR5a in the brain (Nicoletti et al., 2011). At the postsynaptic side, mGluR5 receptors can be physically linked to the NMDA receptor 2 subunits (GluN2) and enhance NMDA receptor function (Nicoletti et al., 2011). Interestingly, a developmental down-regulation of GluN2B subunits was also found in mouse TMN (Fig.3-17B left) (scRT-PCR showed in addition NMDA receptor subunits on one selected HA neuron, Fig.3-17B right). Taken together these data showed how glutamate sensitivity dramatically decreased during brain maturation (Kernder et al., 2014).

Next experiments were directed to demonstrate the contribution of mGluR1/5, AMPA and NMDA receptors for LLEcap maintenance during juvenile stage. Juvenile E2 Tmt-HDC expressing neurons (5 out 6, showed significant increase of firing, all inhibited by RAMH application), were excited by capsaicin 1 µM in the presence of MPEP to $147 \pm 19\%$ of control, during first phase and to $182 \pm 59\%$ of control in the late phase (p<0.05, paired t-test). The amount of capsaicin-mediated excitation during mGluR5 block, showed no difference either during first phase (p=0.2, MWT), or in the late phase (p=0.3, MWT) compared to the drug alone, that indicated no participation of mGluR5 for the maintenance of the excitatory effect. Occurrence between capsaicin application alone and in the presence of an mGluR5 antagonist showed no difference (p=1, FEPT). When AMPA (GluA) and NMDA (GluN) receptors were blocked with 6-cyano-7-nitroquinoxaline-2,3-dione (CNQX, antagonist of alpha-amino-3-hydroxy-5-methyl-4-isoxazolepropionic acid (AMPA) receptor) (20 µM) and D-(-)-2-Amino-5-phosphopentanoic acid (D-AP5, antagonist of N-methyl-D-aspartate (NMDA) receptor) (50 µM), respectively, capsaicin-evoked excitation of HA neurons recorded from juvenile mice was not different from the control experiments (n=9) (Fig.3-18). CNQX and D-AP5 increased *per se* spontaneous firing of HA neurons (Fig.3-18) indicating presence of inhibitory glutamatergic tone under our experimental conditions (it is possible that glutamate uptake is impaired at room temperature). Inhibition of HA neuron activity through NMDA receptors was previously described (Faucard et al., 2006). Thus glutamate can not amplify capsaicin-mediated excictation of HA neurons.
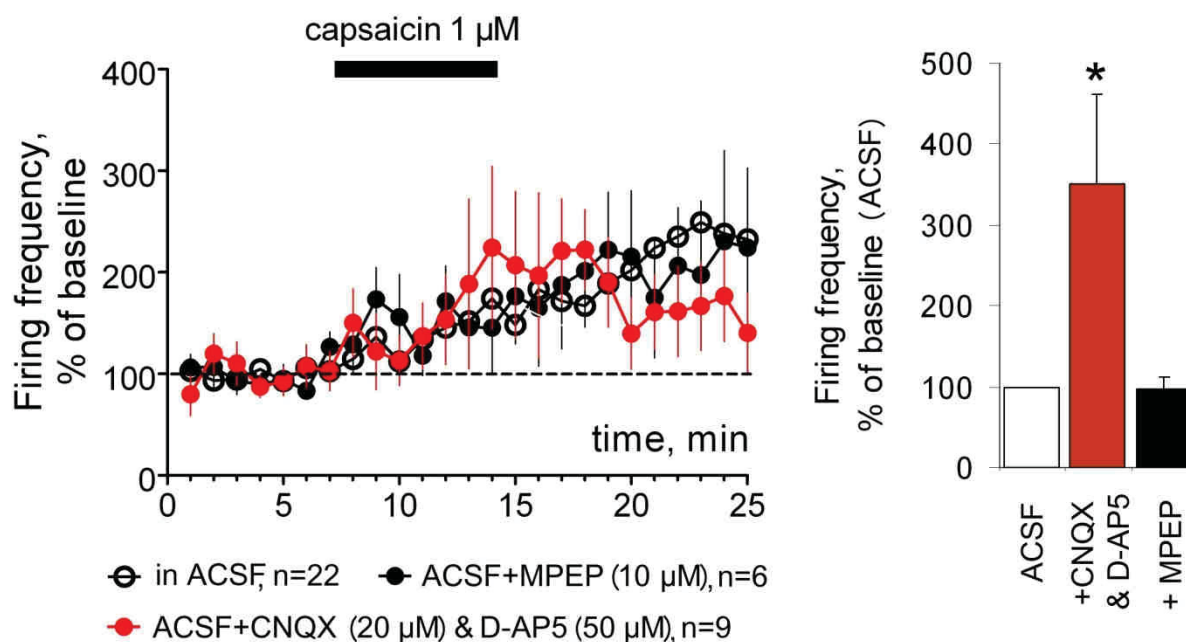
Fig.3-18. Excitation of HA cells of vTMN by capsaicin is independent of glutamate release.
Response to capsaicin in ACSF is compared with the responses obtained in the presence of MPEP (antagonist of mGluR5) and in the presence of ionotropic glutamate receptor antagonists (CNQX and D-AP5). Bar histogram (right) shows change in baseline activity during the first 7 minutes application of CNQX & D-AP5 (* $p < 0.05$, MWT), indicative of ambient glutamate presence in the slices recorded at room temperature.

3.2.2.7. TRPV1–mediated excitation of HA system is amplified by SP acting through the neurokinin 1 receptor (NK1R). Mechanisms of NK1R signalling

Previous studies have already shown that HA neurons synthesize SP (Airaksinen et al., 1992) and receive presynaptic SP-ergic inputs in the cat (Yao et al., 1999), but at the moment it is not known whether HA neurons can release SP together with histamine and whether they can amplify TRPV1-signalling as it was shown in the dorsal root and nodose ganglia (Caterina et al., 1997).

LLEcap induced by TRPV1 activation by capsaicin could be abolished in the presence of NK1 receptor antagonists, namely CP 96345 1 µM and CP 99994 1 µM. Interestingly, the first phase of capsaicin-mediated excitation did not change during the co-application with CP 96345 (in identified HA neurons, $p = 0.4$, MWT; n=4), with reduction of the of late phase only ($p = 0.02$, MWT). The same results were obtained with CP 99994, with the first phase preserved ($p = 0.1$, MWT) and only late phase of capsaicin-induced excitation being reduced ($p = 0.04$, MWT) (Fig.3-19A). The involvement of NK1 receptors in the amplification of

TRPV1-mediated response led to experiments investigating NK1R expression and function on HA neurons.

Results from scRT-PCR showed that NK1R and the precursor of SP (pre-SP) expression were not significantly different between juvenile and adult E2 HDC-positive neurons (p=0.23 and p=0.05, respectively; FEPT). Therefore, calculations of NK1R and pre-SP percentages were made considering juvenile and adults as one group. NK1R transcripts (124 b.p.) were detected in 67% (18 out of 27), while pre-SP (215 b.p.) in 63% (17 out of 27) of HDC-positive neurons in E2 (Fig.3-19B). Moreover qRT-PCR analysis of NK1R and pre-SP levels showed no difference between mRNA levels in adult (100%) and juvenile E2 (Fig.3-19C). Therefore electrophysiological data between these groups were pooled.

NK1R immunostainings in Tmt-HDC-expressing neurons (5 mice) revealed that the majority of Tmt-HDC-positive (n=267) and histamine-containing neurons (n=317) were immune-positive for NK1R (83% and 86%, respectively) without differences between juvenile and adult mice for NK1R-expressing Tmt-HDC-positive and NK1R-positive histamine-expressing neurons, respectively (p=0.84, and p=1, FEPT) (Fig.3-19D).

Electrophysiological recordings confirmed evidences coming from NK1R expression with molecular biology and IHC. The majority of investigated E2 neurons (8 out of 9 HA neurons) were excited by GR 73632 10 nM (a NK1R synthetic agonist) to 174 ± 21% of control, during the bath perfusion (7 minutes) and to 302 ± 61% of control after 10 minutes of drug withdrawal from the bath, at physiological temperature. Neurons were considered responsive if they changed significantly, either during bath perfusion period or 10 minutes after GR 73632 withdrawal, their firing with respect to control (p<0.05, paired t-test). Increase of firing induced by GR 73632 10 nM application was abolished in the presence of one of its antagonists namely CP 99994 100 nM (in all 6 recorded HA neurons) (Fig.3-19E). As expected according to previous observations, the amount of the excitatory response induced by GR 73632, did not differ between juvenile and adult HA neurons (p=1, FEPT). Together with the increase of firing frequency induced by GR 73632 10 nM a significant reduction of eAPC amplitude to 90 ± 2% of control was observed in the majority of HA neurons (83%) excited through NK1R activation (5 out of 6; only neurons with stable eAPC amplitude during control were considered, p<0.05, paired t-test), therefore CC experiments were performed to investigate a possible depolarization induced by GR 73632.

In CC whole-cell configuration application of GR 73632 10 nM (recorded with EGTA 10 mM-containing intracellular solution, at physiological temperature) caused an increase of firing frequency to 123 ± 13% in reference to control (in 4 out of 5 neurons; p<0.05, paired t-

test) that turned to an inhibition by the end of the drug application period ($52 \pm 23\%$, of control). A significant depolarization (3.9 ± 1.4 mV) was observed in all 5 HA neurons recorded ($p<0.05$, paired t-test) during perfusion of the NK1R agonist, which recovered after drug withdrawal (Fig.3-19F). At the same time a significant reduction of AP amplitude (indicating depolarization, $p<0.05$, paired t-test) to $91 \pm 3\%$ respect to control, was observed during GR 73632 10 nM application.

To demonstrate a postsynaptic effect of GR 73632-induced excitation, tetrodotoxin (TTX, a strong inhibitor of voltage-gated sodium channels) and gabazine were co-applied in the bath to abolish completely AP and GABA-mediated pre-AP formation, respectively. The majority of Tmt-HDC-expressing neurons in E2 (4 out of 5) showed a significant depolarization of 5.4 ± 3.1 mV ($p<0.05$, paired t-test), for the whole period of GR 73632 10 nM application (and after its withdrawal) in the presence of TTX 1 µM and gabazine 10 µM.

Loose patch recordings using: CNQX, D-AP5 and gabazine, provided additional evidences of GR 73632-mediated postsynaptic effect. Indeed, all HA E2 neurons investigated (n=5), were excited by GR 73632 10 nM in the presence of CNQX, D-AP5 and gabazine to $175 \pm 37\%$ of control, during first phase and to $170 \pm 53\%$ of control in the late phase ($p<0.05$, paired t-test). Occurrence between GR 73632 application alone and in the presence of AMPA, NMDA and GABA$_A$ receptors antagonists showed no difference ($p=1$, FEPT).

Taken together these data showed that capsaicin LLEcap depends on NK1R expressed on HA neurons without differences during brain maturation. Moreover, GR 73632- induced excitation and depolarization is mainly postsynaptic and could be abolished by one of NK1R antagonists.
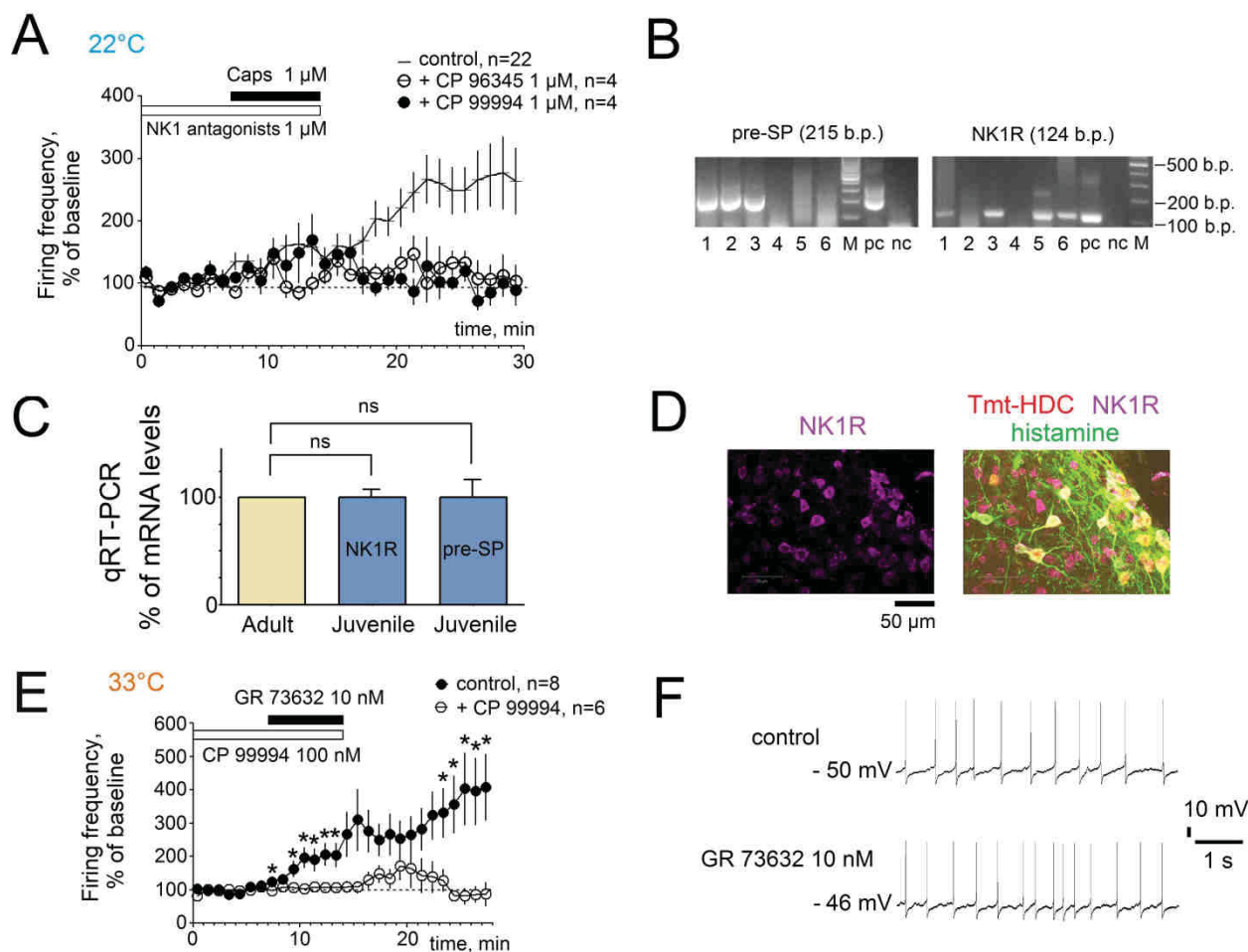
Fig.3-19. NK1R expression and function in mouse TMN.
A. LLEcap was abolished in the presence of NK1R antagonists: CP 96345 or CP 99994. B. scRT-PCR analysis of SP precursor (pre-SP, 215 b.p.) and NK1R (124 b.p.) in 6 neurons acutely dissociated from E2. C. Developmental changes of NK1R signalling. NK1R and pre-SP mRNA levels in juvenile TMN in % of adult values (data from Olga Sergeeva). D. Co-localisation of HA- (in green) and NK1R (in pink)-immunoreactivities with red Tmt-HDC fluorescence in E2. E. Increase of firing during GR 73632 application at physiological temperature. First phase of excitation and LLEGR were abolished by CP 99994 perfusion (* p<0.05, unpaired t-test). F. Example of CC firing recorded in one HA neuron during control and in presence of GR 73632. Activation of NK1R caused increase of firing and depolarization.

The presence of SP expression inside HA neurons was tested as well with IHC.

SP immunostainings in Tmt-HDC-expressing neurons (4 mice) revealed that only a minor fraction of Tmt-HDC-positive (n=78) were immune-positive for SP (23%) without differences between juvenile and adult mice (p=0.6, FEPT) (Fig.3-20).
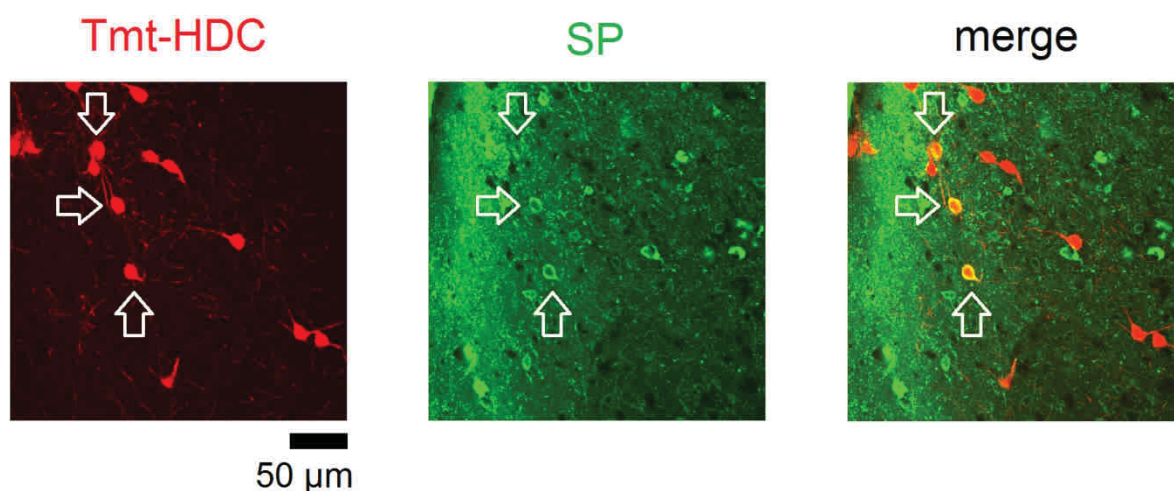
Fig.3.20. SP staining in Tmt-HDC-positive neurons located in vTMN.
Open arrows indicate red Tmt-HDC-expressing neurons which are immuno-positive for SP (in green).

3.2.2.8. Temperature-dependence of NK1R signalling

Different effects of GR 73632 at 22°C and 33°C were investigated either in CC whole-cell or in loose patch recording.

No difference was detected between those temperatures in terms of depolarization (p=0.22, MWT), therefore data were pooled. A significant depolarization (3.2 ± 0.2 mV) was observed in all 12 (5 at 33°C + 7 at 22°C) HA neurons recorded (p<0.05, paired t-test) during GR 73632 perfusion, and later recovered after drug withdrawal (Fig.3-21A).

Increase of firing frequency caused by GR 73632 recorded in loose patch is smaller at 22°C than 33°C in the late phase of excitation (p<0.05, MWT) (Fig.3-21B). Therefore signalling cascade triggered through NK1R activation by GR 73632 action 10 minutes after drug withdrawal (in the frame of 20-25 minutes) was investigated under physiological conditions. Prolonged excitation caused by NK1R at 33°C was defined, like for TRPV1 activation by capsaicin (at 22°C), as long-lasting enhancement by GR 73632 (LLEGR>160%).

3.2.2.9. Second messenger systems recruited by NK1R

NK1 is a well-known G-coupled protein receptor but it is still unclear which phospholipase (PLC) is involved in NK1R signalling on HA neurons. In the cortex SP binds NK1R, activating the phosphatidylcholine-specific PLC (PC-PLC) (Endo et al., 2014), therefore one specific PC-PLC inhibitor, namely D-609, was applied to test this hypothesis.

D-609 30 µM in combination with GR 73632 10 nM is not able to reduce the amount of excitation ($304 \pm 48\%$ of control; n=4) induced by the NK1R agonist alone ($427 \pm 74\%$ of

control, n=6; p=0.12, MWT), leading to the conclusion that PC-PLC did not participate on NK1R-mediated signalling cascade on HA neurons.

The phosphatidylinositol-specific PLC (PI-PLC) was further considered as a possible candidate in NK1R-mediated cascade. A significant reduction of GR 73632 10 nM effect was indeed observed in the presence of U 73122 10 μM (a PI-PLC inhibitor) during the last phase to $181 \pm 35\%$ of control (n=5; p=0.04, MWT).

The common products of PLC specific cleavage are diacyl-glycerol (DAG) and inositol 1,4,5-trisphosphate (PI3). PI3 triggers the release of calcium from intracellular stores activating the phosphatidylinositol-3-kinase (PI3K). LY 294002 10 μM was tested to verify the PI3K inhibition. The PI3K inhibitor reduced the NK1R-induced excitation significantly to $164 \pm 32\%$ of control (n=6; p=0.007, MWT).

The last step of the considered transduction may involve the mitogen-activated protein kinase (MAPK), responsible for the gene expression. Application of MAPK inhibitor, U 0126 10 μM reduced GR 73632-mediated excitation during the last phase to $132 \pm 36\%$ of control (n=4; p=0.01, MWT) (Fig.3-21C right).

Occurrence and amplitude of the response during the first phase of application (8-14 minutes), were not changed for all considered cascade blockers (D-609: $228 \pm 27\%$ of control, p=0.28, MWT; U 73122: $219 \pm 37\%$ of control, p=0.3, MWT; LY 2940042: $163 \pm 21\%$ of control, p=0.24, MWT; U 0126: $160 \pm 15\%$ of control, p=0.56, MWT), compared to the action of GR 73632 10 nM alone (n=8; p=1, FEPT) (Fig.3-21C left).

Taken together these data showed that membrane depolarization caused by GR 73632 did not depend on temperature. Interestingly, not the first but the late phase of GR 73632-mediated excitation was enhanced during physiological conditions and involved PI-PLC, PI3K and MAPK.
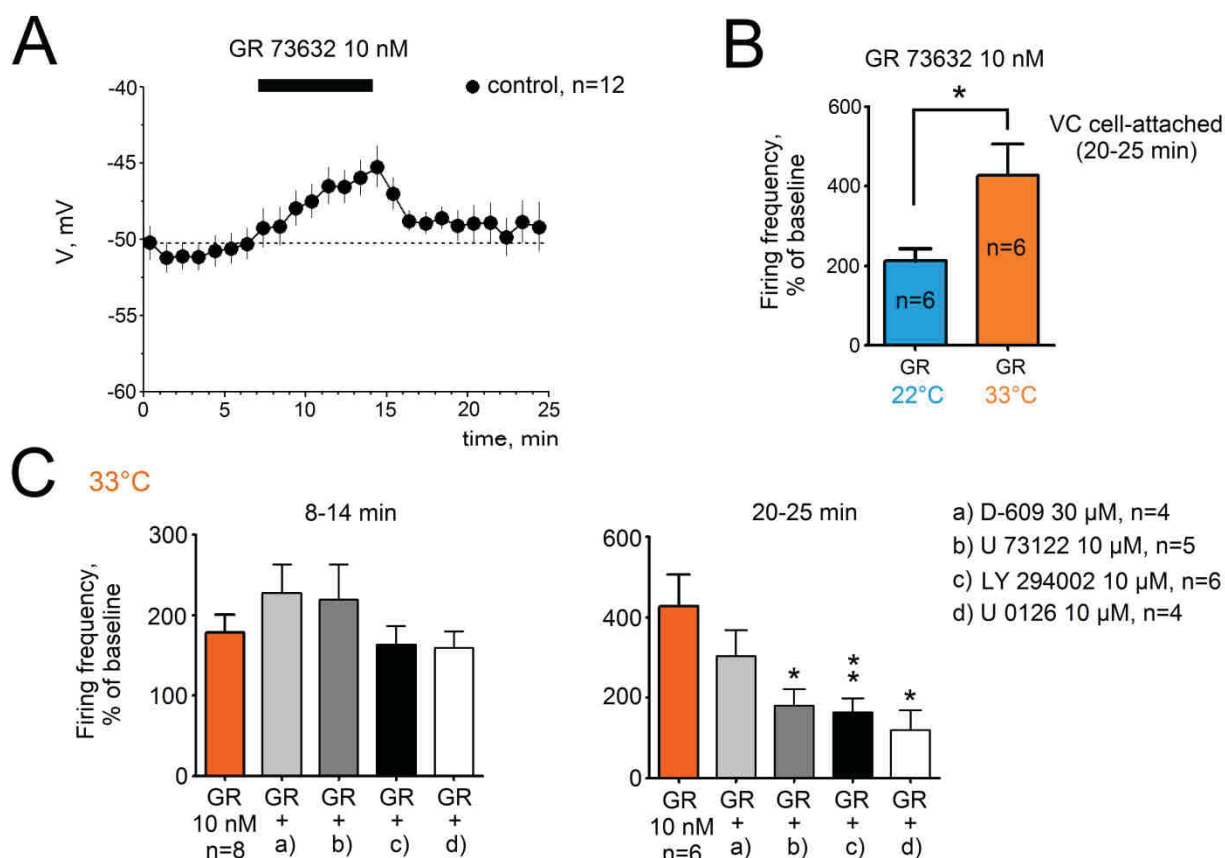
Fig.3-21. NK1R-mediated excitation depends on PI-PLC, PI3K and MAPK.
A. Membrane potential versus time diagram. No difference was seen between the membrane potential shifting between room and physiological temperature in response to GR 73632 on HA neurons (data were pooled). **B.** Bar histograms show relative increase in firing frequency (loose patch) during GR 73632 application is higher at 33 than 22°C. Number of neurons is written in the bars (* p<0.05, MWT). **C.** Block of phosphatidylinositol-specific phospholipase C (PI-PLC) by U73122, but not inhibition of phosphatidylcholine-specific PLC (PC-PLC) with D-609, abolished late phase (20-25 minutes after drug withdrawal) of GR 73632-mediated excitation. Inhibitor of phosphatidylinositol-3-kinase (PI3K) LY294002 and inhibitor of mitogen-activated protein kinase (MAPK) U0126, abolished LLEGR on HA neurons. Note that blockers of NK1R signaling cascade did not affect the first phase (8-14 minutes, after drug withdrawal) of GR 73632-induced excitation (* p<0.05; ** p<0.01, MWT).

3.2.2.10. NK1R activation caused calcium entry on HA neurons

NK1R immunostainings in Tmt-HDC-expressing neurons (4 cultures, p11-p13) revealed that the majority of Tmt-HDC-positive (n=58) and histamine-containing neurons (n=62) were immune-positive for NK1R (79% and 85%, respectively) without differences for NK1R-

expressing Tmt-HDC-positive and NK1R-expressing histamine-positive neurons, respectively (p=0.8, FEPT) (Fig.3-22A).

Histamine-negative Tmt-HDC-expressing neurons were discarded (in culture preparations some Tmt-HDC-positive cells may be non-HA). NK1R staining results in cultured neurons were not different from those calculated in slice about NK1R-co-localization in Tmt-HDC- and histamine-containing neurons (p=0.9 and p=0.1 respectively, FEPT).

In calcium imaging experiments the increase of calcium induced by GR 73632 perfusion was 31 ± 8 $\Delta F/F0$ (KCl was taken as reference) in Tmt-HDC-expressing neurons in culture, indicating a direct involvement of NK1R in calcium-dependent effects on HA neurons (Fig.3-22B).

These data confirmed that NK1R activation triggers the increase of intracellular calcium accompanying by excitation and depolarization on HA neurons.
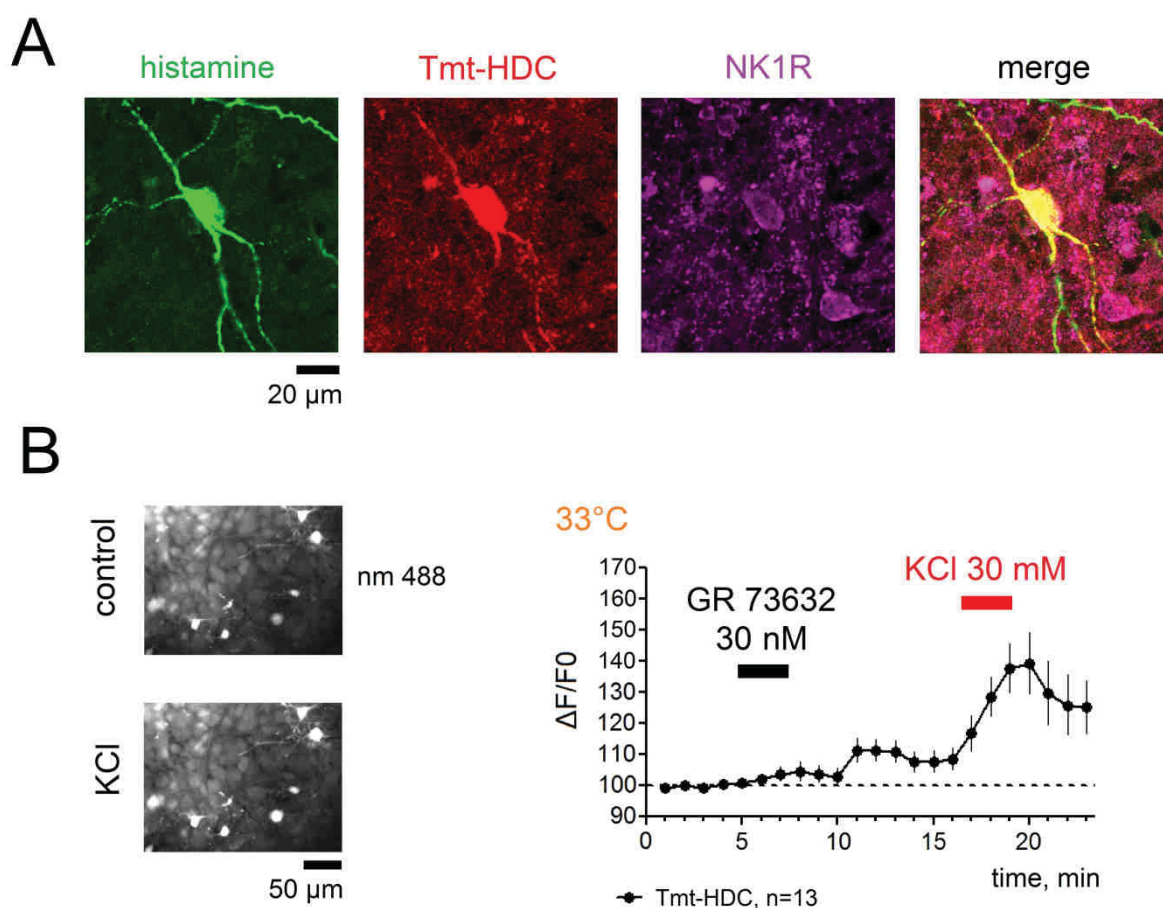
Fig.3-22. Calcium imaging in slice and cultured Tmt-HDC-expressing neurons.
A. Co-localisation of HA-(in green) and NK1R-(in pink) immunoreactivities with red Tmt-HDC fluorescence in mouse TMN primary culture. **B**. Increase of relative calcium fluorescence levels ($\Delta F/F0$) after GR 73632 perfusion in reference to the control in Fluo4-labelled Tmt-HDC/histamine-expressing neurons (right). KCl 30 mM perfusion was taken as positive control to test the specific neuronal responsiveness to the increase of potassium-induced calcium level (left).

3.2.2.11. NK1R activation in calcium-free solution

The majority of investigated HA E2 neurons (8 out of 11, $p<0.05$ paired t-test) was excited by GR 73632 10 nM in calcium-free to $139 \pm 23\%$ of control, during the bath perfusion (7 minutes) and to $154 \pm 25\%$ of control after 10 minutes of drug withdrawal from the bath, at 22°C. Occurrence for GR 73632-mediated response did not change between normal ACSF and calcium-free solution ($p=0.6$, FEPT). Increase of firing was unchanged during first phase ($p=0.1$, MWT) but higher during late phase of NK1R-mediated excitation in HA neurons recorded in normal ACSF compared to calcium-free condition ($p=0.03$, MWT).

3.2.2.12. Glutamate contribution during NK1R-mediated excitation

Since juvenile HA neurons express higher levels of glutamate receptors than adult, in particular mGluR5, the role of glutamate release for the maintenance of NK1R-induced excitation was explored. In addition to AMPA and NMDA receptors antagonists also a mGluR5 antagonist called 2-methyl-6-(phenylethynyl)pyridine (MPEP), was tested.

All juvenile HA E2 neurons investigated (n=4), were excited by GR 73632 10 nM in the presence of MPEP to $174 \pm 58\%$ of control, during first phase and to $296 \pm 52\%$ of control in the late phase ($p<0.05$, paired t-test). The amount of GR 73632-mediated excitation during mGluR5 receptor block, showed no difference during both, the first phase ($p=0.56$, MWT), and the late phase ($p=0.17$, MWT) compared to the drug alone, that indicated no participation mGluR5 for the maintenance of the excitatory effect. Occurrence between GR 73632 application alone and in the presence of mGluR5 antagonist showed no difference ($p=1$, FEPT).

Finally, a possible glutamate contribution through AMPA and NMDA receptor activation in NK1R-mediated excitation was investigated:

The amount of GR 73632-mediated excitation during the blockage of AMPA, NMDA and GABAA receptors, showed no difference during the first phase ($p=0.72$, MWT), but did so in the late phase (less excited to $170 \pm 53\%$ of control, $p=0.03$, MWT) compared to the drug alone, indicating also an AMPA and NMDA-receptors contribution for the maintenance of excitation.

These data showed that LLEGR depends on glutamate release directed to activate AMPA and NMDA receptors in a not age-dependent mechanism. Notably, TRPV1 and NK1R activation by capsaicin and GR 73632 respectively, are not comparable processes. Even though both of them caused LLE and trigger calcium-dependent signalling pathways on HA

neurons, GR 73632-induced depolarization is not sustained like that caused by capsaicin. Moreover, additional extracellular calcium entry through voltage-gated channels that impairs H3R functionality is limited in the absence prolonged depolarization. Accoording to these evidences, all HA neurons recorded after GR 73632 application presented a clear inhibition after RAMH perfusion, indicating a preservation of H3R-mediated auto-inhibition.

3.2.3. OLDA increases firing of HA neurons.

3.2.3.1.TRPV1-mediated effect of OLDA on HA firing frequency in vTMN

OLDA (0.2-2 µM) significantly increased firing frequency of majority of HA neurons of vTMN: 20 out of 22 tested. As no difference was noticed between OLDA concentrations 0.2 and 2 µM data were pooled. In the TRPV1 KO mice first phase of OLDA-induced excitation (during application time) was significantly impaired (Fig.3-23). As SP release is secondary to the TRPV1 activation, involvement of NK1R signalling pathway in the second phase of OLDA-evoked excitation in TRPV1 KO neurons could be excluded. Involvement of cannabinoid receptors was next investigated.
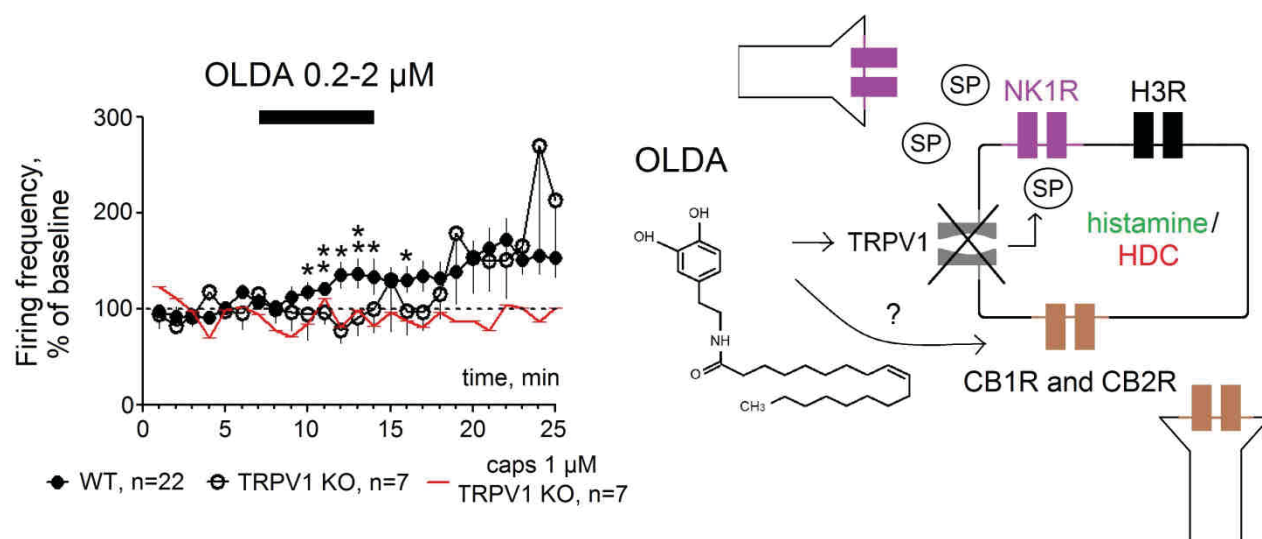
Fig.3-23. OLDA-mediated excitation of vTMN HA neurons is delayed in TRPV1 KO mice.
Second phase of OLDA-mediated excitation is a TRPV1 independent mechanism (* $p < 0.05$; ** $p < 0.01$, MWT).

3.2.3.2. WIN 55-212,2 increases firing frequency of HA neurons of vTMN

As we already observed in midbrain DA neurons CB1R and CB2R activation after OLDA application in TRPV1 KO mice, we first investigated whether WIN 55-212,2 affects the firing frequency of HA neurons. A previous study showed that somata of these neurons are devoid of CB1R immunostaining whereas many axonal endings from yet unidentified

neurons to the TMN region are CB1R-positive (Cenni et al., 2006). We found that 10 nM of WIN 55-212,2 increases the firing frequency of juvenile HA neurons to 300 ± 5% of control (n=7, maximal effect observed during 7 minutes washout period). The effect of WIN 55-212,2 was similar at temperatures 22°C and 33°C, therefore recordings were pooled (Fig.3-24A). In the presence of the selective CB1R antagonist AM251 (1 µM), which did not affect firing of TMN neurons on its own, the effect of WIN 55-212,2 was still present (165 ± 6% of control, during the last part of application period, Fig.3-24A) indicating that CB2R may be also involved. Amplitude of eAPC was not changed in the presence of WIN 55-212,2 (Fig.3-24A, open circles), which demonstrates lack of change in membrane potential. WIN 55-212,2 was not active in the presence of gabazine (10 µM), CNQX (20 µM) and D-AP5 (50 µM) in 4 neurons tested (Fig.3-24B). Furthermore, WIN 55-212,2 at 1 µM enhanced the firing frequency similarly in juvenile and adult HA neurons to 232 ± 5% of control.
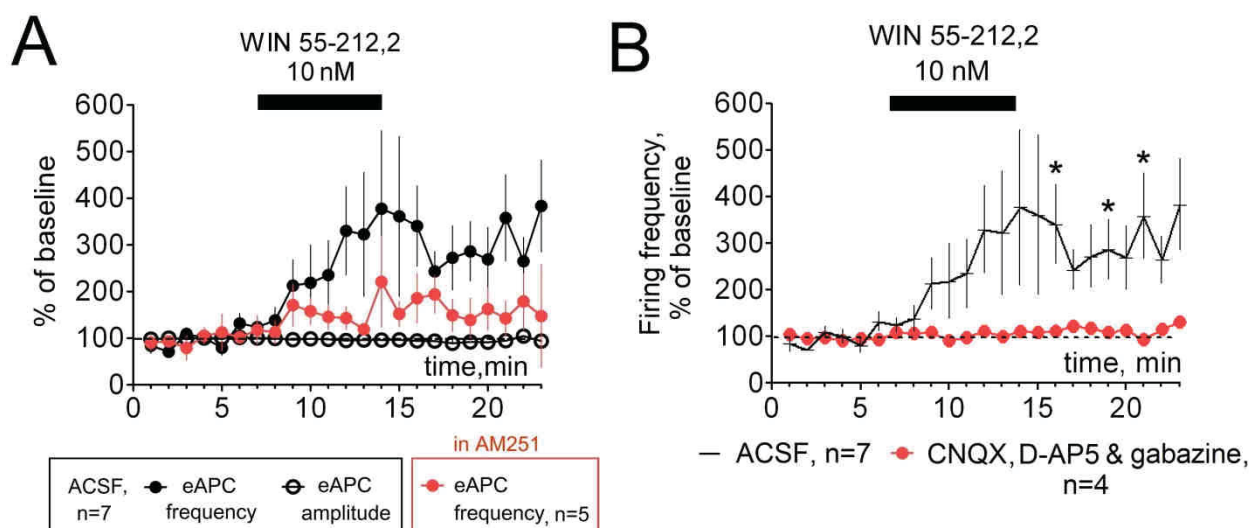
Fig.3-24. CB1 and CB2 receptor expression and function of vTMN HA neurons.
A. Increase in firing frequency of HA neurons of vTMN in response to WIN 55-212,2 is not strongly sensitive to the CB1 receptor antagonist AM251 (1 µM). eAPC amplitude remained unchanged during WIN 55-212, 2 perfusion. **B.** Increase in firing frequency of HA neurons of vTMN in response to WIN 55-212,2 is abolished in the presence of antagonists at ionotropic glutamate and GABA$_A$ receptors (* $p<0.05$, MWT).

GABAergic spontaneous IPSCs recorded from 5 Tmt-HDC neurons of vTMN (E2) displayed a reduced frequency in the presence of WIN 55-212,2 1 µM, whereas in 1 neuron the frequency of sIPSCs was increased, in all cases with no difference in amplitude of sIPSCs respect to control (Fig.3-25A). Thus the effect is presynaptic in line with a previous study (Cenni et al., 2006). We determined with scRT-PCR the expression of CB1 and CB2 receptors in 10 individual HDC-positive TMN neurons: none of them expressed CB1R,

whereas the CB2R-amplimer was detected in one neuron. Positive control processed in 2 ways (without or with RT) showed clear presence of CB1R transcripts in the TMN region, whereas CB2R expression remained unclear: RT+ and RT- samples looked similar on the gels (Fig.3-25B). Thus several lines of evidence support presynaptic expression of CB1R in the TMN region.
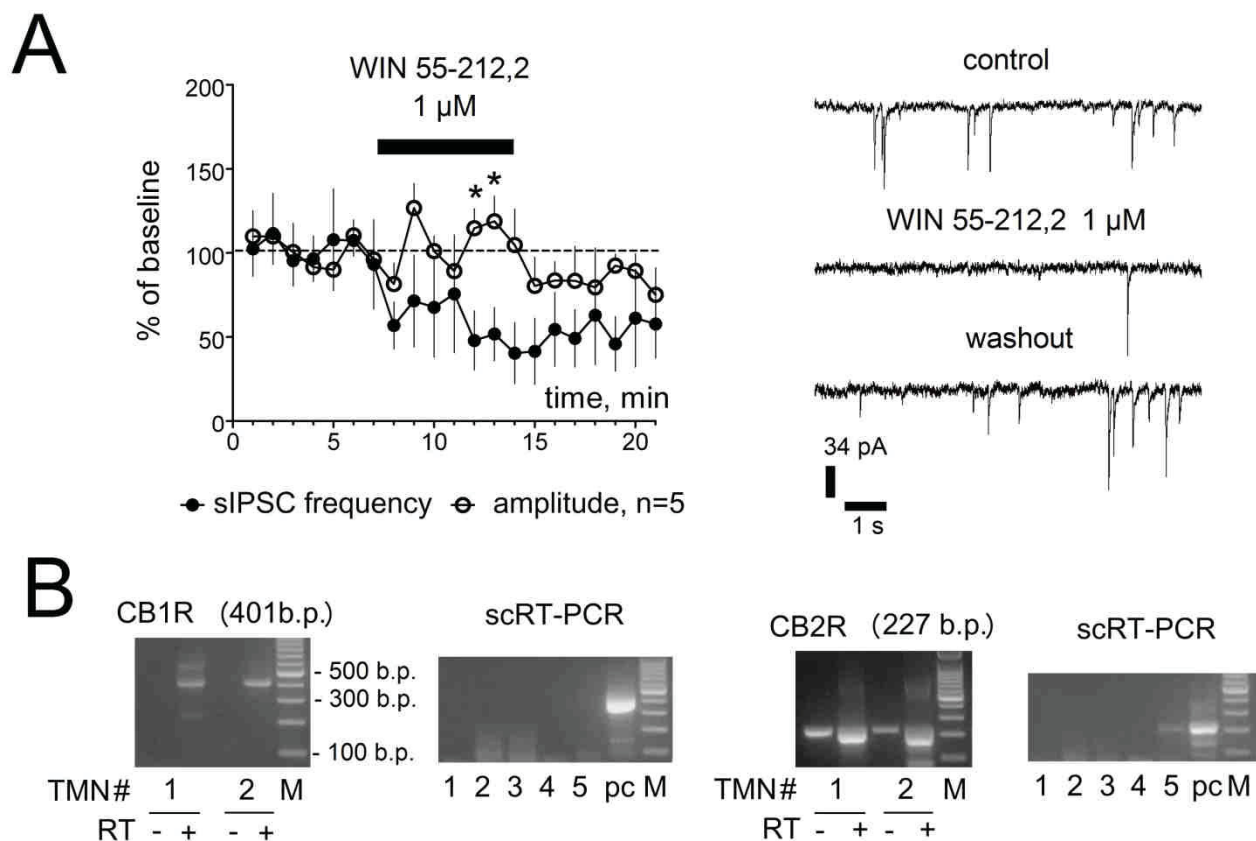
Fig.3-25. WIN 55-212,2 increases firing frequency of HA neurons through presynaptic mechanisms.
A. Time course of sIPSC frequency (closed circles) and amplitude (open circles) on the left and representative sIPSC original recording trace (right) illustrates effect of WIN 55-22,2 (1 μM). **B.** RT-PCR and scRT-PCR analysis of cannabinoid receptor expression in the whole TMN and on HA neurons, respectively (* $p < 0.05$, MWT).

3.2.3.3. OLDA excitation depends on CB1, CB2 and D2-type receptors

As dopamine and L-dopa excite HA neurons of TMN in a sulpiride-sensitive way (D2-type R-mediated) (Yanovsky et al., 2011) we applied OLDA to TRPV1 KO HA neurons in the presence of sulpiride (10 μM). Excitation by OLDA was slightly but not significantly reduced, representing on 23rd to 25th minute of the experiment (Fig.3-26A) $150 \pm 15\%$ and $135 \pm 10\%$ of baseline in control and with antagonist, respectively. When slices were

incubated with antagonists at D2-type R, CB1R (AM251) and CB2R (AM630) the excitation by OLDA was clearly reduced, although only data points at the 23rd minute of experiment reached the significance level (Fig.3-26B).
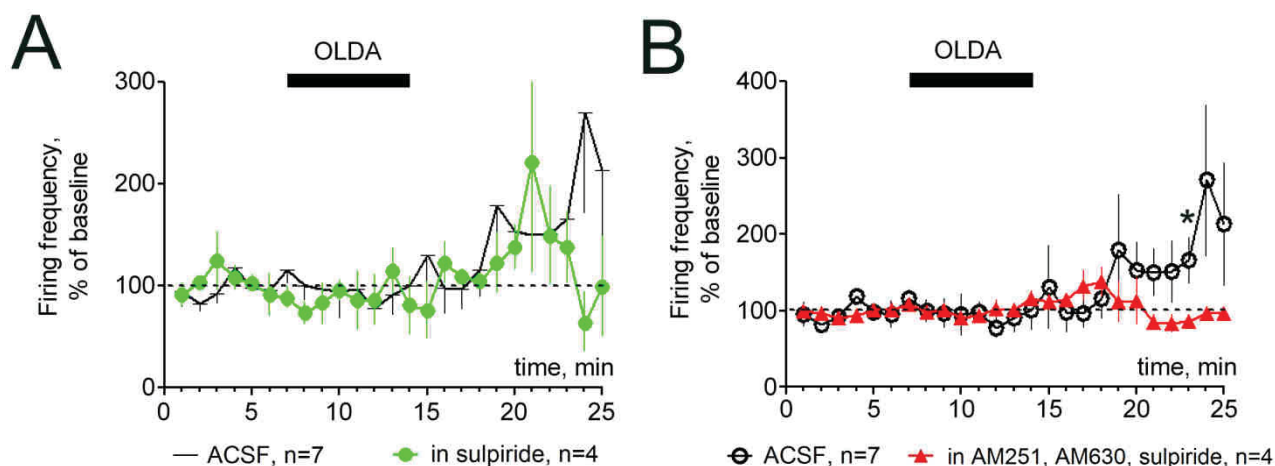
Fig.3-26. In TRPV1 KO mice OLDA-excitation of TMN neurons was abolished by antagonists of cannabinoid receptors and D2-type R.
A. In the presence of the D2-type R antagonist sulpiride (10 µM) OLDA excitation is largely preserved. **B.** In the presence of AM251, AM630 and sulpiride, OLDA does not increase firing frequency of HA neurons. Significant difference between data points is indicated with star (* $p < 0.05$, MWT).

3.2.4. Release of eCB is detected in SNc and vTMN using FAAH inhibitor URB597

The action of OLDA was compared with the action of the known FAAH inhibitor URB597 (1 µM), which lacks activity at dopamine receptors. URB597 significantly increased firing in 4 DA neurons and did not change it significantly in 2 neurons. On average frequency was incresed to $113 \pm 15\%$ of baseline (n=6, 7 minutes of washout period).

TRPV1 KO mice were used in these experiments. Combined application of CB1R/CB2R antagonists abolished the action of URB 597; in none of 4 neurons an increase in firing frequency was observed (Fig.3-27).
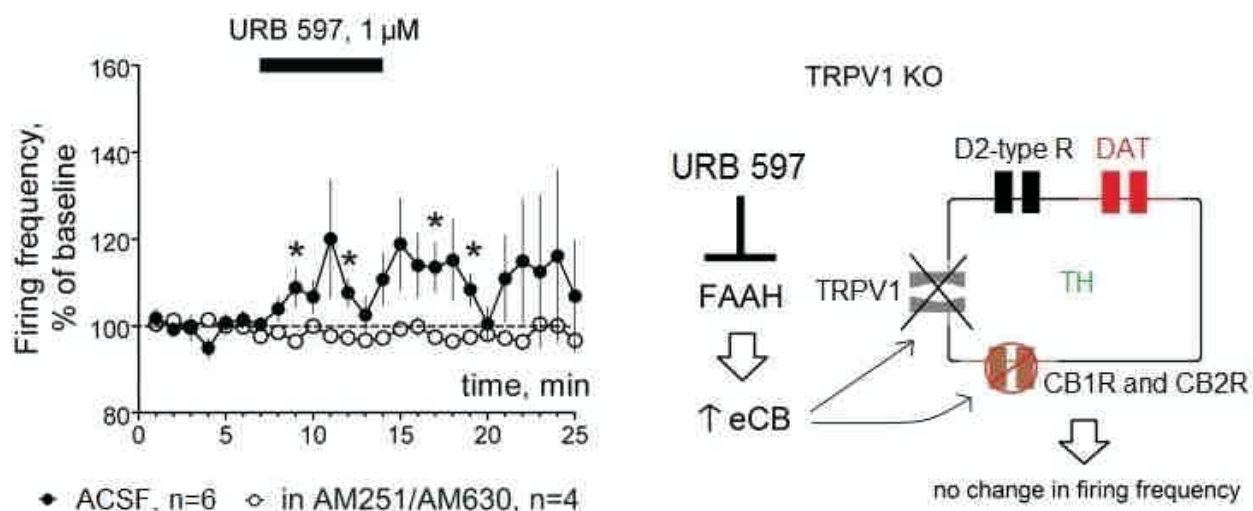
Fig.3-27. The FAAH inhibitor URB 597 increases firing frequency in SNc DA neurons from TRPV1 KO mice.
Antagonists of CB1 and CB2 receptors AM251 and AM630, respectively, abolish URB 597-induced excitation (* $p<0.05$, MWT).

URB597 significantly increased firing in 5 HA neurons of vTMN recorded at 33°C (to 150 ± 16 of baseline, during 7 minutes of washout period) and did not change dramatically firing in 5 neurons recorded at room temperature (107 ± 14% of baseline (7 minutes of washout period) (Fig.3-28). These experiments indicated a spontaneous release of eCB, such as anadamide (Piomelli et al., 2006) in SNc and TMN slices under our experimental conditions. Notably, eCB accumulation is not sufficient to induce a LLEcap-like response on HA neurons, suggesting that TRPV1 activation by eCB is not comparable to the capsaicin-mediated effect (Fig.3-28). H3R mediated auto-inhibition of HA neurons was preserved after OLDA or URB 597 treatment.
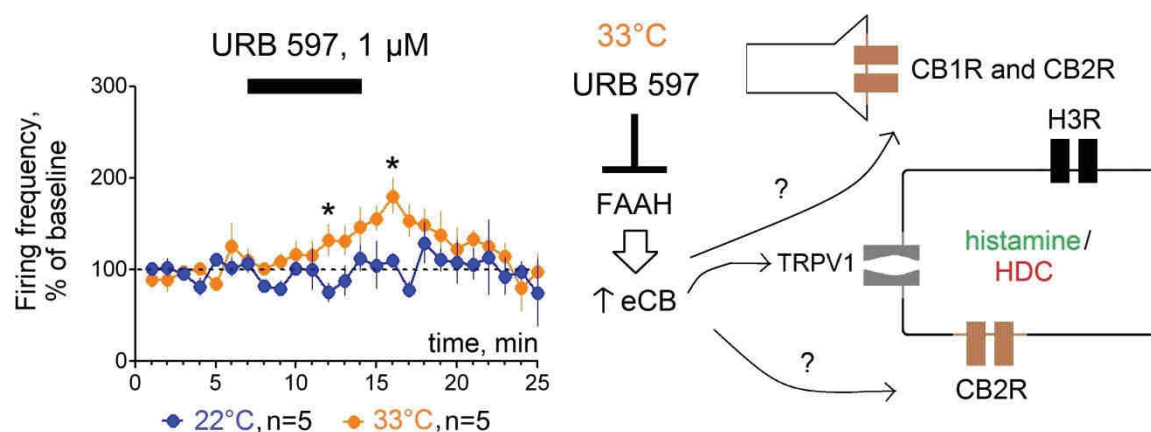
Fig.3-28. URB 597 increases HA firing frequency in a temperature-dependent manner.
URB 597 induces accumulation of some eCB during physiological conditions that in concert activate physiological targets such as CB1R and CB2R and TRPV1, the latter in a smaller extent compared with capsaicin-mediated effect (* $p<0.05$, MWT).

4. Discussion

Major findings of the present study:

(1) <u>Transgenic mouse lines expressing the reporter protein Tmt under control of a cell-specific promoter allow visualization of aminergic neurons in living brain slices.</u> However there is no strict co-localization of Tmt fluorescence with other markers of these neurons. In at least (10%) of aminergic neurons the Tmt protein is not expressed and *vice versa* some Tmt-expressing neurons do not belong to the aminergic group. Therefore pharmacological identification with drugs targeting auto-inhibitory receptors remains the most valid *criterium*. AP width can be used as an additional *criterium* for identification. The Tmt-DAT mouse helped the discovery of a new "conditionally DA" neuronal group in vTMN (E2).

(2) H3R mediated auto-inhibition of HA neurons is impaired by depolarization and low extracellular calcium.

(3) OLDA targets TRPV1 and CBRs in SNc DA neurons. In addition OLDA is a weak agonist at D2-type R (evidence obtained in TRPV1 KO mice).

(4) OLDA targets TRPV1 and CBRs in HA neurons of vTMN.

(5) Action of capsaicin (TRPV1 ligand) on HA neurons.

(sub 5_1) A heterogeneity in response to capsaicin, is described among HA neurons with respect to age, location and projections.

(sub 5_2) TRPV1 expression and function on HA neurons in TMN.

(sub 5_3) Autoinhibition of HA neurons is impaired by capsaicin.

(6) Mechanisms of long-term capsaicin-evoked excitation (LLEcap) of vTMN HA neurons involving SP and glutamate release are investigated.

(7) Release of eCB is detected in SNc and vTMN using the FAAH inhibitor URB 597.

4.1. Transgenic mouse lines expressing the reporter protein Tmt under control of a cell-specific promoter allow visualization of aminergic neurons in living brain slices

The experimental need for a safe identification of HA neurons in TMN led to the generation of HDC-*Cre* mouse lines (Yanovsky et al., 2012;Zecharia et al., 2012), which after crossing to reporter mouse lines such as CgGt(ROSA)26Sortm14(CAG−tdTomato) (JacksonLaboratory) allowed the direct visualization of living HA neurons (Tmt-HDC) in different TMN clusters during recording (Yanovsky et al., 2012). E2 groups of TMN are easily identified under DIC microscopy (in both rat and mouse), in contrast to HA neurons distributed in other clusters. E4 HA neurons are diffusely located around the third ventricle

(3V, a region with many non-HA neurons) and more scattered than E2 HA neurons. Co-localization of histamine immunoreactivity with Tmt-HDC (fluorescent tmt protein expressed under control of HDC promoter) was investigated in the E2 and E4 subdivisions of TMN of juvenile and adult mice. In accordance with a previous study (Yanovsky et al., 2012) 95% of the Tmt-HDC neurons of E2 from juvenile or adult mouse were found immunopositive for histamine.

The E4 region was characterized by Tmt-HDC-expressing neurons of different sizes and stages of maturation, with or without cellular processes in both age groups. Only large adult Tmt-HDC-positive neurons were found to produce histamine. Only 25% of Tmt-HDC E4 neurons in the juvenile stage were immunoreactive for histamine. Furthermore, both E4 and the small fraction of E2 histamine-positive neurons (10-25%) did not express Tmt-HDC, compromising the complete visualization of HA population in the region. For an unknown reason, some HA cells escaped targeting with the Cre-vector, thus remaining invisible in slice preparations. This should be considered for the future planning of experiments with optogenetic stimulation of HDC-Cre neurons or conditional knock-out of genes expressed in these neurons, keeping in mind that some fraction of HA neurons will remain intact.

Using Tmt-HDC reporter mice electrophysiological features of different subgroups of HA neurons (residing in E2 and E4), including Ih current, firing frequency, input resistance, eAPC duration and membrane potential were investigated: there were no differences. Even though E4 HA neurons showed larger HCN-mediated currents compared to E2, no substantial difference in their pacemaker firing pattern was observed.

HA neurons are not the only cell type inhabiting the TMN. Previous studies predicted presence of "conditionally DA" neurons in the caudal hypothalamus (Zoli et al., 1993);(Yanovsky et al., 2011). A DAT-Cre mouse line with 5 copies of the Cre-coding sequence was used to improve detection of transcriptional activity of the DAT-gene, which is expressed in the hypothalamus at a lower level compared to the midbrain DA neurons (Parlato et al., 2006). The function of DAT in this mouse line remains unimpaired as evidenced in experiments on uptake and accumulation of a fluorescent dopamine analog FFN-511 (Romano et al., 2013). The Tmt-DAT mouse line developed for the present study allowed for the first time direct visualization and recordings from hypothalamic DA neurons. We found a small number of Tmt-DAT-expressing neurons (histamine-negative) intermingled with the HA cluster (DAT-negative) in vTMN (De Luca et al., 2016). Focusing mainly on the E2 region a comparative morphological, histochemical, electrophysiological, molecular and pharmacological characterization of Tmt-DAT and HA neurons was

performed. Aminergic neurons possess similarities in their electrophysiological properties (such as: firing, action potential duration longer than 1.5 ms, presence of Ih (HCN) and Ia (delayed potassium current, necessary for the pacemaker activity). This study shows that the Ih current is not present in many HA neurons of the mouse (De Luca et al., 2016) and thus cannot be used for their identification. Interestingly, a similar conclusion was reached in studies on mouse midbrain DA neurons, which, in contrast to the rat neurons, express HCN-mediated currents infrequently (Ungless and Grace, 2012). Full expression of typical DA markers such TH, DDC, DAT and VMAT2, identifies the true DA nature of VTA or SNc neurons. Surprisingly, Tmt-DAT-positive neurons in E2 (vTMN) lacked TH expression, but frequently expressed DDC and VMAT2, suggesting that these neurons could produce, store and release dopamine, if L-dopa is available in the extracellular space. Therefore these neurons were defined as "conditionally DA" (De Luca et al., 2016). Further studies should investigate the functional role and connectivity of these neurons under specific conditions (i.e. under optogenetic stimulation and after L-dopa treatment). Interestingly, HA neurons lacking TH and DAT but expressing DDC and VMAT2, can also produce and release but not store dopamine (Yanovsky et al, 2011). We found that Tmt-DAT neurons share electrophysiological properties with HA neurons either at room or at a more physiological temperature (33°C). Apart from some membrane oscillations seen solely in Tmt-DAT-positive neurons the resting membrane potentials, Ih, input resistances, and firing frequencies were similar between HA and Tmt-DAT neurons. Differences were detected only for AP and eAPC duration (longer on HA neurons) and for the firing pattern, which was more irregular in Tmt-DAT-expressing neurons of vTMN with burst-like events observed in many neurons. The difference in firing patterns between HA and Tmt-DAT neurons was even more pronounced in calcium-free ACSF.

Although the soma size of Tmt-DAT neurons was smaller on average than that of HA neurons, some overlap was noted between individual values. Neuronal somata displaying diameters larger than 18 μm together with spontaneous regular firing safely define HA cells of vTMN. H1R expression was found only on Tmt-DAT neurons. In accordance, histamine-induced excitation recorded in these cells was abolished in the presence of H1R antagonist mepyramine.

In contrast to Tmt-DAT neurons of vTMN, the response to histamine 30 μM was inhibitory on HA neurons of vTMN due to the H3R-activation and lack of the expression of other histamine receptors. In conclusion, reporter mouse models provide the most reliable

identification of living aminergic neurons in vTMN. Pharmacological identification can be done on the basis of histamine receptor expression.

4.2. H3R mediated auto-inhibition of HA neurons is impaired by depolarization and low extracellular calcium

Pharmacological protocols represent the most reliable *criterium* for HA neurons identification. All HA neurons possess functional H3R. Application of RAMH or histamine caused inhibition of firing through selective H3R binding, limiting the activity of voltage-gated calcium channels (Takeshita et al., 1998). This inhibition is abolished in the presence of thioperamide, demonstrating a specific involvement of H3R in the auto-inhibition. The amount of H3R-mediated inhibition was indifferent between randomly recorded E2 HA neurons and those that project to the striatum, revealing that the functional presence of H3R on HA neurons is independent on projection areas (De Luca et al., 2016). This finding is possibly antithetical to conclusions from microdialysis experiments by Giannoni and co-workers (Giannoni et al., 2010;Giannoni et al., 2009). Co-release of histamine and GABA (outside of TMN, (Williams et al., 2014), from HA afferents in striatum or in the cortex, counteracting the pure histamine action on H3R may explain this discrepancy (Yu et al., 2015).

We have here revisited and clarified the patho-physiological conditions in which H3R functionality could be impaired compromising HA neuron auto-inhibition and so their true identification. Previous observations already reported that absence (or low levels) of extracellular calcium reduces significantly the binding affinity of H3R ligands (on presynaptic H3R) (Arrang et al., 1985). Moreover, depolarization of HA neurons increases intracellular calcium (Uteshev and Knot, 2005) through voltage-gated calcium channels. Therefore, histamine responses were studied under different conditions.

Potencies of histamine were compared between experiments done in normal ACSF and in calcium-free solution: the latter condition was accompanied by a dramatic reduction in histamine potency (increase of IC50). As calcium free-ACSF strongly depolarized HA neurons, we could not exclude the possibility that the reason for the reduction of histamine potency was depolarization alone. Sustained depolarization in normal ACSF significantly reduced H3R-mediated inhibition by histamine. Thus, depolarization without and in the presence of extracellular calcium leads to impairments of H3R-mediated inhibition on HA neurons.

Williams et al. (2014) showed that photo-evoked histamine release in vTMN does not affect firing frequency of HA neurons but suppresses GABAergic input to TMN via presynaptic H3 heteroreceptors (on GABAergic axons) thus promoting excitation of HA neurons. Thus, H3 heteroreceptors counteract the function of H3 autoreceptors on HA neurons. We did not see, however, an increase in H3R-mediated response in the presence of a GABA$_A$R antagonist (De Luca et al, 2016). This apparent controversy can be explained considering the differences between response to exogeneous histamine in slices and response to endogenous histamine released by optogenetically-induced prolonged depolarization of HA neurons *in vivo*.

Involvement of intracellular calcium in modulation of auto-inhibition was investigated now with different approaches, including electrophysiological and pharmacological ones. Thus thapsigargin (blocker of calcium ATPase which moves calcium ions from cytosol into intracellular stores) significantly decreased inhibition of firing frequency caused by histamine, which is in line with the previous study by Bongers et al (Bongers et al., 2007). Effector channels mediating H3R autoinhibition of HA neurons were not investigated now. A number of calcium channels are considered candidates as they are partially blocked by H3R activation (Takeshita et al., 1998). Further signalling pathways activated by H3R in HA neurons await characterisation and may employ modulation of potassium currents (Lundius et al., 2010);(Sethi et al., 2011);(Zhou et al., 2006). Moreover, hypertonic or ice-cold medium might affect H3R sensitivity and distribution on the cell membrane, thus increasing desensitization or cellular internalization of this receptor (Osorio-Espinoza et al., 2014).

4.3. OLDA targets TRPV1 and CBRs in SNc DA neurons. In addition OLDA is a weak agonist at D2-type R (evidence obtained in TRPV1 KO mice)

In addition to the development of neuronal identification protocols, a second goal of the present study was analysis of the targets of OLDA in mouse aminergic neurons. As it was known from previous studies that the TRPV1 (or capsaicin receptor) is a major target of OLDA, we used TRPV KO mice in comparison to WT in our recordings from DA and HA neurons. Firing frequencies and eAPC durations were not different between SNc DA neurons recorded from WT and TRPV1 KO mice.

OLDA at 0.2 or 2 µM increased firing on identified DA neurons of SNc in WT mice and slightly but significantly inhibited firing in TRPV1 KO mice suggesting that in this brain region OLDA shows minimal interaction with D2-type R. Involvement of D2-type R was evident from experiments with sulpiride (selective antagonist of D2-type R), which reversed

OLDA-mediated inhibition of firing to an excitation, that was blocked by the CB1- and CB2-receptor antagonists AM251 and AM630, respectively. TRPV1 and eCB receptors expression and functions were already described in the midbrain DA neurons (Marinelli et al., 2003, 2005, 2007). Briefly, CB1R and TRPV1 regulate presynaptically glutamate and GABA release in VTA and SNc, whereas CB2R action is probably postsynaptically inhibitory on VTA neurons (Zhang et al., 2014). The present work shows for the first time that activation of these receptors also affects firing of DA neurons. Application of WIN 55-212,2 and capsaicin showed that cannabinoids and vanilloids, respectively, excite DA neurons of SNc. As responses were small their pharmacology was not further investigated. However, they were comparable in amplitude to the excitatory action of OLDA. Thus interaction with these receptors dominates pharmacological response to OLDA in WT SNc neurons masking inhibition through the D2-type R. Weak D2-type R- mediated inhibition of DA neuron firing revealed in TRPV1 KO mice should be investigated further, e.g. on recombinant D2-type receptors. It is still unclear whether OLDA itself, its metabolites or endogenous dopamine are responsible for the observed effect. It was shown that NADA neither bind to D2-type receptors nor to TRPV1, but interacts with CB1R (Chu et al., 2003), thus possessing distinct from OLDA features.

4.4. OLDA targets TRPV1 and CBRs in HA neurons of vTMN

OLDA action on firing of HA neurons was investigated in WT and TRPV1 KO mice. Firing frequencies and eAPC duration were similar between neurons with these two genotypes.

The first phase of OLDA-evoked excitation of HA neurons was abolished in TRPV1 KO mice. The remaining excitation was further investigated: We can exclude the involvement of SP release and NK1R, as this pathway is located downstream to the TRPV1 activation (see below). We can also exclude release of eCB due to the ability of OLDA to block FAAH (Chu et al., 2003): application of URB 597 had no effect on HA neuron activity recorded at room temperature. Thus reduction of OLDA-mediated excitation by AM251 and AM630 (antagonists of CB1 and CB2 receptors, respectively) indicated direct interaction of OLDA with these receptors. No significant action of sulpiride (D2-type receptor antagonist) was observed on the OLDA response; however combination of all three aforementioned antagonists significantly reduced the last phase of the response. Further receptors could be involved in the OLDA action in TMNv, e.g. GPR119. The action of an anorectic ligand of this receptor, OEA, depending on the intact HA system (Provensi et al., 2014), awaits to be tested on firing activity of HA neurons. The functional role of cannabinoid receptors whose

involvement in the OLDA action was demonstrated in experiments with antagonists was investigated further with WIN 55-212,2, a non selective ligand of CB1 and CB2 receptors (Saez et al., 2014). As the excitatory action of WIN 55-212,2 on neuronal firing was abolished in the presence of GABAA and fast ionotropic glutamate receptors antagonists, we exclude a direct postsynaptic action of this compound. We concluded that CB1 and CB2 receptors regulate presynaptic GABA release on HA neurons (Fig.3-24). HA neurons recorded in slices lack glutamatergic spontaneous synaptic currents (Parmentier et al., 2009). However tonic release of glutamate may decrease excitability of HA neurons through NMDA receptors (Faucard et al., 2006) and CB1R antagonising NMDA action (Liu et al., 2009) may promote excitation of HA neurons. However this possibility needs to be tested in the future. In support of presynaptic action, WIN 55-212,2 decreased frequency of GABAergic sIPSCs without modulation of their amplitude and did not affect amplitude of eAPCs (indicates no change in membrane potential). OLDA action on HA neurons in the presence of GABAA and fast ionotropic glutamate receptors antagonists will clarify participation of presynaptic and postsynaptic sites more precisely in the future.

4.5. Action of capsaicin (TRPV1 ligand) on HA neurons.

4.5.1. A heterogeneity in response to capsaicin, is described among HA neurons with respect to location, age and projections

Action of OLDA was compared with that of the classical ligand of TRPV1 capsaicin.

Functional heterogeneity of HA neurons located in different TMN subdivisions (E2 or E4) in response to capsaicin was detected. Several studies described the HA system as a uniform center with diffuse projections whereas others recognised few specific functions allocated to subgroups E4 & E5 (such as an increase in c-Fos expression after foot shock or insulin-induced hypoglycemia) (Blandina et al., 2012;Miklos and Kovacs, 2003).

The vast majority of adult HA neurons projecting to the striatum were not responsive to capsaicin, whereas the majority of cells retrogradely labelled from the brainstem were excited by capsaicin. Interestingly, NTS and striatum showed low and high expression levels of endogeneous TRPV1 ligands such as: NADA (Huang et al., 2002) and OLDA (Ferreira et al., 2009), respectively. Thus, endogeneous ligands of TRPV1, which are also produced in brain slices (conclusion drawn from our experiments with URB 597) may interfere with action of capsaicin or/and with the expression of TRPV1. This possibility should be further experimentally analysed. Recordings performed now from E4 Tmt-HDC neurons demonstrated that the majority of these neurons responded to capsaicin with an increase in firing, whereas only 25% of adult E2 neurons were responsive. The finding that a majority of

adult Tmt-HDC located around 3V are sensitive to capsaicin is in line with a study by Cavanaugh and co-workers (Cavanaugh et al., 2011), where, using a TRPV1 mouse reporter, unidentified TRPV1-expressing neuronal groups around 3V have been recorded, whereas lateral hypothalamic areas were mostly negative for TRPV1.

In the present study transcription of TRPV1 gene was found higher in adult E4 compared to the E2 region. In line with electrophysiological data, a developmental decline in encoding for TRPV1 mRNA level was observed in E2: it was nearly 3 fold higher in juvenile than in adult vTMN. Thus these data reveal for the first time a region-, projection site- and age- related heterogenity of HA neurons in their responses to TRPV1 ligand capsaicin. Behavioral correlates and the physiological activation mode of these receptors (e.g. by anandamide or OLDA) remain to be investigated in the future.

Possible physiological functions of TRPV1 are briefly discussed below but remain speculative at present. 1) Several studies reported that TRPV1 is involved in cell-death mechanisms inside or outside CNS, through increase of intracellular calcium levels triggering caspase-3 activation (last apoptotic effector) (Leonelli et al., 2011)(Nazıroğlu et al., 2014). Increasing HA excitability by TRPV1 may be useful for the structural organization of E2 during the immature stage in order to reach the final neuronal number during adulthood. E4 shows the interesting feature of a "permanent active" germinal zone especially for HA neurons generation. A possible role of TRPV1 for neuron generation as well as for autonomous functions in this area request further research 2) The maintenance of a fraction of capsaicin-sensitive HA neurons in adult E2 could be related to a cell-to-cell heterogeneity in the regulation of physiological functions, such as breathing or/and chemo-sensing. HA neurons projecting to the NTS possess functional TRPV1 channels and acid sensing ion channels (ASICs) which ensure them a position next to the orexin/hypocretin neurons in central chemosensing (Kernder et al., 2014).

Descending projections of the HA system are largely unexplored but mutual interactions with different systems were previously reported (Haas et al., 2008). The NTS receives, through the glossopharyngeal nerve, peripheral informations about blood chemical composition from the *glomus caroticum* and drives them back to the hypothalamus for the central regulation of vegetative functions. The NTS is characterized by clusters of catecholaminergic neurons that express TH. In addition, a dense HA innervation together with expression of presynaptic H3 and postsynaptic H1 receptors were reported in this region (Kanamaru et al., 1998). HA and glutamate release in NTS can be modulated by several conditions (like a robust induced depolarization) involving respectively H1, H3 receptors and

presynaptic TRPV1 (Fawley et al., 2014), but the role of HA innervation and properties of HA neurons projecting to NTS are still unclear. The present study is a first attempt towards characterization of features of HA neurons regulating vegetative functions.

4.5.2. TRPV1 expression and function in juvenile HA neurons of vTMN

Recordings from the juvenile E2 region showed that the exogenous TRPV1 agonist capsaicin strongly depolarized and increased firing frequency of the majority of HA neurons (17 out of 22 in concentration 1 μM and in 8 out of 10 in concentration 100 nM). Dose-dependent TRPV1-mediated currents have been observed in AIN after capsaicin application, indicating the specific postsynaptic site of action. In accordance with previous studies on neurons (Ferrini et al., 2010) we also detected a presynaptic modulation of GABAergic inputs to HA neurons by capsaicin: thus at 100 nM capsaicin reduced frequency of sIPSCs to 85 ± 3 % of control (n=5) (De Luca and Sergeeva, unpublished observation). Thus both: postsynaptic and presynaptic actions of capsaicin promote excitation of HA neurons.

In the cell-attached mode of patch-clamp recordings we noticed an unusually long lasting excitatory effect of capsaicin (called LLEcap), when a concentration of 1 μM but not of 100 nM was used. The first phase of the capsaicin response and LLEcap were abolished in TRPV1 KO mice. In search for the immunohistochemical evidence for the TRPV1 protein expression in vTMN we performed IHC in WT and TRPV1 KO cultures and brain slices. Unspecific binding of primary antibody in these experiments compromised the results: no difference between genotypes was seen (Fig.3-13).

4.5.3. Autoinhibition of HA neurons is impaired by capsaicin

Capsaicin-induced excitation could impair H3R-mediated inhibition, most likely due to the sustained depolarization and increased intracellular calcium levels following TRPV1 activation. In many retrobeads-containing neurons traced from NTS, which were strongly excited by capsaicin, subsequent application of RAMH did not inhibit firing. On the other hand all recorded E2 neurons traced from striatum were inhibited. In capsaicin-responding Tmt-HDC neurons, which were visually identified in slices before capsaicin application, H3R mediated autoinhibition was significantly impaired (De Luca et al., 2016).

In order to find out the experimental conditions to observe H3R-mediated inhibition after strong TRPV1 activation on HA neurons, capsaicin recordings were performed in calcium-free ACSF. TRPV1 is a channel permeable for both, sodium and calcium; capsaicin-induced excitation of Tmt-HDC-cells was still present but smaller in amplitude in calcium-free ACSF

compared to the control experiments. Surprisingly, H3R-mediated inhibition induced by RAMH was indistinguishable from control experiments in calcium-free ACSF. To conclude, activation of TRPV1 in the absence of extracellular calcium does not impair H3R-mediated autoinhibition. Future steps would be to record retrobeads-containing neurons traced from NTS located in the E2 and E4 regions, in calcium-free solution in order to determine their HA nature though H3R activation.

4.6. Mechanisms of long-term capsaicin-evoked excitation (LLEcap) of vTMN HA neurons involving SP and glutamate release are investigated

As developmental downregulation of TRPV1 expression in posterior hypothalamus and a decrease of the number of vTMN HA neurons responding to capsaicin was found, the underlying mechanisms were further investigated. As glutamate release occurs in the hypothalamus in response to capsaicin (Karlsson et al., 2004)(Bourque et al., 2007) and downregulation of some subunits of ionotropic glutamate receptors was described in TMN with brain maturation (Kernder et al, 2014), the effect of antagonists of metabotropic and ionotropic glutamate receptors on LLEcap was investigated. HA neurons are densely innervated by glutamatergic Hcrt/Orx fibers and also receive projections from preoptic area or lateral hypothalamus (Yang and Hatton, 1997) but the source of glutamate in vTMN is still unclear. Their fast desensitization may have prevented demonstration of an involvement of AMPA receptors in proton-sensing by HA neurons, whereas the role of metabotropic glutamate receptors was demonstrated (Yanovsky et al. 2012). NMDA receptors are also expressed on HA neurons, but their activation can only be detected in magnesium-free solution (Schubring et al., 2012). None of glutamate receptor antagonists significantly affected LLEcap. This may mean that the ambient glutamate level is high at room temperature and in addition, TRPV1-mediated release plays no role; or AMPA /NMDA/mGluR receptors play no role in LLEcap. The role of glutamate receptors in capsaicin or/and OLDA action should be further tested at more physiological temperature (33°C). As activation of presynaptic TRPV1 channels increases release of SP (Julius, 2013), two antagonists of NK1R were tested: each of them abolished LLEcap leaving intact the immediate response through direct activation of postsynaptic TRPV1.

Neuropeptides play a major role in the control of the sleep-awake cycle. Antagonism at SP receptors reduces arousal, facilitating sleep (Ratti et al., 2013). SP was the first detected neuropeptide (von Euler and Pernow, 1956) belonging to the neurokinins (NKs), discovered in brain and enteric nervous systems (Leeman, 1980). SP is a most important "brain-gut

neuropeptide" binding to all three types of NK receptors (NK1R, -2R and -3R), with highest affinity for NK1R (Maggi and Schwartz, 1997). In addition, it is the first neuropeptide acting in pain transmission, expressed in a subgroup of primary C-fibers-expressing in DRG neurons, that project from the spinal horn directly to peripheral tissues. Together with NK1R, TRPV1 is expressed on the postsynaptic membrane of DRG neurons, thus resulting in the transmission of nociceptive informations. Activation of TRPV1 and ASICs (Boillat et al., 2014) promote glutamate release from presynaptic terminals (Kim et al., 2009) triggering the local release of SP and HA (Julius, 2013), that in concert amplify TRPV1 signalling, with NK1R, mGluR1/5 (Crawford et al., 2000) and H1R involved (Kajihara et al., 2010).

qRT-PCR analysis showed that the NK1R was equally expressed in juvenile and adult TMN. Most HA neurons were immunopositive for NK1R. Thus the capsaicin amplifying action of NK1R does not contribute to the developmental downregulation of TRPV1-mediated excitability of HA neurons. The selective agonist of NK1R, GR73632 depolarized HA neurons and increased their firing frequency (effect was significantly larger at 33°C than at room temperature). NK1R-mediated excitation depended on PI-PLC, PI3K and MAPK. GR73632-mediated long-term excitation of HA neurons was significantly reduced in the presence of ionotropic glutamate receptor antagonists and gabazine (GABAA receptor antagonist). Thus LLEcap depends on SP release, involving NK1R. Due to the temperature sensitivity of TRPV1 all experiments were performed at room temperature where pharmacological activation of this channel could be better controlled. A secondary role of glutamate for the LLEcap downstream to the NK1R activation especially at physiological temperature can not be excluded.

4.7. Release of eCB is detected in SNc and vTMN using the FAAH inhibitor URB597

The FAAH inhibitor URB597 (1 µM) was used to compare its action with OLDA, which possesses weak antagonistic properties towards FAAH and is not cleaved by this enzyme. Similarities between the actions of OLDA and a FAAH inhibitor were detected. The increase in firing of SNc DA neurons (in TRPV1 KO mice) in the presence of URB 597 was abolished in the presence of CB1 and CB2 receptors antagonists.

In vTMN URB597 did not affect firing of HA neurons when recordings were done at room temperature. At 33°C URB 597 transiently and reversibly increased firing of HA neurons. Thus eCBs are spontaneously produced and degraded in brain slice preparations; however in TMN these processes are temperature-dependent. Increase in firing frequency of HA neurons by OLDA recorded at room temperature thus is independent of FAAH blockade.

5. Summary

The histaminergic (HA) neurons are located in the tuberomamillary nucleus (TMN) of the posterior hypothalamus and fire exclusively during wakefulness. Through their widely branching projections they control many functions of the central nervous system (CNS), like cortical activation, consciousness, maintaining the waking state as well as the homeostasis of energy administration and the endocrinium. Histamine acts as a neurotransmitter in the mammalian brain mainly through H1R, H2R and H3R (receptors). The H3R are autoreceptors inhibiting histamine synthesis and release as well as the firing of HA neurons. H3R antagonists / inverse agonists increase vigilance; at least one substance is now in clinical use for narcolepsy and other causes of daytime sleepiness: Pitolisant (Wakix) improves also some symptoms of "dopaminergic (DA) diseases" like morbus Parkinson. A previous study (Yanovsky et al., 2011) has shown that L-dopa and dopamine excite HA neurons of rat TMN indicating a synergism between DA and HA systems in the control of arousal.

The present work followed two aims: (1) development of identification protocols for DA and HA neurons in novel transgenic mouse lines; (2) elucidation of mechanisms of action of a conjugate of dopamine with N-oleic acid: N-oleoyl dopamine (OLDA), which is synthesized along with dopamine in catecholaminergic neurons.

Electrophysiological, molecular biological and immunohistochemical methods were employed for the characterization of the ion channels, receptors and signaling pathways mediating OLDA actions. Interactions with dopamine D2-type receptors, the capsaicin receptor (Transient Receptor Vanilloid 1, TRPV1) and cannabinoid receptors in mesencephalic DA neurons and HA neurons of TMN were studied. A heterogeneity of HA neurons in their sensitivity to capsaicin and roles of substance P (SP) and glutamate in the developmental down-regulation of this sensitivity are described. A new population of "conditionally DA" neurons was detected in TMN. New transgenic mouse lines allowing the visual identification of DA and HA neurons in living tissue with fluorescence microscopy were evaluated. In the course of these investigations the mechanism of a particular vulnerability of the H3R mediated autoinhibition was revealed, which needs to be considered in the clinical application of H3R antagonists.

6. Zusammenfassung

Die histaminergen (HA) Neurone liegen exklusiv im hinteren Hypothalamus, feuern strikt ausschließlich während Wachheit und kontrollieren durch weitverzweigte Projektionen über metabotrope Rezeptoren viele Funktionen des zentralen Nervensystems, wie Kognition, Energieverwaltung und das Endokrinium. Sie spielen eine zentral wichtige Rolle in der Aufrechterhaltung des Wachzustandes. Histamin wirkt als Transmitter im Säugerhirn vorwiegend über H1-, H2- und H3-Rezeptoren. Die H3-Rezeptoren sind Autorezeptoren, die Synthese und Freisetzung von Histamin sowie die Aktivität der HA Neurone hemmen. Antagonisten bzw. inverse Agonisten steigern deshalb die Vigilanz und werden derzeit mit der Indikation Narkolepsie und andere Tagesschläfrigkeit in die Klinik eingeführt. Die erste zugelassene Substanz (Pitolisant, Wakix) verbessert auch die Symptomatik „dopaminerger (DA) Erkrankungen" wie M. Parkinson. Eine frühere Arbeit (Yanovsky et al., 2011) hat gezeigt, dass L-Dopa und Dopamin HA Neurone im TMN der Ratte erregen und einen Synergismus zwischen DA und HA Systemen bei der Steuerung der Wachheit vorgeschlagen.

Die vorliegende Arbeit verfolgte zwei Ziele: (1) die Entwicklung von Protokollen zur Identifikation DA und HA Neurone in neuartigen transgenen Mauslinien; (2) Untersuchungen der Wirkungsmechanismen eines Konjugates von Dopamin mit N-oleoylsäure, N-oleoyl dopamin (OLDA), welches neben Dopamin in catecholaminergen Neuronen synthetisiert wird.

Elektrophysiologische, molekularbiologische und immunhistochemische Verfahren wurden herangezogen für die Charakterisierung der Rezeptoren, Ionenkanäle und Signalwege, die die Wirkung von OLDA vermitteln. In mesencephalen Dopamin-Neuronen und Histamin-Neuronen des tuberomamillären Kerns (TMN) im hinteren Hypothalamus wurden Interaktionen mit D2-type Rezeptoren, dem Capsaicin-Rezeptor (Transient Receptor Vanilloid 1, TRPV1) und Cannabinoid-Rezeptoren untersucht. Eine Heterogenität der HA Neurone bezüglich ihrer Sensitivität für Capsaicin und die Rolle von Substanz P sowie Glutamat in der entwicklungsbedingten Abnahme dieser Sensitivität werden beschrieben. Dabei wurde eine neue Population „konditionell DA" Neurone im TMN entdeckt. Neue transgene Mausmodelle wurden generiert und validiert, die die visuelle Identifikation DA und HA Neurone mit Fluoreszenzmikroskopie im lebenden Gewebe erlauben. Dabei wurde der Mechanismus einer Vulnerabilität der H3-Rezeptor-vermittelten Autoinhibition aufgedeckt, welcher bei der klinischen Anwendung dieser Substanzen zu berücksichtigen sein wird.

7. Literature

Abel JJ and Kubota S (1919) Presence of histamine (4-imidozoleethylamine) in the hypophysis cerebri and other tissues of the body and its occurrence among the hydrolytic decomposition products of proteins. J. Pharmacol. 13:243–300.

Agid Y (1991) Parkinson's disease: pathophysiology. Lancet 337:1321-1324.

Airaksinen MS, Alanen S, Szabat E, Visser TJ, Panula P (1992) Multiple neurotransmitters in the tuberomammillary nucleus: comparison of rat, mouse, and guinea pig. J Comp Neurol 323:103-116.

Arnulf I, Leu-Semenescu S (2009) Sleepiness in Parkinson's disease. Parkinsonism Relat Disord 15 Suppl 3:S101-4.

Arrang JM, Garbarg M, Schwartz JC (1983) Auto-inhibition of brain histamine release mediated by a novel class (H3) of histamine receptor. Nature 302:832-837.

Arrang JM, Garbarg M, Schwartz JC (1985) Autoregulation of histamine release in brain by presynaptic H3-receptors. Neuroscience 15:553-562.

Barzilai A, Melamed E (2003) Molecular mechanisms of selective dopaminergic neuronal death in Parkinson's disease. Trends Mol Med 9:126-132.

Begg M, Pacher P, Batkai S, Osei-Hyiaman D, Offertaler L, Mo FM, Liu J, Kunos G (2005) Evidence for novel cannabinoid receptors. Pharmacol Ther 106:133-145.

Berger JR, Vilensky JA (2014) Encephalitis lethargica (von Economo's encephalitis). Handb Clin Neurol 123:745-61.

Bisogno T, Melck D, Bobrov MY, Gretskaya NM, Bezuglov VV, De PL, Di M, V (2000) N-acyl-dopamines: novel synthetic CB(1) cannabinoid-receptor ligands and inhibitors of anandamide inactivation with cannabimimetic activity in vitro and in vivo. Biochem J 351 Pt 3:817-24.:817-824.

Blandina P, Munari L, Provensi G, Passani MB (2012) Histamine neurons in the tuberomamillary nucleus: a whole center or distinct subpopulations? Front Syst Neurosci 6:33.

Boeve BF, Silber MH, Saper CB, Ferman TJ, Dickson DW, Parisi JE, Benarroch EE, Ahlskog JE, Smith GE, Caselli RC, Tippman-Peikert M, Olson EJ, Lin SC, Young T, Wszolek Z, Schenck CH, Mahowald MW, Castillo PR, Del TK, Braak H (2007) Pathophysiology of REM sleep behaviour disorder and relevance to neurodegenerative disease. Brain 130:2770-2788.

Boillat A, Alijevic O, Kellenberger S (2014) Calcium entry via TRPV1 but not ASICs induces neuropeptide release from sensory neurons. Mol Cell Neurosci 61:13-22.

Bongers G, Bakker RA, Leurs R (2007) Molecular aspects of the histamine H3 receptor. Biochem Pharmacol 73:1195-1204.

Bourque CW, Ciura S, Trudel E, Stachniak TJ, Sharif-Naeini R (2007) Neurophysiological characterization of mammalian osmosensitive neurones. Exp Physiol 92:499-505.

Braak H, Del TK, Rub U, de Vos RA, Jansen Steur EN, Braak E (2003) Staging of brain pathology related to sporadic Parkinson's disease. Neurobiol Aging 24:197-211.

Calabresi P, Di FM, Ghiglieri V, Tambasco N, Picconi B (2010) Levodopa-induced dyskinesias in patients with Parkinson's disease: filling the bench-to-bedside gap. Lancet Neurol 9:1106-1117.

Caterina MJ, Leffler A, Malmberg AB, Martin WJ, Trafton J, Petersen-Zeitz KR, Koltzenburg M, Basbaum AI, Julius D (2000) Impaired nociception and pain sensation in mice lacking the capsaicin receptor. Science 288:306-313.

Caterina MJ, Schumacher MA, Tominaga M, Rosen TA, Levine JD, Julius D (1997) The capsaicin receptor: a heat-activated ion channel in the pain pathway. Nature 389:816-824.

Cavanaugh DJ, Chesler AT, Jackson AC, Sigal YM, Yamanaka H, Grant R, O'Donnell D, Nicoll RA, Shah NM, Julius D, Basbaum AI (2011) Trpv1 reporter mice reveal highly restricted brain distribution and functional expression in arteriolar smooth muscle cells. J Neurosci 31:5067-5077.

Cenni G, Blandina P, Mackie K, Nosi D, Formigli L, Giannoni P, Ballini C, Della CL, Mannaioni PF, Passani MB (2006) Differential effect of cannabinoid agonists and endocannabinoids on histamine release from distinct regions of the rat brain. Eur J Neurosci 24:1633-1644.

Chaudhuri KR, Schapira AH (2009) Non-motor symptoms of Parkinson's disease: dopaminergic pathophysiology and treatment. Lancet Neurol 8:464-474.

Chepkova AN, Schonfeld S, Sergeeva OA (2015) Age-related alterations in the expression of genes and synaptic plasticity associated with nitric oxide signaling in the mouse dorsal striatum. Neural Plast 2015:458123.

Chu CJ, Huang SM, De PL, Bisogno T, Ewing SA, Miller JD, Zipkin RE, Daddario N, Appendino G, Di M, V, Walker JM (2003) N-oleoyldopamine, a novel endogenous capsaicin-like lipid that produces hyperalgesia. J Biol Chem 278:13633-13639.

Clapham DE, Julius D, Montell C, Schultz G (2005) International Union of Pharmacology. XLIX. Nomenclature and structure-function relationships of transient receptor potential channels. Pharmacol Rev 57:427-450.

Cooper J, Bloom FE, Roth RH (2003) The Biochemical Basis of Neuropharmacology., 8th ed. Oxford Univerity Press.

Crawford JH, Wainwright A, Heavens R, Pollock J, Martin DJ, Scott RH, Seabrook GR (2000) Mobilisation of intracellular Ca2+ by mGluR5 metabotropic glutamate receptor activation in neonatal rat cultured dorsal root ganglia neurones. Neuropharmacology 39:621-630.

Dauvilliers Y, Bassetti C, Lammers GJ, Arnulf I, Mayer G, Rodenbeck A, Lehert P, Ding CL, Lecomte JM, Schwartz JC (2013) Pitolisant versus placebo or modafinil in patients with narcolepsy: a double-blind, randomised trial. Lancet Neurol 12:1068-1075.

De Luca R, Suvorava T, Yang D, Baumgartel W, Kojda G, Haas HL, Sergeeva OA (2016) Identification of histaminergic neurons through histamine 3 receptor-mediated autoinhibition. Neuropharmacology 106:102-115.

Devane WA, Dysarz FA, Johnson MR, Melvin LS, Howlett AC (1988) Determination and characterization of a cannabinoid receptor in rat brain. Mol Pharmacol 34:605-613.

Di Marzo, V, Fontana A, Cadas H, Schinelli S, Cimino G, Schwartz JC, Piomelli D (1994) Formation and inactivation of endogenous cannabinoid anandamide in central neurons. Nature 372:686-691.

Diewald L, Heimrich B, Busselberg D, Watanabe T, Haas HL (1997) Histaminergic system in co-cultures of hippocampus and posterior hypothalamus: a morphological and electrophysiological study in the rat. Eur J Neurosci 9:2406-2413.

Dinh TP, Carpenter D, Leslie FM, Freund TF, Katona I, Sensi SL, Kathuria S, Piomelli D (2002) Brain monoglyceride lipase participating in endocannabinoid inactivation. Proc Natl Acad Sci U S A 99:10819-10824.

Drutel G, Peitsaro N, Karlstedt K, Wieland K, Smit MJ, Timmerman H, Panula P, Leurs R (2001) Identification of rat H3 receptor isoforms with different brain expression and signaling properties. Mol Pharmacol 59:1-8.

Dzirasa K, Ribeiro S, Costa R, Santos LM, Lin SC, Grosmark A, Sotnikova TD, Gainetdinov RR, Caron MG, Nicolelis MA (2006) Dopaminergic control of sleep-wake states. J Neurosci 26:10577-10589.

Endo T, Yanagawa Y, Komatsu Y (2014) Substance P Activates Ca2+-Permeable Nonselective Cation Channels through a Phosphatidylcholine-Specific Phospholipase C Signaling Pathway in nNOS-Expressing GABAergic Neurons in Visual Cortex. Cereb Cortex 26:669-682.

Ericson H, Kohler C, Blomqvist A (1991) GABA-like immunoreactivity in the tuberomammillary nucleus: an electron microscopic study in the rat. J Comp Neurol 305:462-469.

Ericson H, Watanabe T, Kohler C (1987) Morphological analysis of the tuberomammillary nucleus in the rat brain: delineation of subgroups with antibody against L-histidine decarboxylase as a marker. J Comp Neurol 263:1-24.

Farquhar-Smith WP, Egertova M, Bradbury EJ, McMahon SB, Rice AS, Elphick MR (2000) Cannabinoid CB(1) receptor expression in rat spinal cord. Mol Cell Neurosci 15:510-521.

Faucard R, Armand V, Heron A, Cochois V, Schwartz JC, Arrang JM (2006) N-methyl-D-aspartate receptor antagonists enhance histamine neuron activity in rodent brain. J Neurochem 98:1487-1496.

Fawley JA, Hofmann ME, Andresen MC (2014) Cannabinoid 1 and transient receptor potential vanilloid 1 receptors discretely modulate evoked glutamate separately from spontaneous glutamate transmission. J Neurosci 34:8324-8332.

Ferreira SG, Lomaglio T, Avelino A, Cruz F, Oliveira CR, Cunha RA, Kofalvi A (2009) N-acyldopamines control striatal input terminals via novel ligand-gated cation channels. Neuropharmacology 56:676-683.

Ferrini F, Salio C, Lossi L, Gambino G, Merighi A (2010) Modulation of inhibitory neurotransmission by the vanilloid receptor type 1 (TRPV1) in organotypically cultured mouse substantia gelatinosa neurons. Pain 150:128-140.

Fleck MW, Thomson JL, Hough LB (2012) Histamine-gated ion channels in mammals? Biochem Pharmacol 83:1127-1135.

Franklin KBJ, Paxinos G (2008) The mouse brain in stereotaxic coordinates. Academic Press.

Garbarg M, Javoy-Agid F, Schwartz JC, Agid Y (1983) Brain histidine decarboxylase activity in Parkinson's disease. Lancet 1:74-75.

Garcia-Sanz N, Valente P, Gomis A, Fernandez-Carvajal A, Fernandez-Ballester G, Viana F, Belmonte C, Ferrer-Montiel A (2007) A role of the transient receptor potential domain of vanilloid receptor I in channel gating. J Neurosci 27:11641-11650.

Giannoni P, Medhurst AD, Passani MB, Giovannini MG, Ballini C, Corte LD, Blandina P (2010) Regional differential effects of the novel histamine H3 receptor antagonist 6-[(3-cyclobutyl-2,3,4,5-tetrahydro-1H-3-benzazepin-7-yl)oxy]-N-methyl-3-pyridine carboxamide hydrochloride (GSK189254) on histamine release in the central nervous system of freely moving rats. J Pharmacol Exp Ther 332:164-172.

Giannoni P, Passani MB, Nosi D, Chazot PL, Shenton FC, Medhurst AD, Munari L, Blandina P (2009) Heterogeneity of histaminergic neurons in the tuberomammillary nucleus of the rat. Eur J Neurosci 29:2363-2374.

Giuffrida A, Parsons LH, Kerr TM, Rodriguez de FF, Navarro M, Piomelli D (1999) Dopamine activation of endogenous cannabinoid signaling in dorsal striatum. Nat Neurosci 2:358-363.

Gong JP, Onaivi ES, Ishiguro H, Liu QR, Tagliaferro PA, Brusco A, Uhl GR (2006) Cannabinoid CB2 receptors: immunohistochemical localization in rat brain. Brain Res 1071:10-23.

Grace AA, Bunney BS (1983) Intracellular and extracellular electrophysiology of nigral dopaminergic neurons--2. Action potential generating mechanisms and morphological correlates. Neuroscience 10:317-331.

Grace AA, Floresco SB, Goto Y, Lodge DJ (2007) Regulation of firing of dopaminergic neurons and control of goal-directed behaviors. Trends Neurosci 30:220-227.

Graham DG (1978) Oxidative pathways for catecholamines in the genesis of neuromelanin and cytotoxic quinones. Mol Pharmacol 14:633-643.

Haas H, Panula P (2003) The role of histamine and the tuberomamillary nucleus in the nervous system. Nat Rev Neurosci 4:121-130.

Haas HL, Konnerth A (1983) Histamine and noradrenaline decrease calcium-activated potassium conductance in hippocampal pyramidal cells. Nature 302:432-434.

Haas HL, Reiner PB (1988) Membrane properties of histaminergic tuberomammillary neurones of the rat hypothalamus in vitro. J Physiol 399:633-46.

Haas HL, Sergeeva OA, Selbach O (2008) Histamine in the nervous system. Physiol Rev 88:1183-1241.

Hetherington and Ranson (1940) Nutrition Classics. The Anatomical Record, Volume 78, 1940: Hypothalamic lesions and adiposity in the rat. Nutr Rev 41:124-127.

Hill SJ, Young JM, Marrian DH (1977) Specific binding of 3H-mepyramine to histamine H1 receptors in intestinal smooth muscle. Nature 270:361-363.

Huang SM, Bisogno T, Trevisani M, Al-Hayani A, De PL, Fezza F, Tognetto M, Petros TJ, Krey JF, Chu CJ, Miller JD, Davies SN, Geppetti P, Walker JM, Di M, V (2002) An endogenous capsaicin-like substance with high potency at recombinant and native vanilloid VR1 receptors. Proc Natl Acad Sci U S A 99:8400-8405.

Hurley MJ, Jenner P (2006) What has been learnt from study of dopamine receptors in Parkinson's disease? Pharmacol Ther 111:715-728.

Inagaki N, Yamatodani A, Ando-Yamamoto M, Tohyama M, Watanabe T, Wada H (1988) Organization of histaminergic fibers in the rat brain. J Comp Neurol 273:283-300.

Jaber M, Dumartin B, Sagne C, Haycock JW, Roubert C, Giros B, Bloch B, Caron MG (1999) Differential regulation of tyrosine hydroxylase in the basal ganglia of mice lacking the dopamine transporter. Eur J Neurosci 11:3499-3511.

Jackson MB (2001) Whole-cell voltage clamp recording. Curr Protoc Neurosci Chapter 6:Unit 6.6.

Jellinger KA (1991) Pathology of Parkinson's disease. Changes other than the nigrostriatal pathway. Mol Chem Neuropathol 14:153-197.

Jorgensen EA, Vogelsang TW, Knigge U, Watanabe T, Warberg J, Kjaer A (2006) Increased susceptibility to diet-induced obesity in histamine-deficient mice. Neuroendocrinology 83:289-294.

Julius D (2013) TRP Channels and Pain. Annu Rev Cell Dev Biol 29:355-84.

Kajihara Y, Murakami M, Imagawa T, Otsuguro K, Ito S, Ohta T (2010) Histamine potentiates acid-induced responses mediating transient receptor potential V1 in mouse primary sensory neurons. Neuroscience 166:292-304.

Kanamaru M, Iwase M, Homma I (1998) Autoregulation of histamine release in medulla oblongata via H3-receptors in rabbits. Neurosci Res 31:53-60.

Kandel, E. R., Schwartz, J. H. 1., & Jessell, T. M. (2000). Principles of neural science (4th ed.). New York: McGraw-Hill, Health Professions Division.

Karlstedt K, Jin C, Panula P (2013) Expression of histamine receptor genes Hrh3 and Hrh4 in rat brain endothelial cells. Br J Pharmacol 170:58-66.

Karlsson KA, Kreider JC, Blumberg MS (2004) Hypothalamic contribution to sleep-wake cycle development. Neuroscience 123:575-582.

Kernder A, De Luca R, Yanovsky Y, Haas HL, Sergeeva OA (2014) Acid-sensing hypothalamic neurons controlling arousal. Cell Mol Neurobiol 34:777-789.

Kim SR, Chung YC, Chung ES, Park KW, Won SY, Bok E, Park ES, Jin BK (2007) Roles of transient receptor potential vanilloid subtype 1 and cannabinoid type 1 receptors in the brain: neuroprotection versus neurotoxicity. Mol Neurobiol 35:245-254.

Kim YH, Park CK, Back SK, Lee CJ, Hwang SJ, Bae YC, Na HS, Kim JS, Jung SJ, Oh SB (2009) Membrane-delimited coupling of TRPV1 and mGluR5 on presynaptic terminals of nociceptive neurons. J Neurosci 29:10000-10009.

Kish SJ, Shannak K, Hornykiewicz O (1988) Uneven pattern of dopamine loss in the striatum of patients with idiopathic Parkinson's disease. Pathophysiologic and clinical implications. N Engl J Med 318:876-880.

Kohler C, Swanson LW, Haglund L, Wu JY (1985) The cytoarchitecture, histochemistry and projections of the tuberomammillary nucleus in the rat. Neuroscience 16:85-110.

Lammel S, Hetzel A, Hackel O, Jones I, Liss B, Roeper J (2008) Unique properties of mesoprefrontal neurons within a dual mesocorticolimbic dopamine system. Neuron 57:760-773.

Leeman SE (1980) Substance P and neurotensin: discovery, isolation, chemical characterization and physiological studies. J Exp Biol 89:193-200.:193-200.

Leenders KL, Palmer AJ, Quinn N, Clark JC, Firnau G, Garnett ES, Nahmias C, Jones T, Marsden CD (1986) Brain dopamine metabolism in patients with Parkinson's disease measured with positron emission tomography. J Neurol Neurosurg Psychiatry 49:853-860.

Leonelli M, Martins DO, Britto LR (2011) TRPV1 receptors modulate retinal development. Int J Dev Neurosci 29:405-413.

Leurs R, Traiffort E, Arrang JM, Tardivel-Lacombe J, Ruat M, Schwartz JC (1994) Guinea pig histamine H1 receptor. II. Stable expression in Chinese hamster ovary cells reveals the interaction with three major signal transduction pathways. J Neurochem 62:519-527.

Liem LK, Simard JM, Song Y, Tewari K (1995) The patch clamp technique. Neurosurgery 36:382-392.

Lin JS, Anaclet C, Sergeeva OA, Haas HL (2011) The waking brain: an update. Cell Mol Life Sci 68:2499-2512.

Lin JS, Dauvilliers Y, Arnulf I, Bastuji H, Anaclet C, Parmentier R, Kocher L, Yanagisawa M, Lehert P, Ligneau X, Perrin D, Robert P, Roux M, Lecomte JM, Schwartz JC

(2008) An inverse agonist of the histamine H(3) receptor improves wakefulness in narcolepsy: studies in orexin-/- mice and patients. Neurobiol Dis 30:74-83.

Liu Q, Bhat M, Bowen WD, Cheng J (2009) Signaling pathways from cannabinoid receptor-1 activation to inhibition of N-methyl-D-aspartic acid mediated calcium influx and neurotoxicity in dorsal root ganglion neurons. J Pharmacol Exp Ther 331:1062-1070.

Lichtman AH, Hawkins EG, Griffin G, Cravatt BF (2002) Pharmacological activity of fatty acid amides is regulated, but not mediated, by fatty acid amide hydrolase in vivo. J Pharmacol Exp Ther 302:73-79.

Lundius EG, Sanchez-Alavez M, Ghochani Y, Klaus J, Tabarean IV (2010) Histamine influences body temperature by acting at H1 and H3 receptors on distinct populations of preoptic neurons. J Neurosci 30:4369-4381.

Maggi CA, Schwartz TW (1997) The dual nature of the tachykinin NK1 receptor. Trends Pharmacol Sci 18:351-355.

Marinelli S, Di Marzo, V, Berretta N, Matias I, Maccarrone M, Bernardi G, Mercuri NB (2003) Presynaptic facilitation of glutamatergic synapses to dopaminergic neurons of the rat substantia nigra by endogenous stimulation of vanilloid receptors. J Neurosci 23:3136-3144.

Marinelli S, Pascucci T, Bernardi G, Puglisi-Allegra S, Mercuri NB (2005) Activation of TRPV1 in the VTA excites dopaminergic neurons and increases chemical- and noxious-induced dopamine release in the nucleus accumbens. Neuropsychopharmacology 30:864-870.

Marinelli S, Di Marzo, V, Florenzano F, Fezza F, Viscomi MT, van der Stelt M, Bernardi G, Molinari M, Maccarrone M, Mercuri NB (2007) N-arachidonoyl-dopamine tunes synaptic transmission onto dopaminergic neurons by activating both cannabinoid and vanilloid receptors. Neuropsychopharmacology 32:298-308.

Martinez-Mir MI, Pollard H, Moreau J, Arrang JM, Ruat M, Traiffort E, Schwartz JC, Palacios JM (1990) Three histamine receptors (H1, H2 and H3) visualized in the brain of human and non-human primates. Brain Res 526:322-327.

Meiser J, Weindl D, Hiller K (2013) Complexity of dopamine metabolism. Cell Commun Signal 11:34-11.

Microelectrode array manual http://www.multichannelsystems.com/sites/multi channelsystems.com/files/documents /manuals/MEA_Manual.pdf

Miklos IH, Kovacs KJ (2003) Functional heterogeneity of the responses of histaminergic neuron subpopulations to various stress challenges. Eur J Neurosci 18:3069-3079.

Mizushima J, Takahata K, Kawashima N, Kato M (2012) Successful treatment of dopamine dysregulation syndrome with dopamine D2 partial agonist antipsychotic drug. Ann Gen Psychiatry 11:19-11.

Monti JM, Monti D (2007) The involvement of dopamine in the modulation of sleep and waking. Sleep Med Rev 11:113-133

Moruzzi G (1972) The sleep-waking cycle. Ergeb Physiol 64:1-165.:1-165.

Nakamura S, Ohnishi K, Nishimura M, Suenaga T, Akiguchi I, Kimura J, Kimura T (1996) Large neurons in the tuberomammillary nucleus in patients with Parkinson's disease and multiple system atrophy. Neurology 46:1693-1696.

Naziroglu M, Senol N, Ghazizadeh V, Yuruker V (2014) Neuroprotection induced by N-acetylcysteine and selenium against traumatic brain injury-induced apoptosis and calcium entry in hippocampus of rat. Cell Mol Neurobiol 34:895-903.

Neher E, Sakmann B (1976) Single-channel currents recorded from membrane of denervated frog muscle fibres. Nature 260:799-802.

Nicoletti F, Bockaert J, Collingridge GL, Conn PJ, Ferraguti F, Schoepp DD, Wroblewski JT, Pin JP (2011) Metabotropic glutamate receptors: from the workbench to the bedside. Neuropharmacology 60:1017-1041.

Osorio-Espinoza A, Escamilla-Sanchez J, Aquino-Jarquin G, Arias-Montano JA (2014) Homologous desensitization of human histamine H(3) receptors expressed in CHO-K1 cells. Neuropharmacology 77:387-97. doi: 10.1016/j.neuropharm.2013.09.011. Epub;2013 Oct 23.:387-397.

Paladini CA, Roeper J (2014) Generating bursts (and pauses) in the dopamine midbrain neurons. Neuroscience 282C:109-121.

Panula P, Chazot PL, Cowart M, Gutzmer R, Leurs R, Liu WL, Stark H, Thurmond RL, Haas HL (2015) International Union of Basic and Clinical Pharmacology. XCVIII. Histamine Receptors. Pharmacol Rev 67:601-655.

Panula P, Nuutinen S (2013) The histaminergic network in the brain: basic organization and role in disease. Nat Rev Neurosci 14:472-487.

Panula P, Yang HY, Costa E (1984) Histamine-containing neurons in the rat hypothalamus. Proc Natl Acad Sci U S A 81:2572-2576.

Parlato R, Rieker C, Turiault M, Tronche F, Schutz G (2006) Survival of DA neurons is independent of CREM upregulation in absence of CREB. Genesis 44:454-464.

Parmentier R, Kolbaev S, Klyuch BP, Vandael D, Lin JS, Selbach O, Haas HL, Sergeeva OA (2009) Excitation of histaminergic tuberomamillary neurons by thyrotropin-releasing hormone. J Neurosci 29:4471-4483.

Pechevis M, Clarke CE, Vieregge P, Khoshnood B, Deschaseaux-Voinet C, Berdeaux G, Ziegler M (2005) Effects of dyskinesias in Parkinson's disease on quality of life and health-related costs: a prospective European study. Eur J Neurol 12:956-963.

Pecze L, Blum W, Schwaller B (2013) Mechanism of capsaicin receptor TRPV1-mediated toxicity in pain-sensing neurons focusing on the effects of $Na(+)/Ca(2+)$ fluxes and the $Ca(2+)$-binding protein calretinin. Biochim Biophys Acta 1833:1680-1691.

Perkins KL (2006) Cell-attached voltage-clamp and current-clamp recording and stimulation techniques in brain slices. J Neurosci Methods 154:1-18.

Pertwee RG (1997) Pharmacology of cannabinoid CB1 and CB2 receptors. Pharmacol Ther 74:129-180.

Piomelli D (2003) The molecular logic of endocannabinoid signalling. Nat Rev Neurosci 4:873-884.

Piomelli D, Beltramo M, Glasnapp S, Lin SY, Goutopoulos A, Xie XQ, Makriyannis A (1999) Structural determinants for recognition and translocation by the anandamide transporter. Proc Natl Acad Sci U S A 96:5802-5807.

Piomelli D, Tarzia G, Duranti A, Tontini A, Mor M, Compton TR, Dasse O, Monaghan EP, Parrott JA, Putman D (2006) Pharmacological profile of the selective FAAH inhibitor KDS-4103 (URB597). CNS Drug Rev 12:21-38.

Prell GD, Khandelwal JK, Burns RS, Blandina P, Morrishow AM, Green JP (1991) Levels of pros-methylimidazoleacetic acid: correlation with severity of Parkinson's disease in CSF of patients and with the depletion of striatal dopamine and its metabolites in MPTP-treated mice. J Neural Transm Park Dis Dement Sect 3:109-125.

Provensi G, Coccurello R, Umehara H, Munari L, Giacovazzo G, Galeotti N, Nosi D, Gaetani S, Romano A, Moles A, Blandina P, Passani MB (2014) Satiety factor oleoylethanolamide recruits the brain histaminergic system to inhibit food intake. Proc Natl Acad Sci U S A 111:11527-11532.

Przegalinski E, Filip M, Zajac D, Pokorski M (2006) N-oleoyl-dopamine increases locomotor activity in the rat. Int J Immunopathol Pharmacol 19:897-904.

Purba JS, Hofman MA, Swaab DF (1994) Decreased number of oxytocin-immunoreactive neurons in the paraventricular nucleus of the hypothalamus in Parkinson's disease. Neurology 44:84-89.

Ratti E, Carpenter DJ, Zamuner S, Fernandes S, Squassante L, Danker-Hopfe H, Archer G, Robertson J, Alexander R, Trist DG, Merlo-Pich E (2013) Efficacy of vestipitant, a neurokinin-1 receptor antagonist, in primary insomnia. Sleep 36:1823-1830.

Riley (1965) Histamine and sir Henry Dale. Br Med J 1:1488-1490.

Romano N, Yip SH, Hodson DJ, Guillou A, Parnaudeau S, Kirk S, Tronche F, Bonnefont X, Le TP, Bunn SJ, Grattan DR, Mollard P, Martin AO (2013) Plasticity of hypothalamic dopamine neurons during lactation results in dissociation of electrical activity and release. J Neurosci 33:4424-4433.

Saez TM, Aronne MP, Caltana L, Brusco AH (2014) Prenatal exposure to the CB1 and CB2 cannabinoid receptor agonist WIN 55,212-2 alters migration of early-born glutamatergic neurons and GABAergic interneurons in the rat cerebral cortex. J Neurochem 129:637-648.

Saper CB (2006) Biomedicine. Life,the universe,and body temperature.Science 314:773-774.

Saper CB, Lowell BB (2014) The hypothalamus. Curr Biol 24:R1111-R1116.

Saper CB, Scammell TE, Lu J (2005) Hypothalamic regulation of sleep and circadian rhythms. Nature 437:1257-1263.

Sarvari A, Farkas E, Kadar A, Zseli G, Fuzesi T, Lechan RM, Fekete C (2012) Thyrotropin-releasing hormone-containing axons innervate histaminergic neurons in the tuberomammillary nucleus. Brain Res 1488:72-80.

Schubring SR, Fleischer W, Lin JS, Haas HL, Sergeeva OA (2012) The bile steroid chenodeoxycholate is a potent antagonist at NMDA and GABA(A) receptors. Neurosci Lett 506:322-326.

Schultz W (2007) Behavioral dopamine signals. Trends Neurosci 30:203-210.

Sergeeva OA, Andreeva N, Garret M, Scherer A, Haas HL (2005) Pharmacological properties of GABAA receptors in rat hypothalamic neurons expressing the epsilon-subunit. J Neurosci 25:88-95.

Sergeeva OA, Fleischer W, Chepkova AN, Warskulat U, Haussinger D, Siebler M, Haas HL (2007) GABAA-receptor modification in taurine transporter knockout mice causes striatal disinhibition. J Physiol 585:539-548.

Sethi J, Sanchez-Alavez M, Tabarean IV (2011) Kv4.2 mediates histamine modulation of preoptic neuron activity and body temperature. PLoS One 6:e29134.

Shan L, Bossers K, Unmehopa U, Bao AM, Swaab DF (2012) Alterations in the histaminergic system in Alzheimer's disease: a postmortem study. Neurobiol Aging 33:2585-2598.

Simuni T, Sethi K (2008) Nonmotor manifestations of Parkinson's disease. Ann Neurol 64 Suppl 2:S65-80.

Smart TG, Paoletti P (2012) Synaptic neurotransmitter-gated receptors. Cold Spring Harb Perspect Biol 4:a009662.

Stevens DR, Eriksson KS, Brown RE, Haas HL (2001) The mechanism of spontaneous firing in histamine neurons. Behav Brain Res 124:105-112.

Stoof JC, Kebabian JW (1984) Two dopamine receptors: biochemistry, physiology and pharmacology. Life Sci 35:2281-2296.

Takahashi K, Lin JS, Sakai K (2006) Neuronal activity of histaminergic tuberomammillary neurons during wake-sleep states in the mouse. J Neurosci 26:10292-10298.

Takeshita Y, Watanabe T, Sakata T, Munakata M, Ishibashi H, Akaike N (1998) Histamine modulates high-voltage-activated calcium channels in neurons dissociated from the rat tuberomammillary nucleus. Neuroscience 87:797-805.

Thannickal TC, Lai YY, Siegel JM (2007) Hypocretin (orexin) cell loss in Parkinson's disease. Brain 130:1586-1595.

Tominaga M, Caterina MJ, Malmberg AB, Rosen TA, Gilbert H, Skinner K, Raumann BE, Basbaum AI, Julius D (1998) The cloned capsaicin receptor integrates multiple pain-producing stimuli. Neuron 21:531-543.

Tritsch NX, Sabatini BL (2012) Dopaminergic modulation of synaptic transmission in cortex and striatum. Neuron 76:33-50.

Trottier S, Chotard C, Traiffort E, Unmehopa U, Fisser B, Swaab DF, Schwartz JC (2002) Co-localization of histamine with GABA but not with galanin in the human tuberomamillary nucleus. Brain Res 939:52-64.

Tseng CF, Iwakami S, Mikajiri A, Shibuya M, Hanaoka F, Ebizuka Y, Padmawinata K, Sankawa U (1992) Inhibition of in vitro prostaglandin and leukotriene biosyntheses by cinnamoyl-beta-phenethylamine and N-acyldopamine derivatives. Chem Pharm Bull (Tokyo) 40:396-400.

Umehara H, Mizuguchi H, Fukui H (2012) Identification of a histaminergic circuit in the caudal hypothalamus: an evidence for functional heterogeneity of histaminergic neurons. Neurochem Int 61:942-947.

Ungless MA, Grace AA (2012) Are you or aren't you? Challenges associated with physiologically identifying dopamine neurons. Trends Neurosci 35:422-430.

Ungless MA, Magill PJ, Bolam JP (2004) Uniform inhibition of dopamine neurons in the ventral tegmental area by aversive stimuli. Science 303:2040-2042.

Uteshev VV, Knot HJ (2005) Somatic Ca(2+) dynamics in response to choline-mediated excitation in histaminergic tuberomammillary neurons. Neuroscience 134:133-143.

Verkhratsky A, Krishtal OA, Petersen OH (2006) From Galvani to patch clamp: the development of electrophysiology. Pflugers Arch 453:233-247.

Vetrivelan R, Fuller PM, Yokota S, Lu J, Saper CB (2012) Metabolic effects of chronic sleep restriction in rats. Sleep 35:1511-1520.

von Euler US, Pernow B (1956) Neurotropic effects of substance P. Acta Physiol Scand 36:265-275.

Wada H, Inagaki N, Itowi N, Yamatodani A (1991) Histaminergic neuron system in the brain: distribution and possible functions. Brain Res Bull 27:367-370.

Wang J, Ueda N (2008) Role of the endocannabinoid system in metabolic control. Curr Opin Nephrol Hypertens 17:1-10.

Wang M, Bianchi R, Chuang SC, Zhao W, Wong RK (2007) Group I metabotropic glutamate receptor-dependent TRPC channel trafficking in hippocampal neurons. J Neurochem 101:411-421.

Weiss JL, Cohn CK, Chase TN (1971) Reduction of catechol-O-methyl-transferases activity by chronic L-dopa therapy. Nature 234:218-219.

Watanabe T, Taguchi Y, Shiosaka S, Tanaka J, Kubota H, Terano Y, Tohyama M, Wada H (1984) Distribution of the histaminergic neuron system in the central nervous system of rats; a fluorescent immunohistochemical analysis with histidine decarboxylase as a marker. Brain Res 295:13-25.

Williams RH, Chee MJ, Kroeger D, Ferrari LL, Maratos-Flier E, Scammell TE, Arrigoni E (2014) Optogenetic-mediated release of histamine reveals distal and autoregulatory mechanisms for controlling arousal. J Neurosci 34:6023-6029.

Yang QZ, Hatton GI (1997) Electrophysiology of excitatory and inhibitory afferents to rat histaminergic tuberomammillary nucleus neurons from hypothalamic and forebrain sites. Brain Res 773:162-172.

Yanovsky Y, Li S, Klyuch BP, Yao Q, Blandina P, Passani MB, Lin JS, Haas HL, Sergeeva OA (2011) L-Dopa activates histaminergic neurons. J Physiol 589:1349-1366.

Yanovsky Y, Zigman JM, Kernder A, Bein A, Sakata I, Osborne-Lawrence S, Haas HL, Sergeeva OA (2012) Proton- and ammonium-sensing by histaminergic neurons controlling wakefulness. Front Syst Neurosci 6:23.

Yao R, Rameshwar P, Donnelly RJ, Siegel A (1999) Neurokinin-1 expression and co-localization with glutamate and GABA in the hypothalamus of the cat. Brain Res Mol Brain Res 71:149-158.

Yu X, Ye Z, Houston CM, Zecharia AY, Ma Y, Zhang Z, Uygun DS, Parker S, Vyssotski AL, Yustos R, Franks NP, Brickley SG, Wisden W (2015) Wakefulness Is Governed by GABA and Histamine Cotransmission. Neuron 87:164-178.

Zajac D, Spolnik G, Roszkowski P, Danikiewicz W, Czarnocki Z, Pokorski M (2014) Metabolism of N-acylated-dopamine. PLoS One 9:e85259.

Zecharia AY, Yu X, Gotz T, Ye Z, Carr DR, Wulff P, Bettler B, Vyssotski AL, Brickley SG, Franks NP, Wisden W (2012) GABAergic inhibition of histaminergic neurons regulates active waking but not the sleep-wake switch or propofol-induced loss of consciousness. J Neurosci 19;32:13062-13075.

Zhang HY, Gao M, Liu QR, Bi GH, Li X, Yang HJ, Gardner EL, Wu J, Xi ZX (2014) Cannabinoid CB2 receptors modulate midbrain dopamine neuronal activity and dopamine-related behavior in mice. Proc Natl Acad Sci U S A 111:E5007-E5015.

Zhou FW, Xu JJ, Zhao Y, LeDoux MS, Zhou FM (2006) Opposite functions of histamine H1 and H2 receptors and H3 receptor in substantia nigra pars reticulata. J Neurophysiol 96:1581-1591.

Zoli M, Agnati LF, Tinner B, Steinbusch HW, Fuxe K (1993) Distribution of dopamine-immunoreactive neurons and their relationships to transmitter and hypothalamic hormone-immunoreactive neuronal systems in the rat mediobasal hypothalamus. A morphometric and microdensitometric analysis. J Chem Neuroanat 6:293-310.

8. CV and list of abstracts and publications

8.1. Curriculum Vitae

Name: Roberto De Luca

Date of birth: 10th October 1987

Place of birth: Marino, Rome, Italy

Marital status: Married

2016-   Research Fellow, Sleep Medicine div., Harvard Medical School, Boston, USA

2013-2016 Ph.D, Heinrich-Heine-Universität Düsseldorf, Germany

2011-2013 M.Sc in Biology, "Roma Tre" University, Rome, Italy

2011-2013 Scientific Internship, "Campus Biomedico"University, Rome, Italy

2007-2011 B.Sc in Biological Sciences,"Roma Tre" University, Rome, Italy

2001-2006 Scientific Liceum Diplom, "Giovanni Vailati"Institute, Genzano, Rome, Italy

1998-2001 Middle School Diplom, "Marianna Dionigi"Institute, Lanuvio, Rome, Italy

8.2. List of abstracts and congresses

1. First iBrain kick-off annual meeting, 13th May 2013, Schloss Mickeln, Düsseldorf
2. Society for Neuroscience (SFN) meeting, 7th-13th November 2013, San Diego, USA. Poster presenting author: "TRPV1 expression in central histaminergic neurons of rat and mouse."
3. European Histamine Research Society (EHRS) 43rd Annual meeting,7th-10th May 2014, Lyon, France - as communication and poster non-presenting author of the following projects: "Glutamatergic excitation of histaminergic neurons."; "Substance P amplifies capsaicin signalling in mouse histaminergic neurons."
4. 1st iBrain annual meeting, 8th-9th May 2014, Haus der Universität, Düsseldorf
5. Society for Neuroscience (SFN) meeting, 15th-19th November 2014, Washington DC, USA- Poster presenting author: "Neurokinin 1 and capsaicin receptors in mouse histaminergic neurons."
6. 2nd iBrain annual meeting, 1st-2nd June 2015, SchlossMickeln, Düsseldorf
7. German physiological society (Deutsche Physiologischegesellschaft, DPG) 95th annual meeting, 3rd-5th march 2016, Lübeck, Germany-Poster non-presenting author: "N-oleoyldopamine (OLDA) modulates activity of central aminergic neurons through multiple and region-specific mechanisms".

8.3. List of publications

1. Kernder A, **De Luca R**, Yanovsky Y, Haas HL, Sergeeva OA. Acid-Sensing Hypothalamic Neurons Controlling Arousal. Cellular and Molecular Neurobiology 2014 Aug;34(6):777-89. Epub 2014 May 6. (impact factor: 2,506)

2. Biamonte F, Latini L, Giorgi FS, Zingariello M, Marino R, **De Luca R**, D'Ilio S, Majorani C, Petrucci F, Violante N, Senofonte O, Molinari M, Keller F. Associations among Exposure to Methylmercury, Reduced Reelin Expression, and gender in the Cerebellum of Developing Mice. Neurotoxicology. 2014 Dec;45:67-80. Epub 2014 Oct 14. (impact factor: 3,379)

3. **De Luca R**, Suvorava T, Yang D; Baumgärtel W; Kojda G, Haas HL, Sergeeva OA. Identification of histaminergic neurons through histamine 3 receptor-mediated autoinhibition. Neuropharmacology 106; 102-115 (2016) (impact factor: 5,106)

4. Sergeeva OA, **De Luca R,** Mazur K., Chepkova AN, Haas HL and Bauer A. N-oleoyldopamine (OLDA) modulates activity of midbrain dopaminergic neurons through multiple mechanisms (Neuropharmacology in revision).

9. Acknowledgements

10. Eidesstattliche Erklärung

Ich versichere hiermit an Eides statt, dass die vorliegende Dissertation von mir selbstständig und ohne unzulässige fremde Hilfe unter Beachtung der „Grundsätze zur Sicherung guter wissenschaftlicher Praxis an der Heinrich-Heine-Universität Düsseldorf" erstellt worden ist. Diese Dissertation wurde keiner anderen Fakultät vorgelegt und es gab bisher keine erfolglosen Promotionsversuche.

Düsseldorf, den 22. Februar 2016,
Roberto De Luca

10. Eidesstattliche Erklärung